FINAL REPORT

Degradation of Energetic Compounds Using Zero-Valent Iron (ZVI)

ESTCP Project WP-200524

MARCH 2012

Byung J. Kim
U.S. Army Engineering Research and Development Center

Daniel K. Cha
Pei C. Chiu
Seok-Young Oh
Department of Civil and Environmental Engineering, University of Delaware

ESTCP

Report Documentation Page

Form Approved
OMB No. 0704-0188

1. REPORT DATE	2. REPORT TYPE	3. DATES COVERED
MAR 2012		**00-00-2012 to 00-00-2012**

4. TITLE AND SUBTITLE	5a. CONTRACT NUMBER
Degradation of Energetic Compounds Using Zero-Valent Iron (ZVI)	5b. GRANT NUMBER
	5c. PROGRAM ELEMENT NUMBER
6. AUTHOR(S)	5d. PROJECT NUMBER
	5e. TASK NUMBER
	5f. WORK UNIT NUMBER
7. PERFORMING ORGANIZATION NAME(S) AND ADDRESS(ES) **U.S. Army Engineering Research and Development Center,Construction Engineering Research Laboratory (CERL),3909 Halls Ferry Road,Vicksburg,MS,39180-6199**	8. PERFORMING ORGANIZATION REPORT NUMBER
9. SPONSORING/MONITORING AGENCY NAME(S) AND ADDRESS(ES)	10. SPONSOR/MONITOR'S ACRONYM(S)
	11. SPONSOR/MONITOR'S REPORT NUMBER(S)

12. DISTRIBUTION/AVAILABILITY STATEMENT
Approved for public release; distribution unlimited

13. SUPPLEMENTARY NOTES

14. ABSTRACT

15. SUBJECT TERMS

16. SECURITY CLASSIFICATION OF:			17. LIMITATION OF ABSTRACT	18. NUMBER OF PAGES	19a. NAME OF RESPONSIBLE PERSON
a. REPORT **unclassified**	b. ABSTRACT **unclassified**	c. THIS PAGE **unclassified**	**Same as Report (SAR)**	**106**	

Executive Summary

For the last quarter century, the US Army has been searching for the most appropriate technology to treat pink water other than granular activated carbon (GAC). The major constituents of pink water are 2,4,6-trinitrotoluene (TNT), hexahydro-1,3,5-trinitro-1,3,5-triazine (RDX), octahydro-1,3,5,7-tetranitro-1,3,5,7-tetrazocine (HMX), 2,4-dinitrotoluene (DNT), trinitrobenzene (TNB), and dinitrobenzene (DNB). Among these toxic compounds, TNT and RDX are the major constituents in pink water and both of them are potential human carcinogens. National Defense Center for Environmental Excellence (Concurrent Technologies Corporation, 1995) prioritized all available pink water treatment technologies and selected five top technologies for further development: large aquatic plants, thermophilic biological regeneration of GAC, Fenton's oxidation, electrolytic oxidation and anaerobic fluidized bed reactor. However, we now know that both biological and chemical oxidations of pink water are inefficient due to the oxidized nature of these compounds. As a result, GAC adsorption is the most commonly used method to remove energetic compounds from pink water. The GAC process not only is expensive but generates explosive-laden spent carbon, a hazardous waste that needs to be regenerated or disposed of properly.

The long-term goal of this research was to develop a more cost-effective technology for the treatment of wastewaters containing energetic compounds. As the first phase of this research, we conducted a study to demonstrate the feasibility of using zero-valent iron (ZVI) to treat energetic compounds. ZVI was evaluated as a reductant for the degradation of 2,4,6-trinitrotoluene (TNT), hexahydro-1,3,5-trinitro-1,3,5-triazine (RDX), octahydro-1,3,5,7-tetranitro-1,3,5,7-tetrazocine (HMX), and nitroglycerin (NG). We hypothesized that reduction of these energetic compounds with ZVI would rapidly convert them to products that are either non-toxic or more readily mineralized in a subsequent oxidative treatment. This was demonstrated successfully in a series of laboratory-scale experiments with batch and flow-through reactors, using ZVI treatment alone or ZVI treatment followed by Fenton oxidation.

The reductive degradation of TNT, RDX, and NG in aqueous solution was carried out under anaerobic conditions in batch reactors with ZVI containing commercial cast iron or high-purity iron powder. All three compounds were removed rapidly from solution using either cast iron or high-purity iron. The fitted pseudo-first-order rate constants for the disappearance of TNT, RDX, and NG were 4.4 (± 0.3) x 10^{-2}, 6.3 (± 0.1) x 10^{-2}, and 1.65 (± 0.3) x 10^{-2} $L \cdot m^{-2} \cdot h^{-1}$, respectively. Initial removal of TNT and RDX was partly due to adsorption to iron particles, but the adsorption was reversible and all adsorbed TNT and RDX, as well as their reaction intermediates, were further transformed. The extent of adsorption with cast iron was greater than that with high-purity iron, presumably due to the presence of carbon (mostly graphite) in cast iron. In contrast, adsorption of NG was negligible because of its high water solubility.

Using either cast iron and high-purity iron, TNT was quantitatively reduced to the end product 2,4,6-triaminotoluene (TAT) through dinitroamino- and nitrodiamino-toluenes as intermediates. In contrast to TNT, RDX reduction with iron involved ring cleavage and yielded formaldehyde (69.1%) as the dominant carbonaceous product and NH_4^+ (35.5%) and N_2O (26.9%) as major nitrogenous products. Methylenedinitramine (MDNA) was identified as an intermediate product of RDX and was itself reduced completely to formaldehyde (~100%), NH_4^+ (19.2%), and N_2O (25.4%). Reduction of NG with iron occurred through sequential reductive denitration reactions via 1,2- and 1,3-dinitroglycerins (DNGs) and 1- and 2-mononitroglycerins (MNGs) to glycerol. Each of the denitration reactions released a nitrite, which was further reduced to NH_4^+. A reaction pathway and a kinetic model were proposed to describe the reduction of NG and nitrite with cast iron.

The rapid and quantitative reduction of NG to innocuous and biodegradable glycerol and NH_4^+ suggests that ZVI alone may be a viable method to treat NG-laden wastewaters. For TNT and RDX, an oxidative process following ZVI treatment may be necessary due to potential product toxicity and incomplete mass balance. For this study, we have selected Fenton oxidation to demonstrate the effectiveness of ZVI treatment to enhance the rate and extent of TNT and RDX

oxidation. An integrated treatment system consisting of a ZVI column and a Fenton reactor was proposed, and a bench-scale unit was constructed for this demonstration. A solution of TNT and RDX was passed through a cast iron-packed column (9.7 min residence time). The column effluent, which contained the reduction products of RDX and TNT, was sent to a completely-stirred tank reactor where Fenton reagent (H_2O_2 and Fe^{2+}) was added. Compared to direct Fenton oxidation of TNT and RDX, ZVI treatment enhanced the TOC removal by 20% and 60% for TNT and RDX, respectively. Complete TOC removal for both compounds was achieved under relatively mild conditions following ZVI treatment, whereas mineralization was not achievable without ZVI treatment even at high H_2O_2 and Fe^{2+} concentrations. The result suggests that a sequential ZVI treatment-Fenton oxidation process may be a feasible technology for pink water treatment.

In the second phase, the ZVI-Fenton process was further evaluated against real pink water from the Iowa Army Ammunition Plant (AAP). Result of our batch and column experiments shows that TNT, RDX, and HMX in the pink water were completely degraded and TAT and NH_4^+ were recovered after ZVI treatment. Using the integrated system, 85% of the TOC in the pink water, corresponding to the TOC of TNT, RDX, and HMX combined, was removed under optimal conditions. We also conducted laboratory column experiments with "real" wastewater samples from Holston AAP showed that a complete removal of RDX can be achieved with a column hydraulic residence time of 6.2 minutes. An additional column test carried out at an elevated temperature of 75^{o}C suggested that the iron contact time and thus ZVI reactor size may be further reduced by pre-heating the wastewater with steam.

Laboratory results indicate that elemental iron rapidly reduces nitroaromatics, nitramines, and nitrate esters to non-toxic or more oxidizable products and thus represents a promising new approach to treat energetic compounds in wastewater. The results also strongly justified a pilot - phase study evaluation and demonstration of the proposed ZVI process.

The trailer-mounted ZVI reactor unit was constructed and delivered to Holston AAP for evaluation. Because of lack of coordination for the start up, Holston AAP's operation contractor

wetted and exposed ZVI to the air for two months and exhausted the reduction power of ZVI. ESTCP funding was terminated after one year and another trailer-mounted ZVI reactor was built using Army materiel command (AMC) funding and pilot-phase evaluation was conducted at University of Delaware. The pilot-scale demonstration study (50 gallons/hour) was conducted with RDX solution containing four different RDX concentrations (10 – 40 mg/L) and two different pH values. The results from the pilot-scale iron column study showed that RDX and DNT were readily degraded by ZVI under a wide range of influent conditions. This pilot study demonstrated that ZVI-based treatment process is an efficient way to convert RDX in wastewater into products that is easily degradable through chemical or biological oxidation. For example, about 65% of carbon in influent RDX was recovered as formaldehyde, which can be very easily oxidized in conventional aerobic wastewater treatment plant (WWTP) or by Fenton oxidation.

Table of Contents

Executive Summary 1
Table of Contents 5
List of Tables 7
List of Figures 8
List of Acronyms 10
Acknowledgements 11
Section 1. ZVI Reduction of Energetic Compounds 12
1.1 Introduction 12
1.2 Reduction of TNT and RDX 15
1.2.1 Introduction 15
1.2.2 Materials and Methods 15
1.2.3 Results and Discussion 19
1.3 Reduction of Nitroglycerin 35
1.3.1 Introduction 35
1.3.2 Materials and Methods 35
1.3.3 Results and Discussion 37
Section 2. Enhanced Fenton Oxidation of Energetic Compounds with ZVI 46
2.1 Introduction 46
2.2 Integrated ZVI-Fenton System for Mineralization of TNT an RDX 49
2.2.1 Introduction 49
2.2.2 Materials and Methods 49
2.2.3 Results and Discussion 52
2.3 Validation of Proposed ZVI-Fenton Process with Pink Water 65
2.3.1 Introduction 65
2.3.2 Materials and Methods 65
2.3.3 Results and Discussion 67
Section 3. Pilot-Plant Evaluation of an Integrated ZVI-Fenton Process for RDX Containing Process Water treatment 75
3.1 Introduction 75
3.1.1 Background 75
3.1.2 Objectives of the Demonstration 75
3.2 Technology Description 76
3.2.1 Advantages and Limitations of the Technology 77
3.3 Preliminary Laboratory Testing 78
3.3.1 RDX Process Water from Holston AAP 78
3.4 Design and Construction of Demonstration Unit: Holston AAP 80
3.5 Start-up of ZVI Demonstration Unit: Holston AAP 85

3.5.1 Lesson Learned……85
3.6 Design and Construction of Demonstration Unit at Univ. of Delaware 86
3.7 Results of Pilot-plant Study at UD 90
Section 4. Conclusions and Rcommendations 95
4.1 Conclusions 95
4.2 Recommendations 96
References 97

List of Tables

Table **Page**

1.1 Reactions and rate laws for NG and its reduction products in the proposed pathway (1.11). The correlation coefficient for each compound is also shown (Oh et al., 2004a)……41
1.2 Fitted pseudo-first-order rate constants [hr-1] for the reactions shown in 1.11. The corresponding surface area-normalized rate constants [L·m-2·hr-1] were calculated based on the BET surface area concentration of 258 [m2/L]. The errors are two standard deviations obtained from the model fit (Oh et al., 2004a)……42
2.1 Nitrogen recovery after Fenton oxidation of TNT, RDX, ZVI-treated TNT and ZVI-treated RDX solutions (Oh et al., 2003a)……59
2.2 TOC removal and nitrogen recovery in degradation of TNT and RDX solutions using a bench-scale ZVI column-Fenton oxidation integrated system (Oh et al., 2003a)……..62
2.3 Dissolved explosives, TOC and pH in pink water from the Iowa Army ammunition plant……....67
2.4 Estimated treatment cost of pink water with the integrated ZVI-Fenton process……74
3.1 Chemical characteristics of the wastewater from Holston AAP……...80

List of Figures

Figure **Page**

1.1 Aqueous (a), surface (b) and total (c) concentrations of TNT, TAT, and four intermediates during TNT reduction with scrap iron. The dashed lines in Fig. 1.1(a) represent the aqueous TNT and TAT concentration profiles based on the fitted first-order rate constant of 0.190 ± 0.013 min-1 (r2 = 0.993) for the disappearance of TNT in solution (Oh et al., 2002a)……20
1.2 Aqueous (a), surface (b) and total (c) concentrations of TNT, TAT, and four intermediates during TNT reduction with high-purity iron powder. The dashed lines in Fig. 1.2(a) represent the aqueous TNT and TAT concentration profiles based on the fitted first-order rate constant of 0.096 ± 0.009 min-1 (r2 = 0.990) for the disappearance of TNT in solution (Oh et al., 2002a)……22
1.3 Aqueous (a), surface (b) and total (c) concentrations of RDX during its reduction with scrap iron. Fig. 1.3(a) also shows the LC peak area of a possible RDX reduction product (Oh et al., 2002a)……25
1.4 Aqueous (a), surface (b) and total (c) concentrations of RDX during its reduction with high-purity iron powder……..26
1.5 Concentrations of RDX, MDNA, and formaldehyde during RDX reduction with cast iron (0.1 g). The error bars are based on 5-mL samples from duplicate 8-mL reactors……29
1.6 Concentrations of the (a) carbonaceous and (b) nitrogenous compounds during RDX reduction in 250-mL batch reactors containing cast iron (2 g)……..30
1.7 Concentrations of MDNA, formaldehyde, and NH4+ during MDNA reduction with cast iron (0.1 g)…..32
1.8 Concentrations of the (a) carbonaceous and (b) nitrogenous compounds during MDNA reduction in 250-mL batch reactors containing cast iron (2 g)……33
1.9 Masses of the carbonaceous compounds during NG reduction in batch reactors containing cast iron…...37
1.10 Masses of the nitrogenous compounds during NG reduction in batch reactors containing cast iron……. 38
1.11 Proposed pathway of NG reduction with cast iron…….. 40
1.12 Measured masses of and fitted curves for the carbonaceous compounds during NG reduction with cast iron in batch reactors…… 43
1.13 Measured masses of and fitted curves for the nitrogenous compounds during NG reduction with cast iron in batch reactors ……...44
2.1 A proposed ZVI column-Fenton oxidation integrated system for pink water treatment…….52
2.2 The extent of TOC removal (a) and pseudo-first-order rate constant (b) with various H2O2/Fe2+ molar concentration ratios in Fenton oxidation of TNT and ZVI-treated TNT…….53
2.3 The extent of TOC removal (a) and pseudo-first-order rate constant (b) with various H2O2 and Fe2+ concentrations in Fenton oxidation of TNT and ZVI-treated TNT…….55
2.4 The extent of TOC removal (a) and pseudo-first-order rate constant (b) with various H2O2/Fe2+ molar concentration ratios in Fenton oxidation of RDX and ZVI-treated RDX……56
2.5 The extent of TOC removal (a) and pseudo-first-order rate constant (b) with various H2O2 and Fe2+ concentrations in Fenton oxidation of RDX and ZVI-treated RDX……58
2.6 Concentrations of TNT, RDX, and HMX during reduction of pink water in an unbuffered ZVI-water system……..68
2.7 Concentrations of TNT, RDX, and HMX during reduction of pink water with zero-valent iron……69
2.8 The extent of TOC removal with various H2O2 and Fe2+ concentrations in Fenton oxidation of pink water……70
3.1 Schematic of the proposed ZVI treatment system for the RDX wastewater……76
3.2 Reduction of RDX in Holston AAP wastewater in laboratory ZVI-packed column at 20 °C……..79
3.3 Reduction of RDX in Holston AAP wastewater in laboratory ZVI-packed column at 75 °C……..79
3.4 Layout of the trailer-mounted ZVI reactor system……82

3.5 Schematic Diagram of ZVI reactor system……..83
3.6 Schematic of the dual ZVI reactors……..84
3.7 Schematic layout of trailer-mounted demonstration system at Delaware……88
3.8 Iron columns in the demonstration system……..89
3.9 Removal of DNT by pilot-scale iron columns (Total HRT = 40 min)……90
3.10 Dinitrotoluene as the major products of DNT reduction by ZVI……...91
3.11 Removal of RDX by pilot-scale iron columns (Total HRT = 40 min.; influent pH = 7.5)……92
3.12 Removal of RDX by pilot-scale iron columns (Total HRT = 40 min.; influent pH = 4.5)……93
3.13 Effect of influent pH on effluent ferrous iron concentrations……..94

Acronyms

AAP: Army Ammunition Plant
AMC: Army Materiel Command
ANT: aminonitrotoluene
CERL: Construction Engineering Research Laboratory
CSTR: continuously stirred tank reactor
GAC: Granular Activated Carbon
DNB: dinitorbenzene
DNG: dinitroglycerin
DNT: 2,4-dinitotoluen
DNX: hexahydro-1,3-dinitroso-5nitro-1,3,5-triazine
ERDC: Engineer Research and Development Center
FID: flame ionization detector
GC/MS: gas-chromatography-mass spectrometry
HMX: octahydro-1,3,5,7-tetranitro-1,3,5,7-tetrazocine
HEPES: hydroxyethyl piperazine ethanesulfonic acid
HPLC: high performance liquid chromatography
HRT: hydrolic retention time
LC: liquid chromatography
MDNA: methylenedinitramine
MNG: mononitroglycerin
MNX: hexahydro-1-nitroso-3,5-dinitro-1,3,5-triazine
NG: nitroglycerin
PI: Principal Investigator
PRB: permeable reactive barrier
RDX: hexahydro-1,3,5-trinitor-1,3,5-triazine
TAT: 2,4,6-triaminotoluene
TNB: trinitrobenzene
TNT: 2,4,6- trinitrotoluene
TNX: hexahydro-1,3,5-trinitroso-1,3,5-triazine
TOC: total organic carbon
UV: ultraviolet
WWTP: Wastewater Treatment Plant
ZVI: zero-valent iron

Acknowledgements

This project was partially funded by Environmental security Technology Certification Program (ESTCP) Office and Army Materiel Command (AMC).

Dr. Byung Kim, US Army Engineer Research and Development Center (ERDC)-Construction Engineering Research Laboratory (CERL), was the Principal Investigator (PI).

Dr. Daniel Cha, University of Delaware, Department of Civil and Environmental Engineering was the contracted co-PI. Professor Pei C. Chiu and Dr. Seok-Young Oh were researchers with University of Delaware. Appreciation is extended to a few graduate research assistants (not identified in this report) at Drs. Cha and Pei's laboratory who helped to complete this research while they were pursuing their Master and Ph. D. programs.

Process wastewater (pink water), NG, and RDX samples were provided by Iowa Army Ammunition Plant (AAP), Radford AAP, and Holston AAP, espectively. Treatability studies and final pilot scale tests were conducted at University of Delaware. University of Delaware built two pilot scale trailer-mounted ZVI systems.

Section 1
ZVI Reduction of Energetic Compounds

1.1 Introduction

TNT and RDX are the most widely used explosives in the world (Spain et al., 2000). TNT is known to be carcinogenic and mutagenic and is acutely toxic to microbes, algae, fish, and other organisms (Smock et al., 1976; Won et al., 1976; Kaplan and Kaplan, 1982). RDX is a heterocyclic nitramine which, together with octahydro-1,3,5,7-tetranitro-1,3,5,7-tetrazocine (High Melting Explosive, HMX), is a persistent compound that is toxic to organisms including humans (Yinon, 1990; Harvey et al., 1991). It has been reported that soil and groundwater in the proximity of munitions-manufacturing plants are often contaminated with TNT and RDX (Hundal et al., 1997; Boopathy and Manning, 2000). In addition, explosives-laden wastewater from munitions-manufacturing facilities is difficult to treat because TNT and RDX are resistant to aerobic biodegradation, due to the presence of electron-withdrawing nitro constituents that inhibit electrophilic attack by oxygenase enzymes (Bruhn et al., 1987). Therefore, these energetic compounds are often removed from wastewater by costly physical-chemical processes including advanced oxidation, alkaline hydrolysis, carbon adsorption and incineration (Heilmann et al., 1996; Li et al., 1997; Alnaizy and Akgerman, 1999; Bier et al., 1999).

Nitroglycerin (NG, $CH(ONO_2)(CH_2ONO_2)_2$), or glycerol trinitrate is a nitrate ester explosive, that has been used as the main component in dynamites and propellants (Yinon and Zitrin, 1993). It has been also widely used as a vasodilator for heart diseases, such as angina pectoris (Wendt et al., 1978). Despite its pharmaceutical use, nitroglycerin is known to be toxic to microorganism, fish, rat, and human at high levels (Wendt et al., 1978; Urbański, 1985). At concentrations of 30 to 1,300 mg/kg, NG has been reported to be acutely toxic to mammalian species (Wendt et al., 1978). Chronic human exposure to NG causes headache, palpitation of the heart, nausea, and vomiting (Yinon, 1990). Due to its toxicity, NG-containing wastewater from propellant-manufacturing plants needs to be treated before it is discharged to wastewater treatment plants (Smith et al., 1983; USATHMA, 1989). Granular activated carbon (GAC)

adsorption, alkaline hydrolysis, chemical reduction processes were suggested as treatment methods for NG-containing wastewater (Smith et al., 1983; Meng et al., 1995; Christodoulatos et al., 1997). However, these treatment methods are costly and have additional drawbacks. The GAC adsorption process requires periodic regeneration of spent GAC and further treatment to completely degrade adsorbed NG. For alkaline hydrolysis and chemical reduction processes, large amounts of chemicals (e.g., Na(OH) or Na_2SO_3) are required and the products, such as nitrate and nitrite, need to be removed through denitrification. Biological treatment methods have been increasingly studied as a simple and cost-effective alternative (Wendt et al., 1978; Meng et al., 1995; Christodoulatos et al., 1997). However, NG is not readily biodegradable in aerobic mixed cultures (Pesari and Grasso, 1993), and studies show that biodegradation of NG is a co-metabolic process, which requires an external carbon source, such as ethanol. These studies showed that NG was transformed to glycerol through enzymatic reduction or hydrolysis (Pesari and Grasso, 1993; Meng et al., 1995; French et al., 1996; White et al., 1996; Bhaumik, 1997; Blehert et al., 1997; Zhang et al., 1997). However, the transformation was often slow and incomplete, resulting in the accumulation of dinitroglycerin (DNG) and mononitroglycerin (MNG) isomers in aerobic or anaerobic condition. It was currently reported that NG could be completely biotransformed by a mixed bacterial culture as the sole carbon, nitrogen, and energy source under aerobic condition (Accashian et al., 1998). However the transformation of NG was also shown to be slow. Therefore, a simple and cost-effective treatment process has been needed for NG-containing wastewater.

Elemental iron, often known as zero-valent iron (ZVI), usually in the form of scrap iron, has been increasingly used in recent years in permeable reactive barriers for the remediation of contaminated groundwater (Vidic and Pohland, 1996). Through reductive transformation or precipitation, iron has been shown to remove chlorinated solvents, nitrate, heavy metals, and radionuclides from water (Orth and Gillham, 1996; Roberts et al., 1996; Blowes et al., 1997; Huang et al., 1998; Gu et al., 1998; Nam and Tratnyek, 2000). It was also shown that ZVI can enhance the degradation of azo- and nitro-aromatic pollutants in water by reductively transforming them to more biologically amenable compounds (Perey et al., 2002). It may also be possible to use ZVI to pre-treat wastewater containing TNT and RDX provided the reduction of

these compounds with iron is sufficiently rapid. While the reduction of many pollutants with ZVI has been studied, the transformation of NG with ZVI has not been examined.

In this study, we examined whether and how rapidly ZVI is capable of reductively transforming these energetic compounds. We studied the effect of adsorption and the factors controlling the reduction of TNT and RDX with ZVI. We investigated the kinetics, pathway, and yield of products in the reduction of these energetic compounds (TNT, RDX, and NG) in an iron-water system through batch reduction experiments.

1.2 Reduction of TNT and RDX

1.2.1 Introduction

This study was conducted to determine the extent of adsorption to iron during reductive transformation of TNT and RDX and the effect of adsorption on the transformation rates. In addition to extraction from aqueous samples, adsorbed molecules were extracted and analyzed at different times. The effect of ZVI type on adsorption and transformation was investigated using high-purity iron powder and scrap iron having the same surface area. Data were also analyzed to examine whether TNT reduction and TAT formation rates were mass transfer-controlled. We were also trying to identify the reduction products of RDX with ZVI through batch reduction experiments in a closed system. We analyzed several possible compounds (e.g., MDNA, formaldehyde, and N_2O), which were detected previously in anaerobic biotransformation of RDX, to determine the mass recovery after the reduction with ZVI. Formation of volatile reduction products was examined using a GC-MS.

1.2.2 Materials and Methods

Chemicals

TNT (>99%) and RDX (>99%) were provided by Holston AAP (Kingsport, TN). 2-Amino-4,6-dinitrotoluene (2A46DNT; 99%) and 4-amino-2,6-dinitrotoluene (4A26DNT; 99.5%) were obtained from Chem Service (West Chester, PA). 2,4-Diamino-6-nitrotoluene (24DA6NT; 0.1 mg/mL standard in acetonitrile), 2,6-diamino-4-nitrotoluene (26DA4NT; 0.1 mg/mL standard in acetonitrile) and 2,4,6-triaminotoluene trihydrochloride (~100%) were purchased from Accustandard (New Haven, CT). Methylenedinitramine (MDNA, $CH_2(NH)_2(NO_2)_2$, >99%) was purchased from SRI International (Menlo Park, CA). Formaldehyde (HCHO, >99.8%) and HEPES [N-(2-hydroxyethyl)piperazine-N'-(ethanesulfonic acid)] were purchased from Sigma (St. Louis, MO). N_2O (99%) and acetonitrile (HPLC grade) were obtained from Aldrich (Pittsburgh, PA). Acetonitrile (≥99.9%) was purchased from Fisher Scientific (Pittsburgh, PA). All chemicals were used as received.

Two types of ZVI were used for this study. Master Builders iron was chosen as a representative scrap iron because it has been widely used in groundwater remediation work and its elemental composition has been determined (Reardon, 1995; Hardy and Gillham, 1996; Gu et al., 1998). High-purity iron powder (<10 μm, >99.5%) was purchased from Alfa Aesar (Ward Hill, MA). These irons were used as received without pretreatment. Specific surface areas of Master Builders iron and the high-purity iron powder were 1.29 and 0.19 m^2/g, respectively, as determined by the BET method with N_2.

Batch Reduction Experiments

Batch reduction experiments were conducted in an anaerobic glove box (95% N_2 + 5% H_2, Coy, MI) using 8 mL borosilicate vials containing 5 mL of aqueous solution and either 1 g of scrap iron or 6.8 g of high-purity iron powder. The different iron masses were used to give the same surface area of 1.29 m^2. Replicate vials were set up for each experiment. TNT and RDX solutions contained 0.1 M HEPES buffer to maintain a constant pH of 7.4 throughout the experiments. The solutions were purged in a glove box to completely remove oxygen. Initial concentrations of TNT and RDX were 0.206 ± 0.003 mM and 0.202 ± 0.006 mM (or 0.173 ± 0.004 mM), respectively. After iron was added, the vials were shaken in a horizontal position using an orbital shaker at 100 rpm. At different elapsed times, one of the vials was sacrificed and 4.5 mL of the supernatant was filtered through a 0.22 μm mixed cellulose membrane filter (Millipore, Bedford, MA) for analysis using a high performance liquid chromatograph (HPLC). Acetonitrile extraction of used filters indicated that TNT and RDX did not adsorb to the filters. Another batch reduction experiment was also performed to examine the possible transformation of MDNA, an intermediate during RDX reduction with cast iron. The experiments were conducted under the same conditions. The initial concentration of MDNA was 0.082 ± 0.001 mM.

In order to quantify volatile products such as N_2O or N_2, similar batch reduction experiments were performed for RDX and MDNA using a headspace method in a closed system. All experimental procedures to make a closed system were performed in a glove bag ($I^2R^®$, Cheltenham, PA) filled with Ar. Replicate amber glass vials (250 mL) were used containing 2 g

of cast iron and 125 mL of RDX solution. The solution was deoxygenated by purging with Ar for more than 30 min. The pH of the solution was controlled at 7.4 through the experiment using 0.1 M HEPES buffer. The initial concentration of RDX was 0.173 ± 0.004 mM. Mininert® valves (VICI Precision Sampling Inc, Baton Rouge, LA) were used to close the vials, and the gap between valves and the vials was tightly sealed by taping with vinyl tape (Scotch™ Brand 471, 3M, St. Paul, MN) to make a gas-tight closed system. Preliminary test showed that the prepared gas-tight sealing system lasted more than 2 weeks. The vials were shaken in a 45° inclined position at 100 rpm using a platform rotator. At elapsed sampling times, the replicates were sacrificed and the gas phase of the vial was sampled using a gas-tight syringe (VICI Precision Sampling Inc, Baton Rouge, LA) through the Mininert® valve for the injection to GC and GC-MS. At the same sampling times, the aqueous phase of the vial was sampled and filtered through 0.22-μm cellulose filter (Millipore, MA) for the analysis of RDX, MDNA, and formaldehyde. The identical batch reduction experiments were also conducted with MDNA. The initial MDNA concentration was 0.074 ± 0.005 mM.

Extraction of Adsorbed Compounds

After 4.5 mL of supernatant was removed, the iron (and 0.5 mL of solution) remaining in the vial was extracted once for high-purity iron powder and twice for scrap iron filings, each using 2 mL of acetonitrile, to recover adsorbed molecules. Additional extraction did not yield meaningful increases in recovery. For high-purity iron, after 2 mL of acetonitrile was added, the vial was vigorously shaken for 1.5 min using a vortex mixer, 2 mL of the supernatant was withdrawn and passed through a glass fiber filter, and the filtrate was analyzed by HPLC. Surface concentrations of adsorbates, defined as adsorbed mass divided by initial solution volume (5 mL), were calculated using eq. 1.1.

$$C_S = (C_e \cdot V_e - C_a \cdot V_a) / V_T \tag{1.1}$$

where C_S is the surface concentration (mM; the adsorbed mass divided by initial solution volume (V_T)), C_e is the concentration in extract (mM), obtained from HPLC analysis, C_a is the aqueous

concentration (mM), obtained from HPLC analysis, V_a is the volume of solution extracted by acetonitrile (0.5 mL), V_e is the extract volume (2.5 mL), V_T is the initial solution volume (5 mL), respectively.

For scrap iron, the extraction was repeated with another 2 mL of acetonitrile. Total surface concentration was taken to be the sum of the two surface concentrations calculated based on the two extract concentrations, using eqs 1.2-1.4. The first and second extraction efficiencies, defined as C_{S1}/C_S and C_{S2}/C_S, were 82.5 ± 0.3% and 17.5 ± 0.3%, respectively, for TNT.

$$C_{S1} = (C_{e1} \cdot V_e - C_a \cdot V_a)/ V_T \tag{1.2}$$

$$C_{S2} = (C_{e2} \cdot V_e - C_{e1} \cdot V_a)/ V_T \tag{1.3}$$

$$C_S = C_{S1} + C_{S2} \tag{1.4}$$

where C_{S1} and C_{S2} are surface concentrations based on first and second extractions (mM), respectively. C_{e1} are C_{e2} are concentrations in the first and second extracts (mM), respectively.

Analytical Methods

The TNT, 2A46DNT, 4A26DNT, 24DA6NT, 26DA4NT, RDX, MDNA, and a soluble RDX reduction product (see Results and Discussion) were analyzed using a Varian HPLC (Walnut Creek, CA) equipped with a Supelguard guard column (20×4.6 mm, Supelco, Bellefonte, PA), a Supelco LC- 18 column (250×4.6 mm, 5-µm particle size), an ultraviolet (UV) detector (2510 Varian, Walnut Creek, CA) and an isocratic pump (2550 Varian, Walnut Creek, CA). Methanol-water mixture (55:45, v/v) was used as the mobile phase at a flow rate of 1.0 mL/min. 2,4,6-Triaminotoluene (TAT) was analyzed by HPLC with an Alltima C18 column (250×4.6 mm, 5-µm particle size, Alltech, Deerfield, IL) and an Alltima guard column (7.5×4.6 mm, Alltech). Acetonitrile-phosphate buffer (40 mM, pH 3.2, 10:90, v/v) was used as an eluent at 1.0 mL/min. The injection volume for all samples was 10 µL and the wavelength for the UV detector was 254 nm.

Formaldehyde was analyzed using the HPLC through derivatization with Nash's reagent (0.02M of 2,4-pentanedione and 2 M ammonium acetate, pH 6) (Summer, 1990). Dissolved formaldehyde in aqueous sample (1 mL) was derivatized with 1 mL of Nash's reagent for 1 hour at 60 ^{o}C in a water bath (Precision, Winchester, VA). After the samples cooled down to ambient temperature, the derivatized formaldehyde was analyzed using the Varian HPLC with the UV detector (λ = 410 nm). The mixture of acetonitrile and deionized water (40/60, v/v) was used as an eluent at a flow rate of 1.0 mL/min and the injection volume of the sample was 10 μL. The identical procedure was applied for formaldehyde standard solution dissolved in deionized water. Correlation coefficient for the obtained calibration curve for formaldehyde was 0.999.

N_2O was analyzed using a GC (HP5890, Hewlett Packard, Palo Alto, CA) equipped with a 25-m Ultra-2 capillary column (0.2 mm i.d., 0.33 μm film thickness, J&W, Wilmington, DE) and a flame ionization detector (FID). The injected volume of gas sample was 100 μL and the oven temperature was 60 ^{o}C. The standard samples were prepared by injecting several different volumes of pure N_2O gas into the headspace in the vial (250 mL) having 125 mL of 0.1 M HEPES and 2 g of cast iron. The total mass of N_2O in aqueous and gas phases was quantified using Henry's constant of N_2O (40 atm/M at 25 ^{o}C). Mass spectrum of the gas sample was obtained using a GC (6890N, Agilent Technology, Palo Alto, CA) equipped with a column (model 122-0732, 0.25 mm i.d., 30 m length, 0.25 μm film thickness, Agilent Technology, Palo Alto, CA) and mass selective detector (5973N, Agilent Technology, Palo Alto, CA). The oven temperature was raised from 40 ^{o}C (1 min) to 230 ^{o}C (1 min) at the rate of 23.75 ^{o}C/min.

Total organic carbon (TOC) was analyzed using a TOC analyzer (DC-190 Dohrmann, Santa Clara, CA). The NH_4^+ was analyzed by the salicylate method (Hach Co., 1998) using a UV-vis spectrophotometer (DR2010, HACH, Loveland, CO). Nitrate and nitrite were analyzed using an ion chromatograph (Dionex, Sunnyvale, CA) equipped with a Dionex Ionpac AS11 column.

1.2.3 Results and Discussion

Reduction of TNT with Scrap Iron and High-Purity Iron Powder

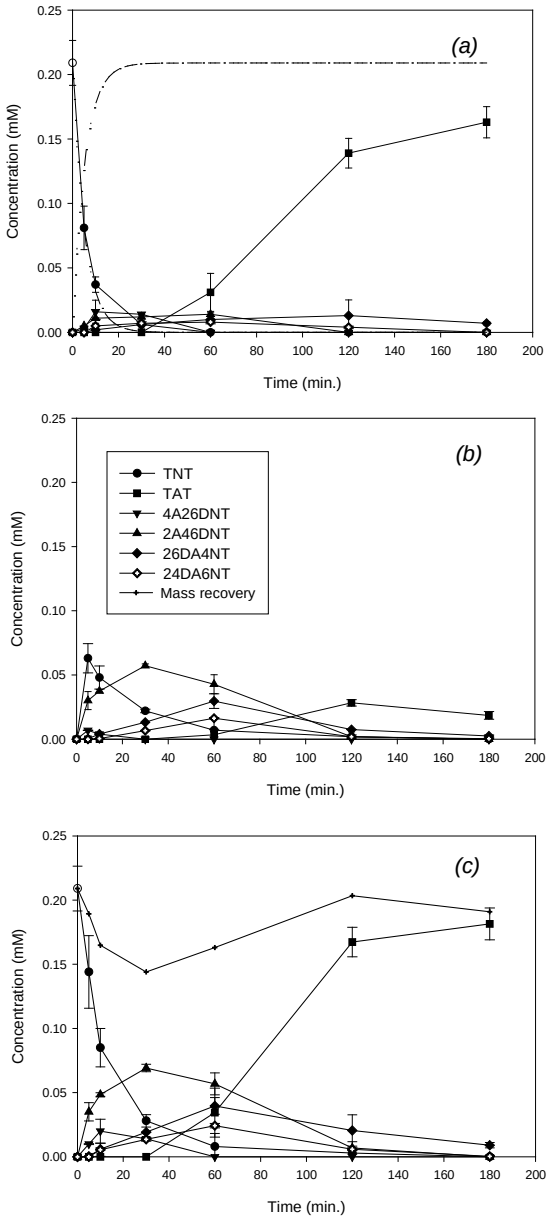

Figure 1.1 Aqueous (a), surface (b) and total (c) concentrations of TNT, TAT, and four intermediates during TNT reduction with scrap iron. The dashed lines in Figure 1.1(a) represent the aqueous TNT and TAT concentration profiles based on the fitted first-order rate constant of 0.190 ± 0.013 min^{-1} (r^2 = 0.993) for the disappearance of TNT in solution (Oh et al., 2002a)

Figure 1.1 shows the aqueous, surface, and total concentrations of TNT and the major reduction intermediates (2A46DNT, 4A26DNT, 24DA6NT, 26DA4NT) and end product (TAT) during reduction with scrap iron. The error bars in all figures indicate the standard deviation, which was calculated by data from analyses of replicate reactors. Aqueous TNT concentration rapidly decreased to zero within 30 min, but only low quantities of the intermediates were detected in solution during this period (Figure 1.1a). Over 75% of the initial TNT was recovered as TAT after 3 h. The surface concentrations of adsorbed compounds, however, presented a very different picture. As shown in Figures 1.1a and 1.1b, almost half of the TNT removed from water in the first 5 min (~0.13 mM) was adsorbed to scrap iron, and the amounts of intermediates adsorbed were greater than that found in solution. In comparison, TAT was only weakly adsorbed due to its relatively high water solubility. 2A46DNT was the dominant intermediate, indicating reduction of the *ortho* nitro group was the principal reaction in TNT reduction pathway with scrap iron. Reduction of the *ortho* nitro group was also a major reaction for 2A46DNT, as shown by the high yields of 26DA4NT. Figure 1.1c shows the total concentrations of TNT and its daughter products, which were obtained by adding the aqueous and surface concentrations. These profiles represent concentration changes due only to transformation. Complete reduction of TNT to TAT took more than 3 h, as reaction rate decreased with decreasing number of nitro groups. Mass balance during the experiment ranged from 70.1 to 97.3%. The lower mass balance at early times might be ascribed to the TNT reduction products that were not measured (e.g., nitroso compounds).

Figure 1.2 shows the aqueous, surface, and total concentration profiles during TNT reduction with high-purity iron powder. Similar to the data in Figure 1.1a, TNT was completely removed from solution within 30 min (Figure 1.2a). The intermediates found in the aqueous phase were 24DA6NT and 4A26DNT but only in minute quantities (Figure 1.2a). In contrast to Figure 1.1a, aqueous TAT appeared very early and its concentration quickly approached the initial TNT concentration. This suggested that TNT and intermediates adsorbed on high-purity iron were transformed much faster than those adsorbed on scrap iron. Indeed, Figure 1.2b shows that all adsorbed TNT reacted within 30 min, adsorbed TAT appeared immediately, and no intermediates accumulated at the surface. These observations are in sharp

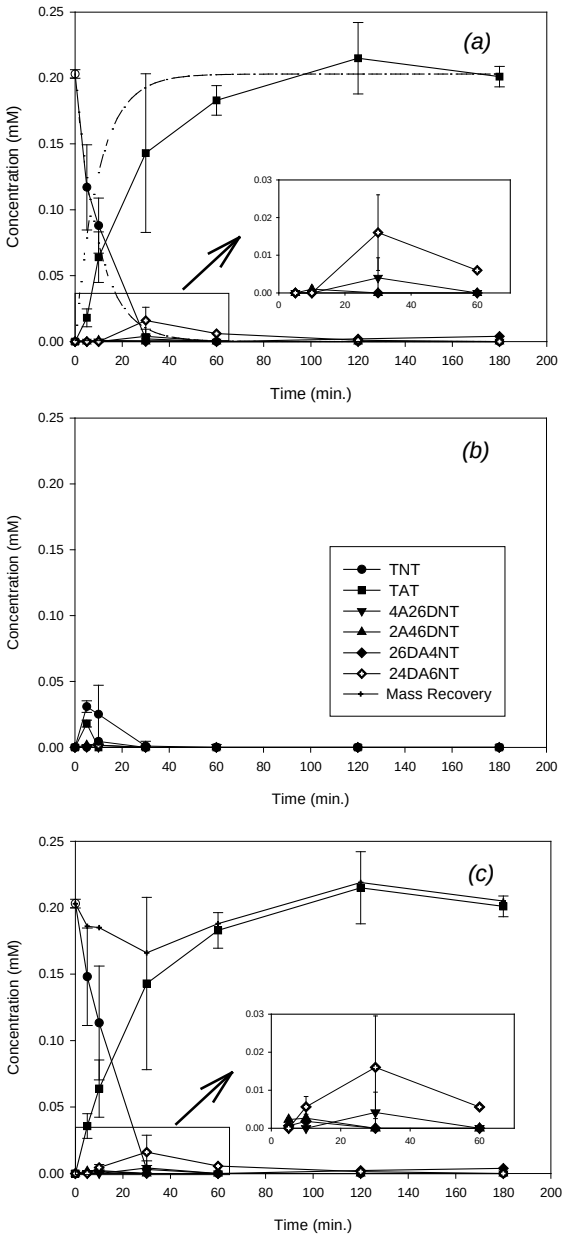

Figure 1.2 Aqueous (a), surface (b) and total (c) concentrations of TNT, TAT, and four intermediates during TNT reduction with high-purity iron powder. The dashed lines in Figure 1.2(a) represent the aqueous TNT and TAT concentration profiles based on the fitted first-order rate constant of 0.096 ± 0.009 min^{-1} (r^2 = 0.990) for the disappearance of TNT in solution (Oh et al., 2002a)

contrast to Figure 1.1b. All TNT was fully reduced and recovered as TAT in solution and the mass balance ranged from 82 to 108% during the experiment (Figure 1.2c).

From the results shown in Figures 1.1 and 1.2, it is clear that adsorption of TNT and its daughter products was more pronounced with scrap iron. This may be attributed to the carbon in scrap iron. Master Builders iron is known to contain 2-4% carbon and other elements (Reardon, 1995; Hardy and Gillham, 1996; Burris et al., 1998). Adsorption of chlorinated ethenes to scrap iron has been proposed to occur at non-reactive sites, such as graphite inclusions (Burris et al., 1998). In contrast to the studies with chlorinated ethenes (Burris et al., 1995; Allen-King et al., 1997; Burris et al., 1998), however, adsorbed TNT on scrap iron was reduced much more rapidly. Rapid consumption of aqueous TNT could have shifted the equilibrium and caused TNT to desorb from the non-reactive sites. Alternatively, the more pronounced adsorption of TNT with scrap iron could be due to adsorption to another type of reactive sites, which were different from and less reactive than those found in pure iron. The mechanism through which adsorbed TNT is transformed was interesting topic in the future research.

The results also suggest that, for pure iron powder, the overall rate of TNT reduction to TAT was controlled by either mass transfer or adsorption of TNT in solution. Equation 1.5 shows a simplified reaction sequence of TNT reduction to TAT. Note that all steps were assumed to be first-order and desorption of the intermediates was omitted for simplicity. If the removal of TNT from solution controlled the overall rate of the reaction, then either the TNT mass transfer rate constant ($k_{MT,TNT}$) or the adsorption rate constant (k_{ads}) would be approximately equal to the overall rate constant ($k_{overall}$, eq. 1.6). In that case, the sequence can be modeled as a single-step, first-order reaction (eq. 1.6) and the aqueous concentrations of TNT and TAT can be calculated using equations 1.7 and 1.8. The predicted concentration profiles of aqueous TAT with scrap iron and pure iron are shown in Figures 1.1a and 1.2a (dash lines). Fitted pseudo-first-order rate constants for the disappearance of aqueous TNT (fitted curves also shown in the Figures) were used. Note that these empirical rate constants may correspond to either $k_{MT,TNT}$ or k_{ads}, as mass transfer and adsorption could not be differentiated in our experiments. For scrap iron, the model prediction differs greatly from the actual aqueous concentrations of TAT,

suggesting that TAT formation was controlled not by TNT removal from solution but by subsequent steps in the sequence. For high-purity iron, the model fits the observed TAT data quite well, which suggests that either mass transfer or adsorption of aqueous TNT was the rate-limiting step in the sequence (eq. 1.5).

$$\mathrm{TNT_{(aq)} \xrightarrow{k_{MT,TNT}} \xrightarrow{k_{ads}} \xrightarrow{k_{R1}} \xrightarrow{k_{R2}} \rightarrow\rightarrow \xrightarrow{k_{Rn}} \xrightarrow{k_{des}} \xrightarrow{k_{MT,TAT}} TAT_{(aq)}} \quad (1.5)$$

$$TNT_{(aq)} \xrightarrow{k_{overall}} TAT_{(aq)} \quad (1.6)$$

$$[TNT]_{(aq)} = [TNT]_{o\,(aq)} \cdot e^{-k_{overall}t} \quad (1.7)$$

$$[TAT]_{(aq)} = [TNT]_{o\,(aq)} \cdot (1 - e^{-k_{overall}t}) \quad (1.8)$$

where k_{R1}, k_{R2}, and k_{Rn} are the rate constants of sequential reactions, k_{des} is the desorption rate constant, and t is time.

Reduction of RDX with Scrap Iron and High-Purity Iron Powder

Figures 1.3 and 1.4 show the changes of aqueous, surface, and total concentrations of RDX during its reduction with scrap iron and high-purity iron, respectively. RDX disappeared from the aqueous phase within 30 min regardless of the iron type, as was observed for TNT. However, in contrast to the TNT data with scrap iron (Figure 1.1b), adsorbed RDX was transformed within 30 min with both pure iron and scrap iron (though slightly faster with pure iron). It thus appears that RDX adsorbed to scrap iron either desorbed or reacted more rapidly than adsorbed TNT.

Using the same LC conditions as for RDX analysis, we detected a large peak with a retention time of 2.2 ± 0.1 min during RDX reduction with both irons. The area of the peak increased with time initially and then slowly decreased (Figures 1.3a and 1.4a), suggesting that it was an RDX reduction intermediate. This compound was water-soluble and could not be solvent-extracted for analysis by gas chromatography-mass spectrometry (GC/MS). In soil

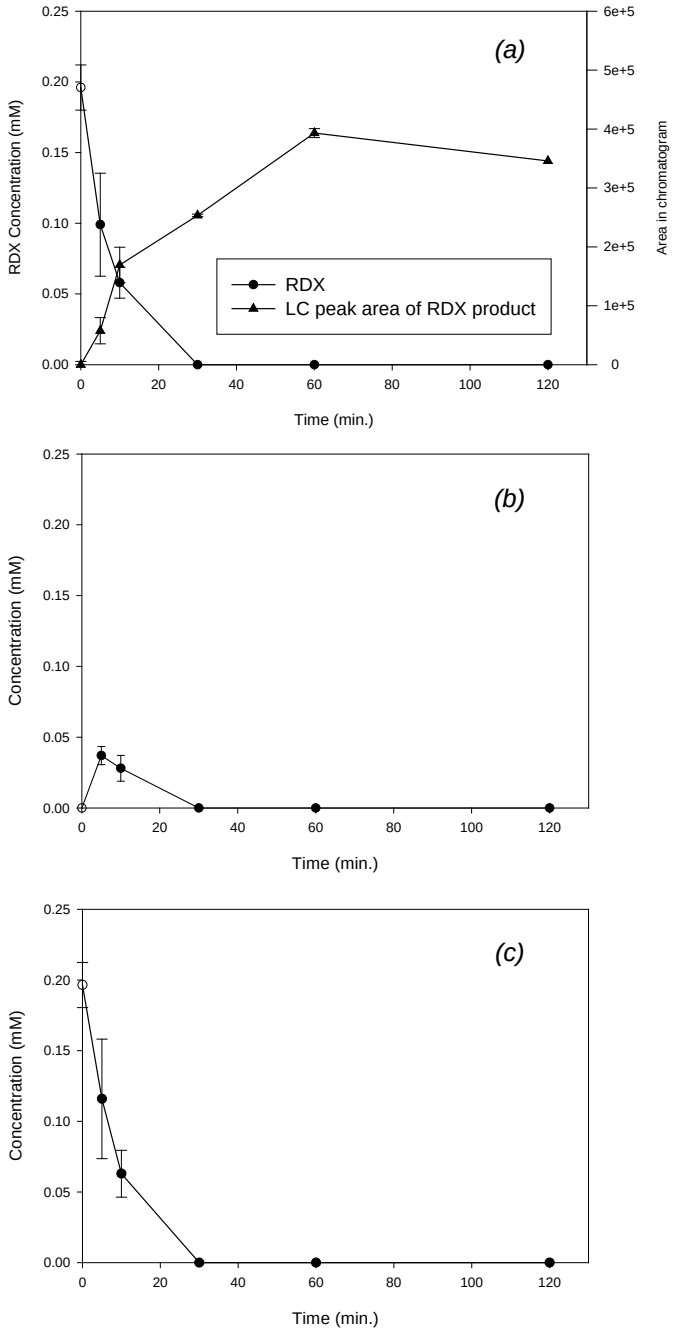

Figure 1.3 Aqueous (a), surface (b) and total (c) concentrations of RDX during its reduction with scrap iron. Figure 1.3(a) also shows the LC peak area of a possible RDX reduction product (Oh et al., 2002a)

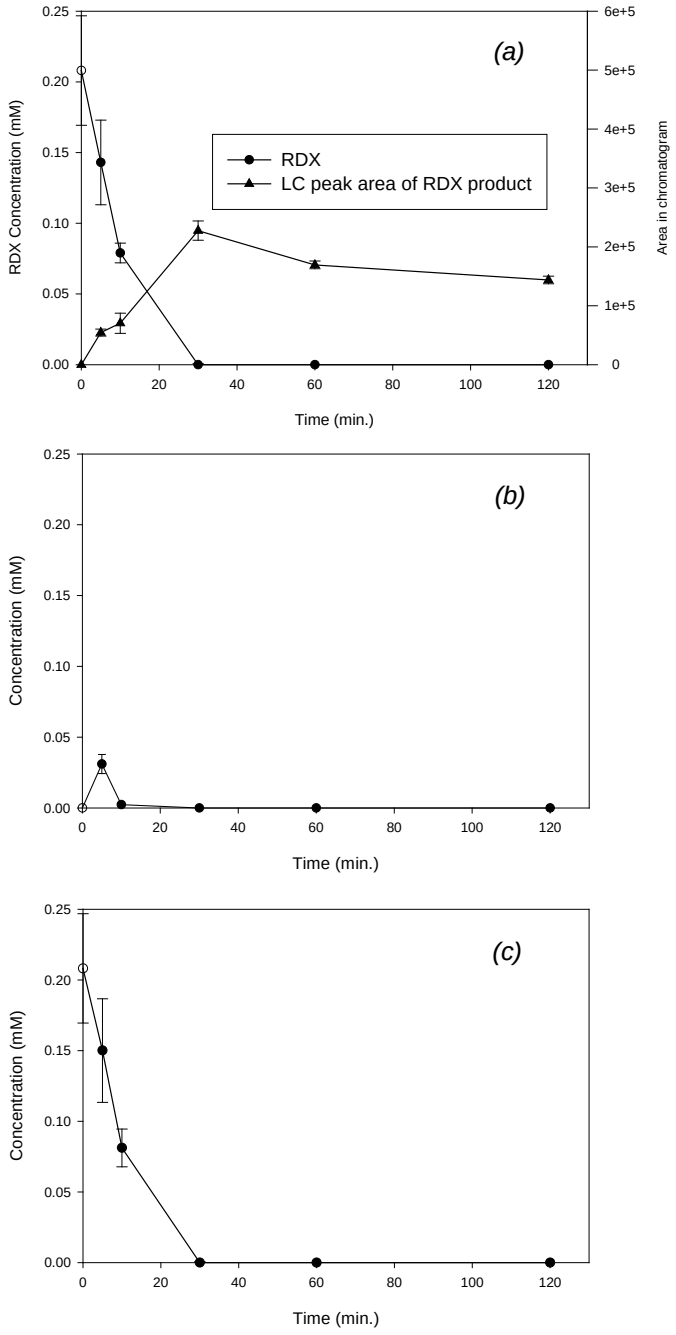

Figure 1.4 Aqueous (a), surface (b) and total (c) concentrations of RDX during its reduction with high-purity iron powder. Figure 1.4(a) also shows the LC peak area of an unidentified reduction product of RDX (Oh et al., 2002a).

microcosms containing ZVI, Oh et al. (2001) identified methylenedinitramine (MDNA) to be a soluble RDX reduction product using LC/MS/MS. Whether the LC peak we observed corresponds to MDNA remains to be determined.

Although the pathway for RDX reduction with ZVI is not resolved, a pathway for biological RDX reduction has been proposed. Under anaerobic conditions, RDX was shown by McCormick and coworkers (1981) to transform in a stepwise fashion to hexahydro-1-nitroso-3,5-dinitro-1,3,5-triazine (MNX), hexahydro-1,3-dinitroso-5-nitro-1,3,5-triazine (DNX), and hexahydro-1,3,5-trinitroso-1,3,5-triazine (TNX). Further degradation involved cleavage of the triazine ring and formation of hydrazine, 1,1-dimethylhydrazine, 1,2-dimethylhydrazine, formaldehyde, and methanol. Another possible reduction pathway was shown by Hawari and coworkers in anaerobic sludge (Hawari et al., 2000), who proposed that the triazine ring of RDX was cleaved through enzymatic hydrolysis to form MDNA and bis(hydroxymethyl)nitramine. These compounds were further degraded abiotically to give formaldehyde, methanol, nitrous oxide (N_2O), and water. Formaldehyde and methanol were eventually converted to CO_2 and CH_4.

In an experiment conducted in deionized water (i.e., HEPES buffer was omitted), we found that the TOC remained constant before (12.4 mg/L) and after (12.2 mg/L) complete RDX transformation with scrap iron. This indicates that the carbon in the triazine ring was not mineralized. Using liquid-liquid extraction with hexane or ether followed by GC/MS analysis, we did not detect either formaldehyde or methanol. In fact, no MS peaks were observed, suggesting that the carbonaceous products were highly polar or charged.

Attempts were also made to establish nitrogen balance by measuring NH_4^+, NO_2^-, and NO_3^- in solution during RDX transformation. NH_4^+ appeared immediately and, within 1 hour, its concentration reached a plateau, which corresponded to approximately 50% of the total RDX nitrogen (data not shown). The rapid formation of NH_4^+ indicated that the N-N bonds in RDX were cleaved early in the reaction. No NO_2^- or NO_3^- was detected during the experiment. These ions were either not formed during RDX reduction or were rapidly reduced with iron to NH_4^+ and did not accumulate (Huang et al., 1998; Kielemoes et al., 2000).

Mass Transfer Rates and Rate-Limiting Steps

Mass transfer rates in our batch experiments with high-purity and scrap iron were estimated using the procedures suggested by Arnold et al. (1999) (Jafarpour et al., 2003). They also performed mathematical modeling of 2,4-DNT reduction with high-purity and scrap iron to estimate the rates of surface reaction, adsorption, and desorption at graphite and iron (hydr/oxide) sites. Estimated mass transfer rate constants for the high-purity iron and scrap iron systems were 210 (min^{-1}) and 9 (min^{-1}), respectively. Those values were 2 to 3 orders of magnitude larger than the estimated rate constants of surface reaction, adsorption, and desorption of DNT. The estimated mass transfer rates in our experimental conditions were also 2 to 3 orders of magnitude larger than the pseudo-first-order rate constants of TNT (Figures 1.1 and 1.2). These results suggest that external mass transfer are not the rate-limiting step in our batch experiments and that surface reaction, adsorption, or desorption may be responsible for the overall reaction of TNT and DNT in high-purity iron and scrap iron systems.

Products of RDX Reduction with Cast Iron

RDX was rapidly and completely removed from the solution within 2 hrs in the batch system (Figure 1.5). Pseudo-first-order rate constant for RDX was estimated to be 0.027 ± 0.005 (min^{-1}) ($R^2 = 0.961$). Surface area-normalized rate constant was calculated to be $(6.3 \pm 0.1) \times 10^{-2}$ ($L \cdot m^{-2} \cdot hr^{-1}$), which closed to the measured value for Fisher iron filing ($\sim 10^{-2}$ ($L \cdot m^{-2} \cdot hr^{-1}$)) (Singh et al., 1999; Alowitz and Scherer, 2002) As shown in Figure 1.5, MDNA was shown up as RDX disappeared. After 360 min, MDNA was completely removed from the solution, indicating that MDNA was not a product but an intermediate. Maximum C concentration of MDNA in the solution was 0.037 mM at 60 min, which was much less than the initial C concentration of RDX (0.519 mM). This implies that the rate of MDNA removal may be higher than that of its formation or other intermediates may be formed along with MDNA. The reductive transformation of MDNA with cast iron will be further discussed in a next section. Formaldehyde was also produced as RDX was removed from the solution. It appears that, after 120 min, the C concentration of formaldehyde might be constant. The final C concentration of formaldehyde was 0.336 mM, corresponding to 65.4% of initial C concentration of RDX. Batch

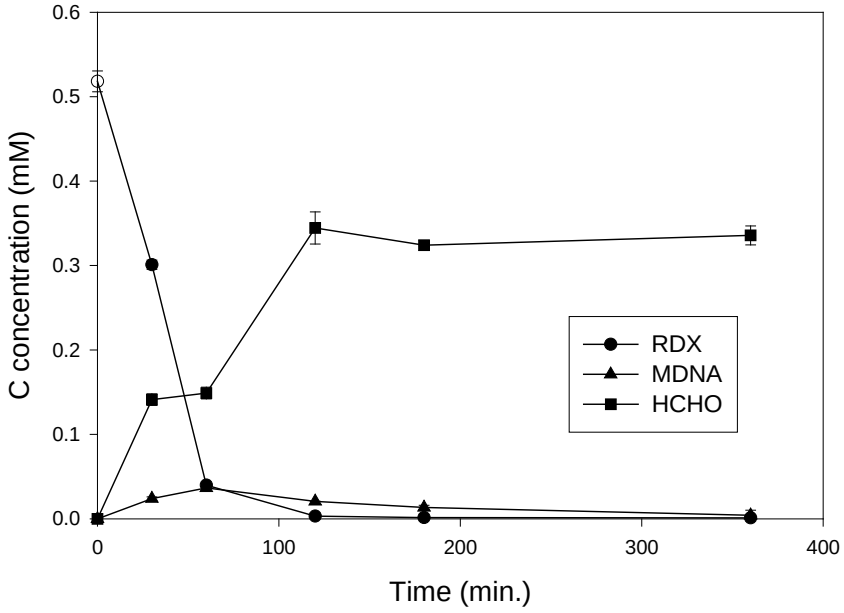

Figure 1.5 Concentrations of RDX, MDNA, and formaldehyde during RDX reduction with cast iron (0.1 g). The error bars are based on 5-mL samples from duplicate 8-mL reactors.

iron reduction experiments with formaldehyde showed that formaldehyde was inert in the iron system under the identical conditions (data not shown). This suggests that formate and methanol, known to be products of transformation of formaldehyde in biological reduction of RDX (Hawari et al., 2000), may not be formed from MDNA in RDX reduction with elemental iron.

The batch reduction experiments with a headspace method showed a similar distribution of products in the batch reactor. As RDX was reduced, MDNA and formaldehyde were produced as an intermediate and a product, respectively (Figure 1.6a). After 5 days, MDNA completely disappeared from the solution and the final C concentration of formaldehyde (0.358 mM) responsible for 69.1 % of C mass recovery. GC-MS analysis of headspace samples could not identify any possible C-containing products, indicating that no volatile carbonaceous products were produced in the iron system. Figure 1.6b shows the profiles of N-containing products during RDX reduction with cast iron in the same batch reactor. N_2O and NH_4^+ were

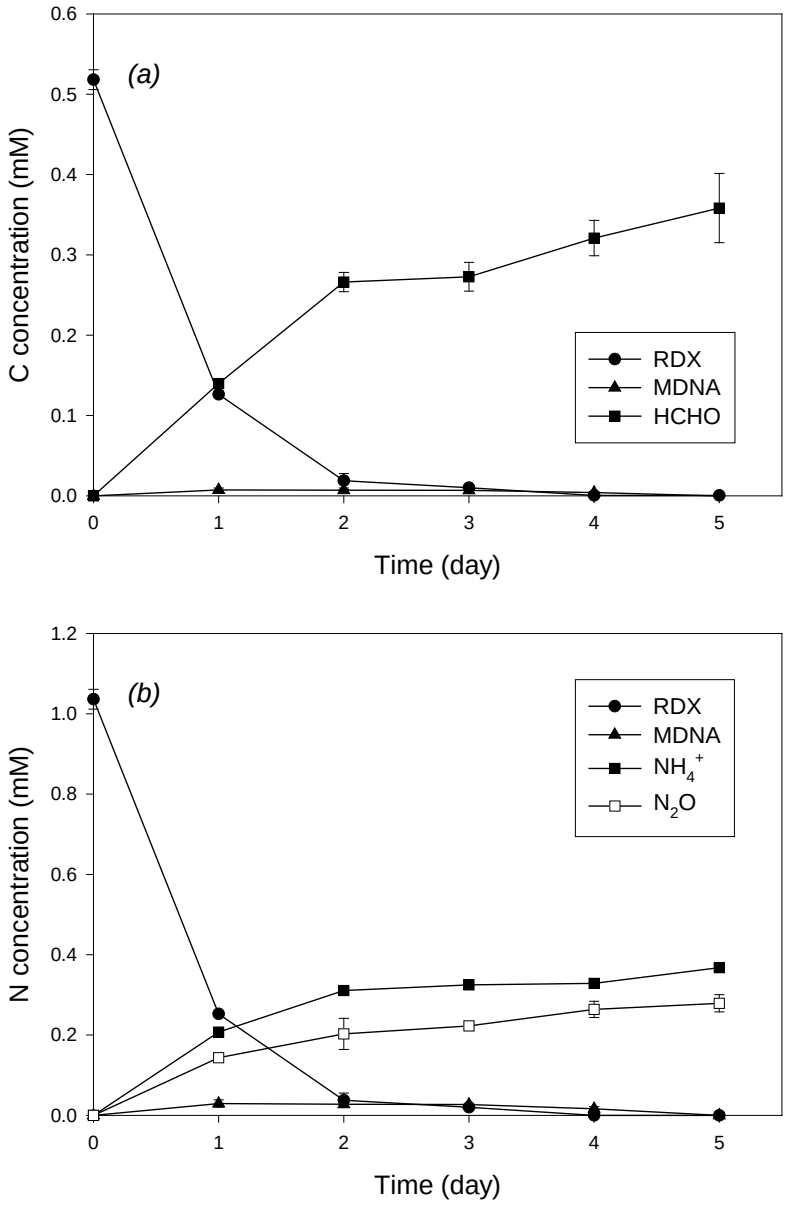

Figure 1.6 Concentrations of the (a) carbonaceous and (b) nitrogenous compounds during RDX reduction in 250-mL batch reactors containing cast iron (2 g). The error bars are based on 125-mL samples from duplicate reactors.

produced as N-containing products in the iron system. After 5 days, N concentrations of N_2O and NH_4^+ were 0.279 mM and 0.368 mM, the sum of which accounted for 62.4% of initial N concentration. GC-MS analysis of headspace samples confirmed that N_2 was not produced in the iron system. It appears that unexplained C and/or N-containing products (31-33% for C, 38% for N) might be water soluble and non-volatile.

MDNA Reduction with Cast Iron

In order to determine the transformation of MDNA during RDX reduction with cast iron, the kinetics and products in MDNA reduction with cast iron were examined through the batch reduction experiments. MDNA was gradually removed from the solution until 360 min with producing formaldehyde and NH_4^+ (Figure 1.7). Complete C mass recovery was achieved as formaldehyde after 360 min (0.094 ± 0.020 mM). The concentration of NH_4^+ at 360 min (0.129 mM) corresponded to 26.0% of initial N concentration. The pseudo-first-order rate constant for MDNA was 0.007 ± 0.001 (min^{-1}) (R^2 = 0.965), which was much less than that of RDX in the iron system (0.027 ± 0.005 (min^{-1})). This slow reduction rate of MDNA and the low concentrations of MDNA in profiles (Figures 1.5 and 1.6a) directly indicated that, besides MDNA, other intermediates existed during RDX reduction with cast iron. Control experiments without iron showed that MDNA was stable through the experiments, indicating that hydrolysis was not involved in the transformation of MDNA (data not shown). The batch experiments with a headspace method also showed complete reductive transformation of MDNA to formaldehyde with cast iron (Figure 1.8a). N_2O (0.076 mM, 25.4%) as well as NH_4^+ (0.057 mM, 19.2%) was identified as a N-containing product through a headspace method (Figure 1.8b). Interestingly, different from the yields of NH_4^+ and N_2O in RDX reduction with cast iron (Figure 1.6b), N_2O is more dominant than NH_4^+. This also suggests that, besides the reduction path of RDX $\rightarrow$ MDNA $\rightarrow$ Formaldehyde, other reduction paths producing more NH_4^+ than N_2O may be involved in RDX reduction with cast iron.

In summary, our results show that TNT molecules removed from water may persist for hours at scrap iron surface, although all adsorbed TNT was eventually reduced to TAT. The

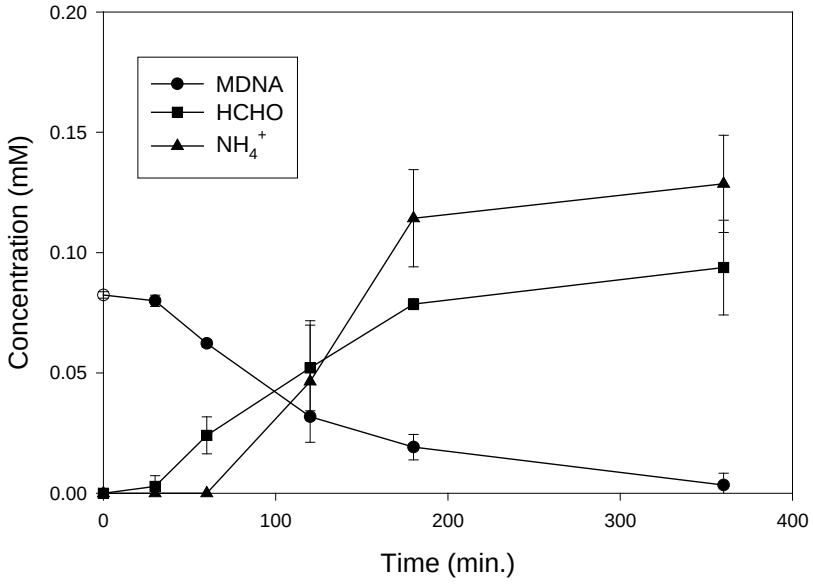

Figure 1.7 Concentrations of MDNA, formaldehyde, and NH_4^+ during MDNA reduction with cast iron (0.1 g). The error bars are based on 5-mL samples from duplicate 8-mL reactors.

ortho nitro group of TNT appeared to be preferentially reduced with scrap iron. In contrast to TNT, reduction of adsorbed RDX was faster and less affected by iron type. No TOC removal was observed during RDX reduction with scrap iron. Through batch reduction experiments using a headspace method, we identified products of RDX reduction with cast iron: MDNA, formaldehyde (69.1%), N_2O (26.9%), and NH_4^+ (35.5%). No other volatile reduction products were detected in GC-MS analysis. MDNA were further reduced to formaldehyde (100%), N_2O (25.4%), and NH_4^+ (19.2%) in the cast iron system. The rapid reduction of adsorbed TNT and RDX suggests that elemental iron may be useful for treating munitions-manufacturing wastewater if combined with a subsequent treatment process to achieve complete mineralization of these energetic compounds.

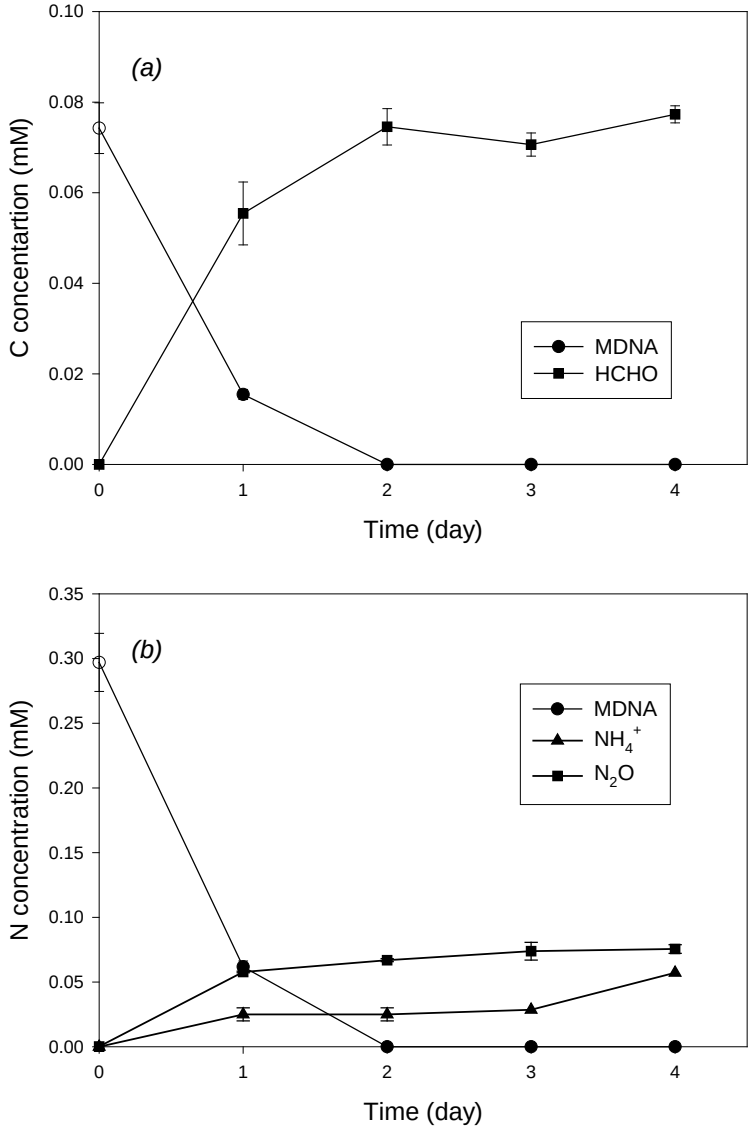

Figure 1.8 Concentrations of the (a) carbonaceous and (b) nitrogenous compounds during MDNA reduction in 250-mL batch reactors containing cast iron (2 g). The error bars are based on 125-mL samples from duplicate reactors.

1.3 Reduction of Nitroglycerin

1.3.1 Introduction

In this study, we investigated kinetics and pathway of nitroglycerin (NG) reduction with ZVI. We hypothesized that NG reduction with ZVI may enhance its biodegradability by rapid transformation of NG to easily biodegradable glycerol. We examined NG reduction with ZVI through batch reduction experiments to determine the reduction kinetics and pathway of NG in ZVI-water system.

1.3.2 Materials and Methods

Chemicals

Nitroglycerin (NG), dissolved in deionized water (497.3 ± 0.7 mg/L), was provided by Redford AAP (Redford, VA). NG standard solution in ethanol (0.1 mg/mL) was purchased from Accustandard (New Haven, CT). Standard solutions in acetonitrile (100 μg/mL each) of 1,3-dinitroglycerin (1,3-DNG), 1,2-dinitroglycerin (1,2-DNG), 1-mononitroglycerin (1-MNG) and 2-mononitroglycerin (2-MNG) were obtained from Cerilliant (Round Rock, TX). Glycerol (>99.5%) and HEPES (N-[2-hydroxyethyl]piperazine-N'-[ethanesulfonic acid]) were purchased from Sigma (St. Louis, MO). Acetonitrile (HPLC grade) was obtained from Fisher (Pittsburgh, PA).

Master Builders cast iron was used for ZVI because it has been widely used and its elemental composition has been determined (Burris et al., 1995; Allen-King et al., 1997; Burris et al., 1998). The iron was used as received without pretreatment. Specific surface areas of Master Builders iron was 1.29 m^2/g (Perey et al., 2002).

Batch Reduction Experiments

Detailed procedure on batch reduction experiments and extraction of adsorbed molecules was described in Chapter 1.2. Batch reduction experiments were conducted in an anaerobic glove box (95% N_2 + 5% H_2, Coy laboratory, Grass Lake, MI). Borosilicate vials (8 mL) were each filled with 5 mL of completely deoxygenated nitroglycerin solution containing 0.1 M HEPES buffer (pH 7.4). Initial concentration of nitroglycerin was 0.395 ± 0.023 mM.

Iron (1 g) was added in each vial, and the vials were tightly closed with Teflon-coated caps and shaken at 100 rpm in a horizontal position using an orbital shaker. At pre-determined elapsed times, replicate vials were sacrificed and 4.5 mL solutions were filtered through a 0.22 μm mixed cellulose filter (Millipore, MA) for analysis of the aqueous samples. Molecules adsorbed to iron surface were extracted once using 2 mL acetonitrile and analyzed for surface masses. Additional extractions with acetonitrile did not recover additional mass.

Chemical Analysis

Nitroglycerin was analyzed using a Varian HPLC (Walnut Creek, CA) equipped with a Supelguard guard column (20×4.6 mm, Supelco, Bellefonte, PA), a SUPELCO LC-18 column (250×4.6 mm, 5 μm, Supelco, Bellefonte, PA), a UV detector (Varian 2510, Walnut Creek, CA) and an isocratic pump (Varian 2550, Walnut Creek, CA). Methanol-water mixture (70/30, v/v) was used as the mobile phase at a flow rate of 1.0 mL/min. 1,3-DNG, 1,2-DNG, 1-MNG, and 2-MNG were analyzed by the HPLC with an Alltima C18 column (250×4.6 mm, 5 μm, Alltech, Deerfield, IL) and an Alltima guard column (7.5×4.6 mm, Alltech). Fifty/fifty and 10/90 (v/v) methanol-water mixtures were used as an eluent at 1.0 mL/min for dinitroglycerin and mononitroglycerin isomers, respectively. The wavelength for the UV detector was set at 214 nm. The injection volume for all samples was 10 μL.

Glycerol was analyzed by a gas chromatograph (5890 Hewlett Packard, Palo Alto, CA) equipped with an Ultra-2 capillary column (25 m length, 0.2 mm i.d., 0.33 μm film thickness, J&W, Wilmington, DE) and a frame ionization detector (FID). Pretreatment was conducted to remove water from samples. Aqueous samples (1 mL) were completely dried in a vacuum oven (model 5821, Napco, Winchester, VA) at approximately 40 ºC for 15 hours and 0.1 mL of acetone was added to each 5-mL vial. A calibration curve was made following the same evaporation procedure with standard solutions of glycerol in water. The calibration curve was obtained from 5 level duplicate standard solutions. Quadratic fit ($r^2 = 0.995$) was used to construct the calibration curve due to increasing recovery with increasing concentration (from 55% at 5 mg/L to 80% at 100 mg/L). Detection limit of this procedure was approximately 3 mg/L.

NO_2^- and NO_3^- were analyzed using a Varian HPLC with a UV detector and an OmniPac Pax-100 column (Dionex, Sunnyvale, CA). Na_2CO_3 (1.8 mM) and $NaHCO_3$ (1.7 mM) solution was used as an eluent at 1.0 mL/min. The injection volume was 10 μL and the wavelength for the UV detector was 214 nm. NH_4^+ was analyzed with an UV-vis spectrophotometer (DR2010, HACH, Loveland, CO) using the salicylate method (Hach Co., 1998). pH was measured using a pH-30 pH sensor (Corning, Big Flats, NY).

Data Analysis

We assumed that the NG and its products were removed or formed in a pseudo-first-order manner with respect to the parent compounds in a ZVI-water system. By using rate laws, a kinetic model was determined by sets of ordinary differential equations representing the stepwise pseudo-first-order reactions in NG reduction to glycerol. The pseudo-first-order rate constants were estimated from two replicate raw data sets using the kinetic modeling software package, Scientist (MicroMath, Salt Lake City, UT). The ordinary differential equations were solved by numerical integration using EPISODE, an ordinary differential equation solver provided by the Scientist.

1.3.3 Results and Discussion

Reduction Pathway of Nitroglycerin

The masses of NG, 1,2- and 1,3-DNG, 1- and 2-MNG, and glycerol during NG reduction with cast iron are shown in Figure 1.9. Each mass is the sum of aqueous and surface masses and thus the mass changes represent transformation rather than sorption. Despite the significant carbon content of Master Builders iron (2 - 4 wt% (Burris et al., 1995; Allen-King et al., 1997; Burris et al., 1998)), adsorption of NG and its reduction products was minimal. This is presumably due to their high water solubility: 1.5, 80, and 700 g/L for NG, 1,2- and 1,3-DNG, and 1- and 2-MNG, respectively (Spain et al., 2000). The adsorbed mass of NG and its daughter products was consistently below 0.05 μmol (2.5% of the total mass) throughout the experiment. This is in contrast to nitroaromatic compounds which adsorb to cast iron to a much greater extent (Oh et al., 2002a; Oh et al., 2002b). As NG was transformed, 1,2- and 1,3-DNG were produced

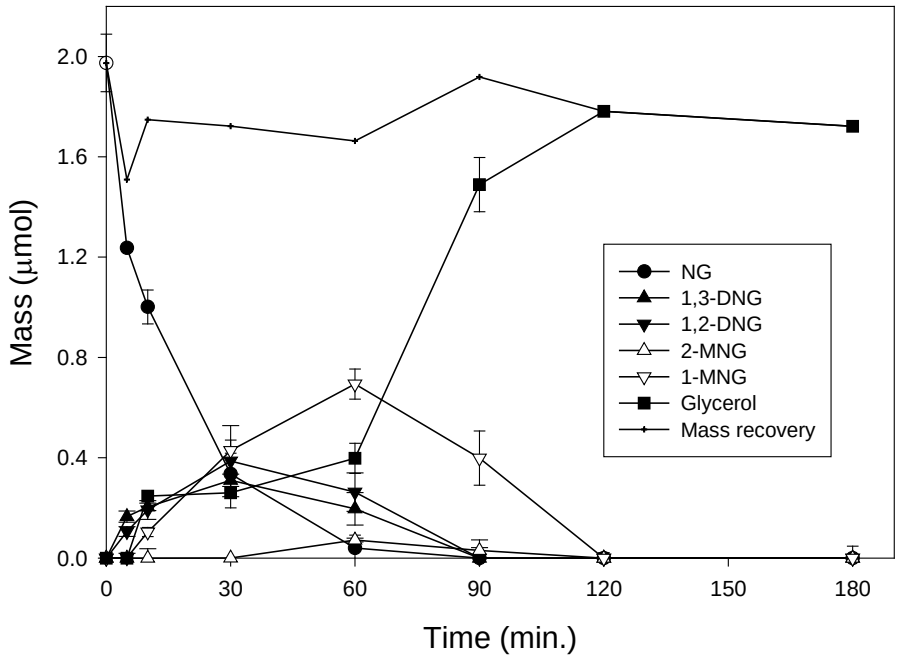

Figure 1.9 Masses of the carbonaceous compounds during NG reduction in batch reactors containing cast iron. The error bars are based on samples from duplicate reactors (Oh et al., 2004a).

concurrently. This was followed shortly by the appearance of 1- and 2-MNG, with 1-MNG being the dominant isomer (up to 0.70 μmol, or 10 times the 2-MNG concentration, at 60 min). NG and the intermediates were transformed completely within 2 h, and the amount of glycerol recovered at 2 h was 1.78 μmol, or 90.2% of the initial of NG. The carbon balance during the reaction was 77.4% – 97.2%. The incomplete recovery was most likely due to errors associated with glycerol analysis, particularly at low concentrations.

In addition to the nitrate esters, we also measured NH_4^+, NO_2^-, and NO_3^- in the aqueous phase to establish a nitrogen balance. As shown in Figure 1.10, NO_2^- was released as NG was reduced to DNGs and MNGs, suggesting that reduction of the nitrate function (+V) of NG to NO_2^- (+III) was the first step in NG reduction with cast iron. It is also possible, albeit not probable in a buffered solution, that NG was transformed through hydrolysis to form NO_3^- (+V),

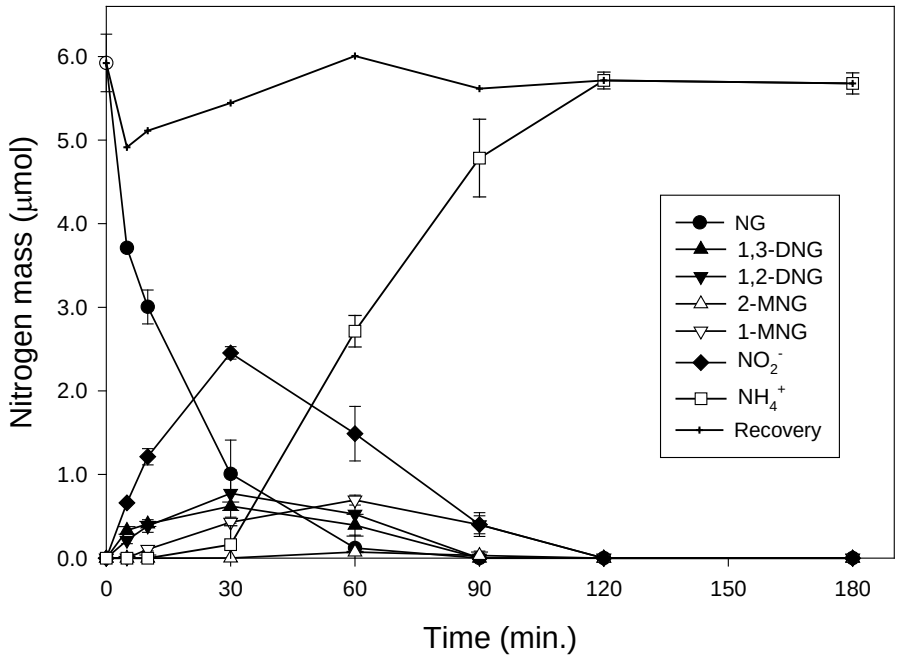

Figure 1.10 Masses of the nitrogenous compounds during NG reduction in batch reactors containing cast iron. The error bars are based on samples from duplicate reactors (Oh et al., 2004a).

which was subsequently reduced to NO_2^- by cast iron. However, NO_3^- was never detected during our experiments. Our control experiments further showed that NG was stable at pH 7.4 without iron, and that NO_3^- was reduced only very slowly in the ZVI-water system under identical conditions (data not shown). Therefore, it appears that NO_2^- rather than NO_3^- was a product of NG transformation with cast iron, and that the reaction was reductive rather than hydrolytic. The reaction of NG with iron is thus similar to its reductive transformation in some biological systems (Christodoulatos et al., 1997). The amount of NO_2^- started to decrease after 30 min as NO_2^- was further reduced to NH_4^+. After 2 h, 96.5% of the initial nitrogen was recovered as NH_4^+, indicating that the NO_2^- produced was completely converted to NH_4^+ as the dominant nitrogen-bearing end product of NG. The nitrogen recovery during the experiment ranged from 83.0% to 101.4%.

From the data in Figures 1.9 and 1.10, it appears that NG was reductively denitrated step-wise to glycerol with concomitant release of NO_2^-, which was further reduced quantitatively to NH_4^+. Based on this result, a pathway for NG reduction with cast iron was proposed (Figure 1.11). In an iron-water system, NG may be reduced to glycerol following one of the three reduction paths: 1) NG —> 1,3-DNG —> 1-MNG —> glycerol, 2) NG —> 1,2-DNG —> 1-MNG —> glycerol, and 3) NG —> 1,2-DNG —> 2-MNG —> glycerol. All the compounds in the pathway were detected in our batch experiments. Each step involves transfer of two electrons and release of a NO_2^- ion (eqs. 1.9-1.11), which was further reduced to NH_4^+ (eq. 1.12). The complete reduction of 1 mole of NG to glycerol and ammonium ion requires 24 moles of electrons (eq. 1.13).

$$C_3H_5(ONO_2)_3 + 2e^- + H_2O \text{ —> } C_3H_5(ONO_2)_2(OH) + NO_2^- + OH^- \quad (1.9)$$

$$C_3H_5(ONO_2)_2(OH) + 2e^- + H_2O \text{ —> } C_3H_5(ONO_2)(OH)_2 + NO_2^- + OH^- \quad (1.10)$$

$$C_3H_5(ONO_2)(OH)_2 + 2e^- + H_2O \text{ —> } C_3H_5(OH)_3 + NO_2^- + OH^- \quad (1.11)$$

$$NO_2^- + 6e^- + 6H_2O \text{ —> } NH_4^+ + 8OH^- \quad (1.12)$$

$$C_3H_5(ONO_2)_3 + 24e^- + 21H_2O \text{ —> } C_3H_5(OH)_3 + 3NH_4^+ + 27OH^- \quad (1.13)$$

Reduction Kinetics of Nitroglycerin

Based on the proposed NG reduction pathway and assuming that each step in the pathway is a pseudo-first-order process, the reactions can be described by a kinetic model consisting of a series of differential equations (i.e., rate laws), which can be solved to obtain a rate constant for each reaction step. Table 1.1 summarizes the rate law and the reactions involved in the formation and transformation of each of the eight compounds shown in Figure 1.11. The pseudo-first-order rate constants for the eight reactions in the pathway, obtained though least-square fitting, are shown in Table 1.2, along with the corresponding surface area-normalized rate constants. The kinetic model fits the data rather well, as indicated by the R^2 values in Table 1.1 and the fitted curves of NG and its daughter products in Figure 1.12. The overall correlation coefficient for the model fit is 0.975. The error associated with the curve fit

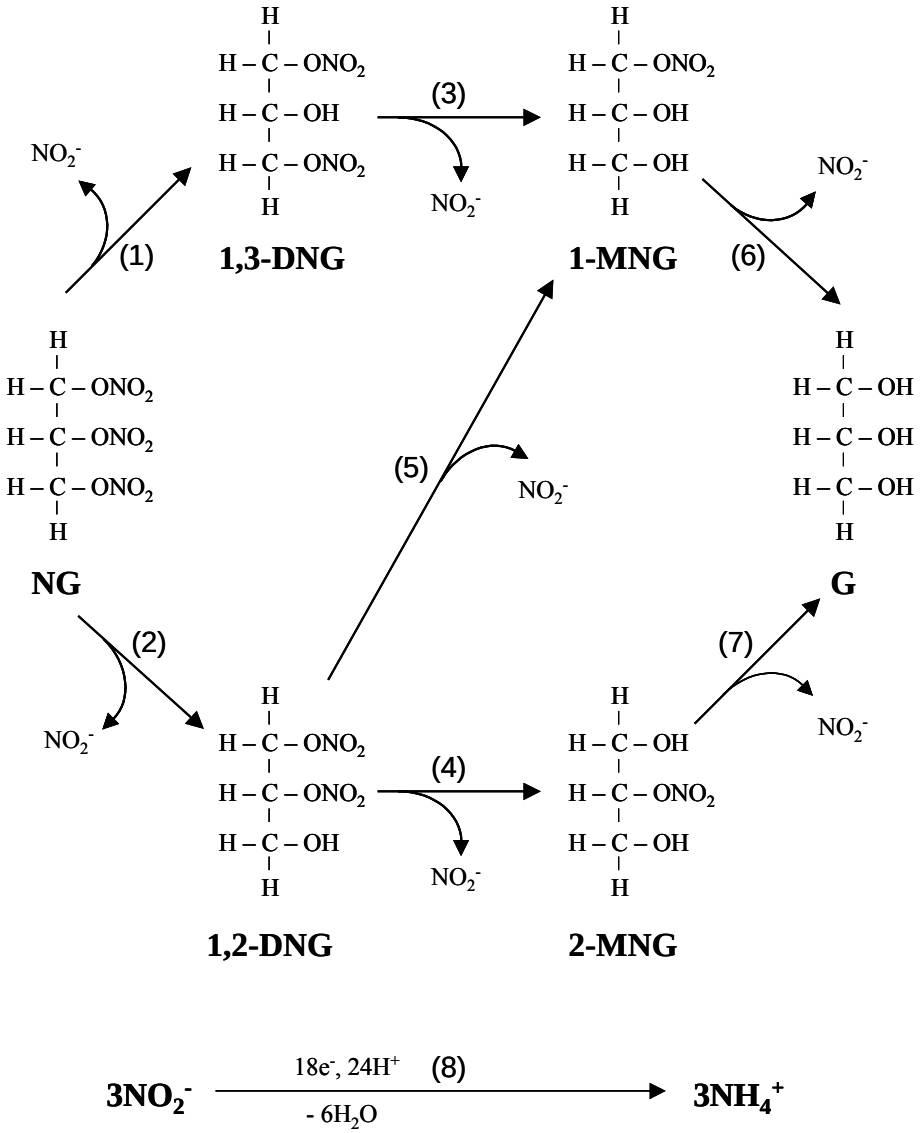

Figure 1.11 Proposed pathway of NG reduction with cast iron (Oh et al., 2004a).

Table 1.1 Reactions and rate laws for NG and its reduction products in the proposed pathway (Figure 1.11). The correlation coefficient for each compound is also shown (Oh et al., 2004a).

Compound	Reaction(s) involved	Rate law	Correlation coefficient
NG	(1), (2)	$-d\{NG\}/dt = k_1\{NG\} + k_2\{NG\}$	$R^2_{NG} = 0.992$
1,3-DNG	(1), (3)	$-d\{1,3\text{-DNG}\}/dt = k_3\{1,3\text{-DNG}\} - k_1\{NG\}$	$R^2_{1,3\text{-DNG}} = 0.905$
1,2-DNG	(2), (4), (5)	$-d\{1,2\text{-DNG}\}/dt = k_4\{1,3\text{-DNG}\} + k_5\{1,3\text{-DNG}\} - k_2\{NG\}$	$R^2_{1,2\text{-DNG}} = 0.860$
1-MNG	(3), (5), (6)	$-d\{1\text{-MNG}\}/dt = k_6\{1\text{-MNG}\} - k_3\{1,3\text{-DNG}\} - k_5\{1,2\text{-DNG}\}$	$R^2_{1\text{-MNG}} = 0.921$
2-MNG	(4), (7)	$-d\{2\text{-MNG}\}/dt = k_7\{2\text{-MNG}\} - k_4\{1,2\text{-DNG}\}$	$R^2_{2\text{-MNG}} = 0.699$
Glycerol (G)	(6), (7)	$d\{G\}/dt = k_6\{1\text{-MNG}\} + k_7\{2\text{-MNG}\}$	$R^2_{G} = 0.956$
NO_2^-	(1), (2), (3), (4), (5), (6), (7), (8)	$-d\{NO_2^-\}/dt = 1/3\ k_1\{NG\text{-}N\} + 1/3\ k_2\{NG\text{-}N\} + 1/2\ k_3\{1,3\text{-DNG-}N\} + 1/2\ k_4\{1,2\text{-DNG-}N\} + 1/2\ k_5\{1,2\text{-DNG-}N\} + k_6\{1\text{-MNG-}N\} + k_7\{2\text{-MNG-}N\} - k_8\{NO_2^-\}$	$R^2_{NO2-} = 0.923$
NH_4^+	(8)	$d\{NH_4^+\}/dt = k_8\{NO_2^-\}$	$R^2_{NH4+} = 0.983$

Table 1.2 Fitted pseudo-first-order rate constants [hr^{-1}] for the reactions shown in Figure 1.11. The corresponding surface area-normalized rate constants [$L \cdot m^{-2} \cdot hr^{-1}$] were calculated based on the BET surface area concentration of 258 [m^2/L]. The errors are two standard deviations obtained from the model fit (Oh et al., 2004a).

Reaction	Fitted pseudo-first-order rate constant [hr^{-1}]	Area-normalized rate constant [$L \cdot m^{-2} \cdot hr^{-1}$]
(1) NG —> 1,3-DNG	2.238 ± 0.390	$(0.87 \pm 0.15) \times 10^{-2}$
(2) NG —> 1,2-DNG	2.022 ± 0.378	$(0.78 \pm 0.15) \times 10^{-2}$
(3) 1,3-DNG —> 1-MNG	4.074 ± 1.110	$(1.58 \pm 0.43) \times 10^{-2}$
(4) 1,2-DNG —> 2-MNG	0.546 ± 0.246	$(0.21 \pm 0.10) \times 10^{-2}$
(5) 1,2-DNG —> 1-MNG	2.074 ± 0.852	$(0.80 \pm 0.33) \times 10^{-2}$
(6) 1-MNG —> Glycerol	2.381 ± 0.292	$(0.92 \pm 0.11) \times 10^{-2}$
(7) 2-MNG —> Glycerol	0.752 ± 0.363	$(0.29 \pm 0.14) \times 10^{-2}$
(8) NO_2^- —> NH_4^+	2.014 ± 0.239	$(0.78 \pm 0.09) \times 10^{-2}$

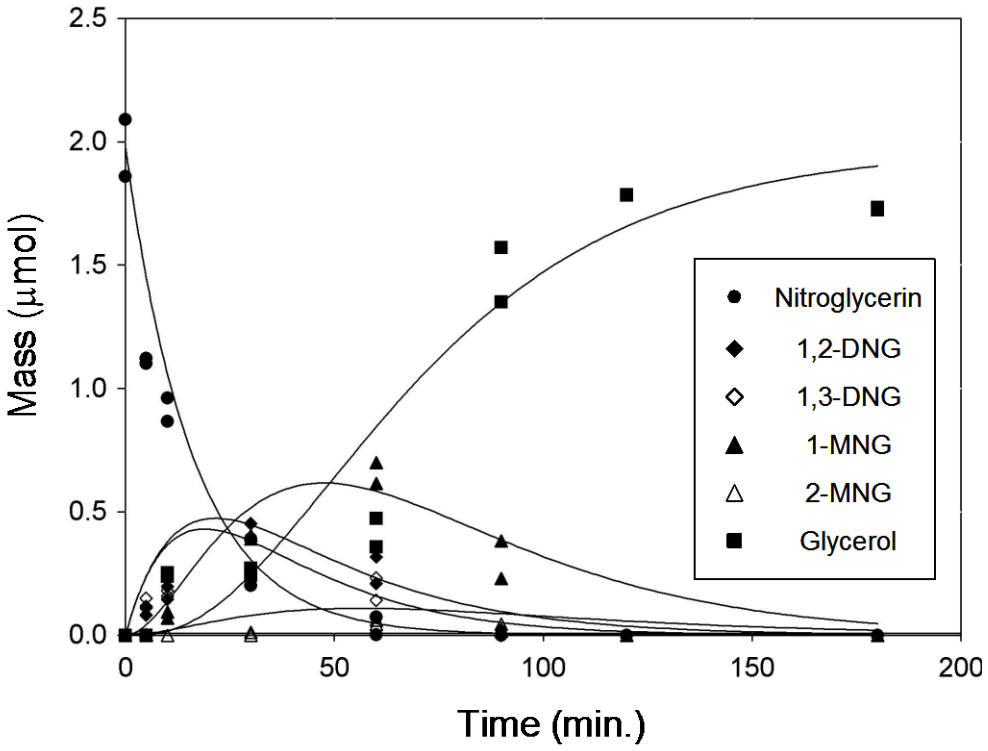

Figure 1.12 Measured masses of and fitted curves for the carbonaceous compounds during NG reduction with cast iron in batch reactors (Oh et al., 2004a).

for 2-MNG was greater than that for the other compounds due to the low concentrations of 2-MNG.

Using the fitted values of k_1 to k_7, we also estimated the pseudo-first-order rate constant for NO_2^- reduction to NH_4^+ ($k_8 = 2.014 \pm 0.239$ hr^{-1}, Table 1.2). The surface area-normalized rate constant ($7.8 \pm 0.9 \times 10^{-3}$ $L \cdot m^{-2} \cdot hr^{-1}$) obtained from modeling is comparable to the measured rate constants for NO_2^- reduction with Fisher, Connelly, and Peerless irons at pH 7.0 (8.8×10^{-3} to 9.1×10^{-3} $L \cdot m^{-2} \cdot hr^{-1}$ (Alowitz and Scherer, 2002). The model curves for NO_2^- and NH_4^+ using the estimated k_8 value fit the experimental data well, as shown in Figure 1.13.

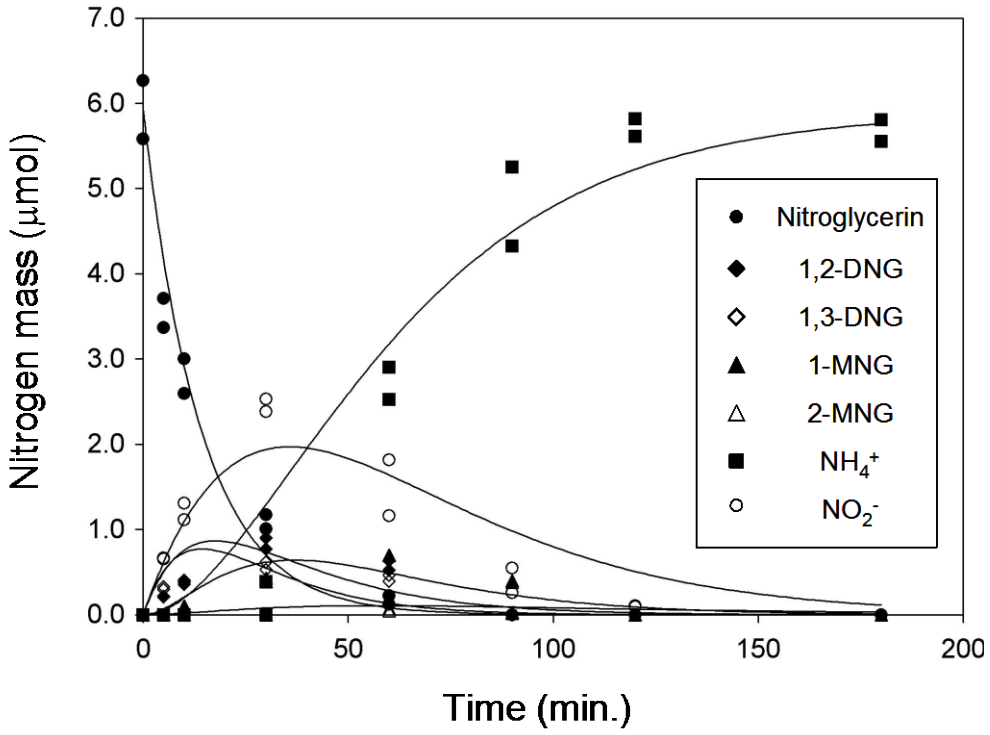

Figure 1.13 Measured masses of and fitted curves for the nitrogenous compounds during NG reduction with cast iron in batch reactors (Oh et al., 2004a).

Although the fitted pseudo-first-order rate constants describe the profiles of NG and its daughter products satisfactorily, it is not clear to what physical or chemical process these rate constants correspond. The possible rate-limiting processes may include external mass transfer from the bulk solution to the iron particle surface, intra-particle diffusion, adsorption to a reactive site, and reduction of the adsorbed molecule. While there is insufficient information to ascertain the rate-limiting step, it is possible to independently estimate the external mass transfer coefficient in batch reactors using the method employed by Arnold et al. (1999) (Jafarpour et al., 2003). Using an assumed iron particle diameter of 1 mm and an estimated molecular diffusivity for NG of 6 x 10^{-6} cm^2/s, the external mass transfer coefficient for the reaction vials was calculated to be 540 hr^{-1}. This value is more than 2 orders of magnitude larger than all the fitted

pseudo-first-order rate constants in Table 1.2, suggesting that external mass transfer was not the rate-limiting step for NG reduction in our batch system. Therefore, the fitted pseudo-first-order rate constants may correspond to diffusion within iron particles, adsorption, or surface reaction. Which of these processes controls the overall rate of NG reduction remains to be elucidated.

The fitted pseudo-first-order rate constant for 1,3-DNG production ($k_1 = 2.238 \pm 0.390\ hr^{-1}$) is similar to that for 1,2-DNG formation ($k_2 = 2.022 \pm 0.378\ hr^{-1}$). Since NG contains two identical terminal nitrate groups, the result suggests that the nitrate group at the 2-position is about two times as likely to be reduced as each terminal nitrate group. This regio-selectivity, which can not be explained by physical processes such as intra-particle diffusion, suggests that the rate-limiting step for NG reduction is probably a chemical process, such as adsorption or redox reaction. One possible explanation for this selectivity is that the nitrate group at the 2-position of NG is more susceptible to reduction than the terminal nitrate groups. Consistent with this explanation, 1,2-DNG was reduced faster to 1-DNG ($k_5 = 2.074 \pm 0.852\ hr^{-1}$) than to 2-DNG ($k_4 = 0.546 \pm 0.246\ hr^{-1}$), again indicating the central nitrate group is more likely to be reduced by cast iron. This regio-selectivity might be related to the electron-deficient (and thus electron-withdrawing) nature of the carbon atom at the 2-position relative to the terminal carbon atoms.

In summary, our results demonstrate that cast iron can rapidly reduce NG to relatively benign end products, glycerol and NH_4^+, and thus represents a promising new approach to treat NG-laden wastewaters. Cast iron may be used, for example, as a reactive component in a packed column to treat ammunition wastewater, as has been suggested for the treatment of wastewater containing other energetic compounds (Oh et al., 2003a; Oh et al., 2003b). Further study will be needed to make sure the complete reduction of NG with iron in a continuous flow system.

Section 2
Enhanced Fenton Oxidation of Energetic Compounds with ZVI

2.1 Introduction

Pink water is wastewater generated from loading, assembling, packing, and demilitarization activities in Army ammunition plants. In 1998, 77 million pounds of pink water were generated from munitions-manufacturing plants in the U.S. (Adrian and Campbell, 1999). Pink water contains nitro constituents such as 2,4,6-trinitrotoluene (TNT), hexahydro-1,3,5-trinitro-1,3,5-triazine (RDX), octahydro-1,3,5,7-tetranitro-1,3,5,7-tetrazocine (HMX), 2,4-dinitrotoluene (DNT), trinitrobenzene (TNB), and dinitrobenzene (DNB). Composition of pink water varies widely depending on munitions manufacturing processes and demilitarization facilities (Concurrent Technologies Corporation, 1995). However, among those toxic compounds, TNT and RDX are known to be the major constituents in pink water (Spain et al., 2000). Concentrations of TNT and RDX in pink water were reported to be around 112 and 76 mg/L, respectively (Concurrent Technologies Corporation, 1995). Due to the toxicity and possible carcinogenicity of TNT and RDX (Won et al., 1976; Kaplan and Kaplan, 1982; Yinon, 1990), these explosive compounds are removed from wastewater before its discharge to environment.

Conventional biological wastewater treatment processes (e.g., activated sludge) are not effective in treating pink water because the electron withdrawing nitro constituents in these explosives inhibit the electrophilic attack by enzymes (Bruhn et al., 1987; Knackmuss, 1996). Chemical oxidation methods (e.g., advanced oxidation processes) are also ineffective because of the hindrance to oxidation by the nitro functions (Schmelling et al., 1996). Consequently, adsorption to granular activated carbon (GAC) has been the method of choice for pink water treatment (Concurrent Technologies Corporation, 1995). Use of GAC may need to be combined with additional treatment processes, such as alkaline hydrolysis or incineration, in order to chemically degrade adsorbed energetic compounds (Heilmann et al., 1996; Hwang et al., 1998).

In efforts to develop a cost-effective pink water treatment system, studies have examined biological or chemical processes to transform the nitro groups in explosives to overcome the hindrance to oxidation. Studies showed that TNT could be biologically transformed to triaminotoluene (TAT) through intermediates (e.g., aminonitrotoluenes and hydroxyaminotoluenes) by pure and mixed cultures under anaerobic conditions (Preuss et al., 1993; Lewis et al., 1996; Hawari et al., 1998; Hwang et al., 2000). In theses studies, it was found that TAT was unstable and could be transformed to phenolic products depending on pH. Hawari and coworkers (2000) proposed that the triazine ring of RDX was cleaved through enzymatic hydrolysis to form methylenedinitramine (MDNA) and bis(hydroxymethyl)nitramine in anaerobic sludge. These compounds were further degraded abiotically to formaldehyde, methanol, nitrous oxide (N_2O), and water (Hawari et al., 2000; Halasz et al, 2002).

Two-stage anaerobic-aerobic biotransformation process was also studied for the treatment of TNT and 2,4-dinitrotoluene (DNT) containing wastewater (Berchtold et al., 1995; VanderLoop et al., 1998). VanderLoop et al. (1998) observed that reduction products of TNT and DNT from an anaerobic fluidized-bed granular activated carbon bioreactor were readily oxidized in a subsequent activated sludge process. Similarly, RDX was easily degraded as a nitrogen source using a two-stage anaerobic-aerobic system in the sequencing batch reactor (Brenner et al., 2000).

DNT and TNT were also shown to be electrochemically reduced to 2,4-diaminotoluene (DAT) and TAT, respectively (Jolas et al, 2000; Rodgers and Bunce, 2001). Rodgers and Bunce (2001) observed that electrochemical reduction products of DNT and TNT (e.g., DAT, 2,6-diamino-4-nitrotoluene) were removed more easily by oxidation with horseradish peroxidase and H_2O_2 than DNT and TNT. They also suggested sequential electrochemical reduction-oxidation process for treatment of DNT and TNT in munitions waste.

ZVI has been used for permeable reactive barrier (PRB) to remediate groundwater contaminated with chlorinated solvents and heavy metals (Orth and Gillham, 1996; Roberts et al., 1996; Blowes et al., 1997; Tratnyek et al., 1997; Gu et al., 1998, Puls et al., 1999; Deng, 1999; U.S. EPA, 1999; Phillip et al., 2000). It has also been shown that TNT and RDX can be rapidly reduced with ZVI (Devlin et al., 1998; Singh et al., 1998). In addition, several

researchers used elemental iron reduction process for the pretreatment of wastewater containing nitro aromatics and azo dyes (Mantha et al., 2001; Perey et al., 2002). Pretreatment with ZVI was suggested since the iron can reductively transform electron withdrawing constituents and make recalcitrant compounds more amenable for subsequent oxidation process. Perey et al. (2002) demonstrated that the recalcitrant azo dyes could be aerobically biodegraded in an activated sludge system after iron pretreatment.

In this study, we determined whether and how effectively a ZVI treatment process enhances the extent and rate of subsequent oxidation of energetic compounds with Fenton's reagent. We determined the optimal condition and the enhancement of mineralization of energetic compounds in subsequent Fenton oxidation. In addition, we evaluated an integrated ZVI treatment-Fenton oxidation process and proved the integrated system was effective treating explosive-containing process water and pink water.

2.2 Integrated ZVI-Fenton System for Mineralization of TNT an RDX

2.2.1 Introduction

We evaluated Fenton oxidation as a subsequent oxidation process following the ZVI pretreatment. Fenton oxidation is the most common advanced oxidation process for the treatment of organic contaminants because of its simplicity and non-selectivity (Huang et al., 1993). Previous research showed that a large amount of H_2O_2 (a range of 0.1%) was required to remove TNT and RDX from explosive-contaminated water in a batch reactor using Fenton oxidation and that TNT and RDX were not completely mineralized in short period of time (Li et al., 1997; Bier et al., 1999).

Since the reductive transformation of nitro function to amino group would lower Gibbs free energy of the compound (e.g., ΔG = -243.1 kJ/mol in reduction of nitrobenzene to aniline) (Schwarzenbach et al., 1993), we hypothesized that reduction with zero-valent iron will make refractory explosives thermodynamically more favorable for oxidation and, thus enhance the extent and rate of mineralization in Fenton oxidation. In this section, we examined the effect of ZVI pretreatment on the mineralization of TNT and RDX by Fenton oxidation. TNT and RDX solutions were initially reduced with ZVI and subsequently oxidized in a laboratory-scale continuously stirred tank reactor (CSTR). Total organic carbon (TOC) concentration in the reactor effluent was used to determine the extent and rate of mineralization in the CSTR.

2.2.2 Materials and Methods

Chemicals

TNT (>99%) and RDX (>99%) were provided by the Holston Army Ammunition Plant (Kingsport, TN). $FeSO_4 \cdot 7H_2O$ (>99%) was purchased from Sigma (St. Louis, MO) and H_2O_2 (30%) was obtained from Fisher Scientific (Pittsburgh, PA). Scrap iron used in this study was obtained from Master Builders, Inc. (Aurora, OH). Specific surface areas of Master Builders iron was 1.29 m^2/g (Perey et al., 2002). The iron was used as received without pretreatment.

ZVI-treated TNT and RDX

ZVI-treated TNT and RDX solutions were prepared by passing solutions of TNT (0.24 mM or 20 mg/L TOC) and RDX (0.25 mM or 9.0 mg/L TOC) through a glass column (2.5 cm i.d. × 30 cm L, Ace Glass, Vineland, NJ) packed with Master Builder's iron (porosity = 0.66). TNT and RDX solutions were prepared with deionized water, purged with N_2 for at least 20 minutes, and then pumped into the column using a peristaltic pump in an upward direction at a flow rate of 10 mL/min. This gave a retention time in the column of approximately 9.7 minutes. HPLC analysis of the column effluents indicated that TNT and RDX were completely transformed. TNT was fully reduced to TAT and no aminonitrotoluene intermediates were detected. The steady-state concentration of ferrous ion in the effluent was below 0.1 mg/L. The column effluents were passed through a 0.22-μm cellulose membrane filter (Millipore, Bedford, MA) to remove particles. The filtered solution was collected in a 2.5-L glass bottle and used for the Fenton oxidation experiments within three days.

Fenton Oxidation in a CSTR

Fenton oxidation experiments were conducted using an acrylic, cylindrical CSTR (8.8 cm dia. × 3.5 cm effective height). Solutions of $FeSO_4 \cdot 7H_2O$ and H_2O_2, and the test solution containing TNT, RDX, or their reduction products were pumped into a CSTR using peristaltic pumps (Cole-Parmer, Vernon Hills, IL). The test solution and Fenton's reagent were mixed in the CSTR using a magnetic stirrer (950 ± 50 rpm, as measured using a tachometer). The flow rate of Fe^{2+} and H_2O_2 solutions were 0.04 mL/min and that of the test solution were 3.5 mL/min. The pH of the reaction mixture was controlled at 3.0 ± 0.1 using an automatic pH controller (Cole-Parmer, Vernon Hills, IL) with 0.1-N NaOH solution. After more than three HRTs, CSTR effluent was collected and filtered with a glass fiber filter (1.5-mm, Whatman, Clifton, NJ) prior to TOC, nitrate, and ammonia analyses. Preliminary result with 2 mM H_2O_2 and 2 mM Fe^{2+} showed that increasing hydraulic retention time (HRT) from 40 min to 2 hours did not result in meaningful increase in TOC removal for TNT (from 29.0 ± 3.0% to 31.6 ± 5.0%) and iron-treated TNT (from 51.8 ± 1.0% to 52.3 ± 0.5%). Therefore, an HRT of 1 hour was used for all CSTR experiments.

The effect of H_2O_2-to-Fe^{2+} ratio was examined by increasing the influent H_2O_2 concentration while keeping the Fe^{2+} dosing rate constant. The optimal H_2O_2-to-Fe^{2+} ratio was taken to be the ratio corresponding to the highest TOC removal. TOC removal for the iron-treated products was compared to control experiments with untreated TNT and RDX performed under identical conditions. Assuming TOC removal by Fenton oxidation is pseudo-first-order, the rate constant for TOC removal in the CSTR can be calculated using eq. 2.1.

$$k_{obs} = \frac{(C_{in} - C_{eff})}{C_{eff} \cdot \tau} \tag{2.1}$$

where k_{obs} is the pseudo-first-order rate constant for TOC removal (hr^{-1}), C_{in} is the TOC in the influent test solution (mg/L), C_{eff} is the TOC in the effluent (mg/L) and τ is the HRT in the CSTR (1 h). Where C_{eff} was below the detection limit of 0.2 mg/L for the TOC analyzer (Rosemount Analytical Inc., 1994), C_{eff} was taken to be 0.2 mg/L to obtain a low estimate of k_{obs}.

Degradation in a Bench-Scale Integrated System

A bench-scale integrated system (shown in Figure 2.1 schematic drawing) was constructed to further evaluate the feasibility of the proposed process to mineralize TNT and RDX. The integrated system was constructed by connecting the iron column and the CSTR described previously with silicone tubing and a glass fiber filter. The same column described above was used. Deoxygenated TNT or RDX solution was pumped into the iron column at a flow rate of 3.5 mL/min. Initial concentrations of TNT and RDX solutions were 0.196 ± 0.008 mM (16.0 ± 1.2 mg/L TOC) and 0.180 ± 0.006 mM (6.5 ± 0.2 mg/L TOC), respectively. TNT and RDX solutions were passed individually through the column on a continuous basis for over two weeks to ensure steady-state conditions. The concentrations of H_2O_2 and Fe^{2+} and the mole ratio were chosen based on results of previous CSTR experiments. The concentrations of TNT and RDX, TOC, NH_4^+, and NO_3^- in the influent, iron column effluent, and CSTR effluent were monitored over time and recorded when the concentrations became constant.

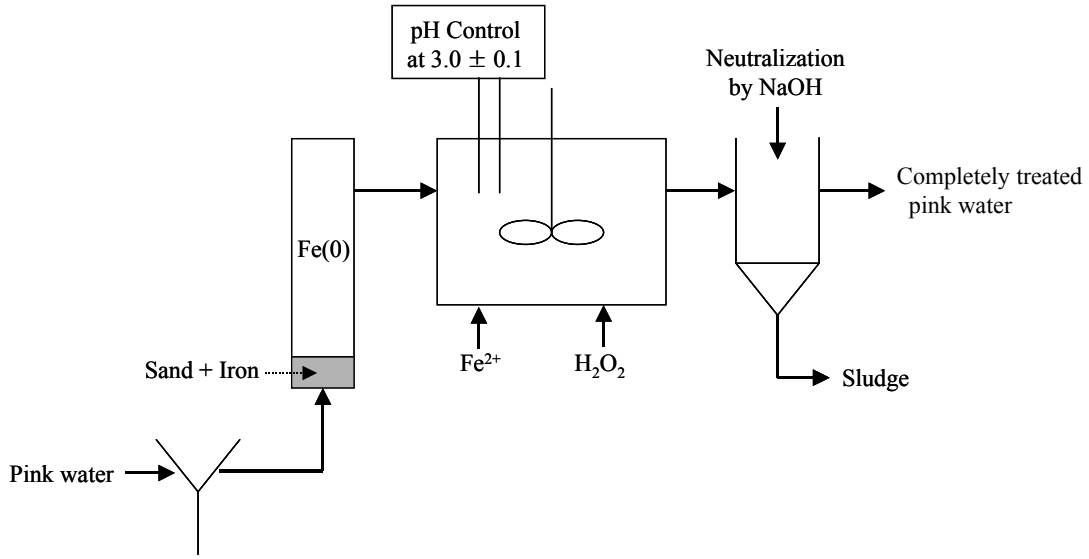

Figure 2.1 A proposed ZVI column-Fenton oxidation integrated system for pink water treatment (Oh et al., 2003a).

2.2.3 Results and Discussion

TOC Removal by Fenton Oxidation of TNT and ZVI -Treated TNT

The effect of H_2O_2-to-Fe^{2+} mole ratio on TOC removal during Fenton oxidation of TNT and ZVI-treated TNT is shown in Figure 2.2. The error bars in all figures indicate the standard deviation, which was calculated by data from analyses of replicates. Using 2 mM Fe^{2+} and an H_2O_2-to-Fe^{2+} ratio of 1 to 20, the extent of TOC removal for iron-treated TNT solution was 20-30 % higher than that for untreated TNT solution, which supports our hypothesis that reduction of the nitro functions of TNT enhances the extent of organic carbon oxidation by Fenton reagent. As shown in Figure 2.2(a), the optimal H_2O_2-to-Fe^{2+} ratio for TOC removal was 10 for TNT and 5 for ZVI-treated TNT, although the differences in TOC removal between the two mole ratios were small. If we assume that TOC removal during Fenton oxidation in the CSTR was pseudo-first-order, then a TOC removal rate constant (k_{obs}) for each H_2O_2-to-Fe^{2+}

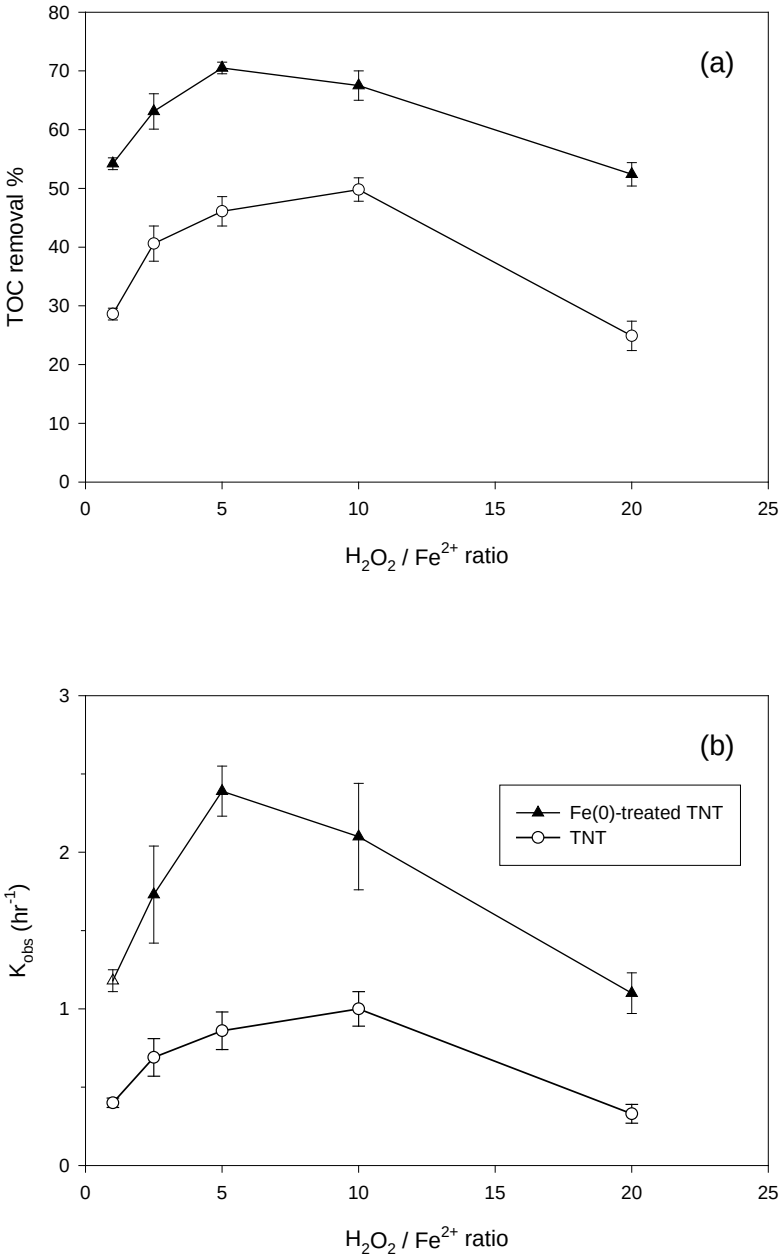

Figure 2.2 The extent of TOC removal (a) and pseudo-first-order rate constant (b) with various H_2O_2/Fe^{2+} molar concentration ratios in Fenton oxidation of TNT and ZVI-treated TNT. Fe^{2+} concentration is 2 mM and initial concentration of TNT and ZVI-treated TNT is 20.0-20.8 mg/L TOC (Oh et al., 2003a).

ratio can be calculated using eq. 2.1. As shown in Figure 2.2(b), the TOC oxidation rate constant for ZVI-treated TNT was 2 to 3 times higher than that for untreated TNT. Figure 2.2 also shows that, using 2 mM of Fe^{2+}, the maximum TOC removal in ZVI-treated TNT solution in the CSTR was only 70.5 ± 1.0% under the optimal conditions, suggesting that, even with ZVI pretreatment, higher dosages of Fenton reagent are needed to achieve complete mineralization of TNT.

Figure 2.3(a) shows the effect of increasing H_2O_2 and Fe^{2+} concentrations on TOC removal for TNT and iron-treated TNT. Both the optimal H_2O_2-to-Fe^{2+} ratio (5:1) and the stoichiometric ratio (1:1) for hydroxyl radical (OH·) formation (Walling, 1975) were examined. Compared to the 1:1 ratio, the optimal ratio (i.e., 5-fold increase in H_2O_2 concentration) gave a 10-20% higher TOC removal for both TNT and ZVI treated TNT (except at very high TOC removal efficiencies). For both ratios, ZVI pretreatment enhanced the TOC removal by 20-40%. For ZVI-treated TNT, the TOC removal increased with increasing H_2O_2 and Fe^{2+} dosages and complete mineralization was achieved with 5 mM Fe^{2+} and 25 mM H_2O_2. In comparison, Fenton oxidation of TNT was less efficient as indicated by the smaller increase in TOC removal with increasing Fe^{2+} and H_2O_2 dosages and incomplete TOC removal (81.4 ± 1.5%) even with 50 mM H_2O_2 and 10 mM Fe^{2+}. Figure 2.3(b) shows that ZVI pretreatment enhanced the TOC oxidation rate (k_{obs}, by as much as two orders of magnitude) and the rate of increase in k_{obs} (on a log scale) with increasing H_2O_2 and Fe^{2+} concentrations. The result suggests that the payoff of increasing Fenton reagent dosage to treat TNT is greater with ZVI pretreatment.

TOC Removal by Fenton Oxidation of RDX and Iron-Treated RDX

Figure 2.4 shows the effect of H_2O_2-to-Fe^{2+} ratio on TOC removal during Fenton oxidation of RDX and ZVI-treated RDX in the CSTR. A molar ratio of 5:1 appeared to be optimal for RDX (with 2 mM Fe^{2+}) and ZVI-treated RDX (with 1 mM Fe^{2+}); ZVI pretreatment enhanced the mineralization of RDX by 50-60%. In addition, the enhancement of TOC removal in ZVI-treated RDX is substantially higher than ZVI-treated TNT. This difference may be due to ZVI-treated RDX being much more easily oxidized than ZVI-treated TNT. It has been reported that the ZVI pretreatment results in the cleavage of triazine ring in RDX and formation of NH_4^+ and a linear structure of C-N compounds (e.g. methylenedinitramine) as products (as discussed

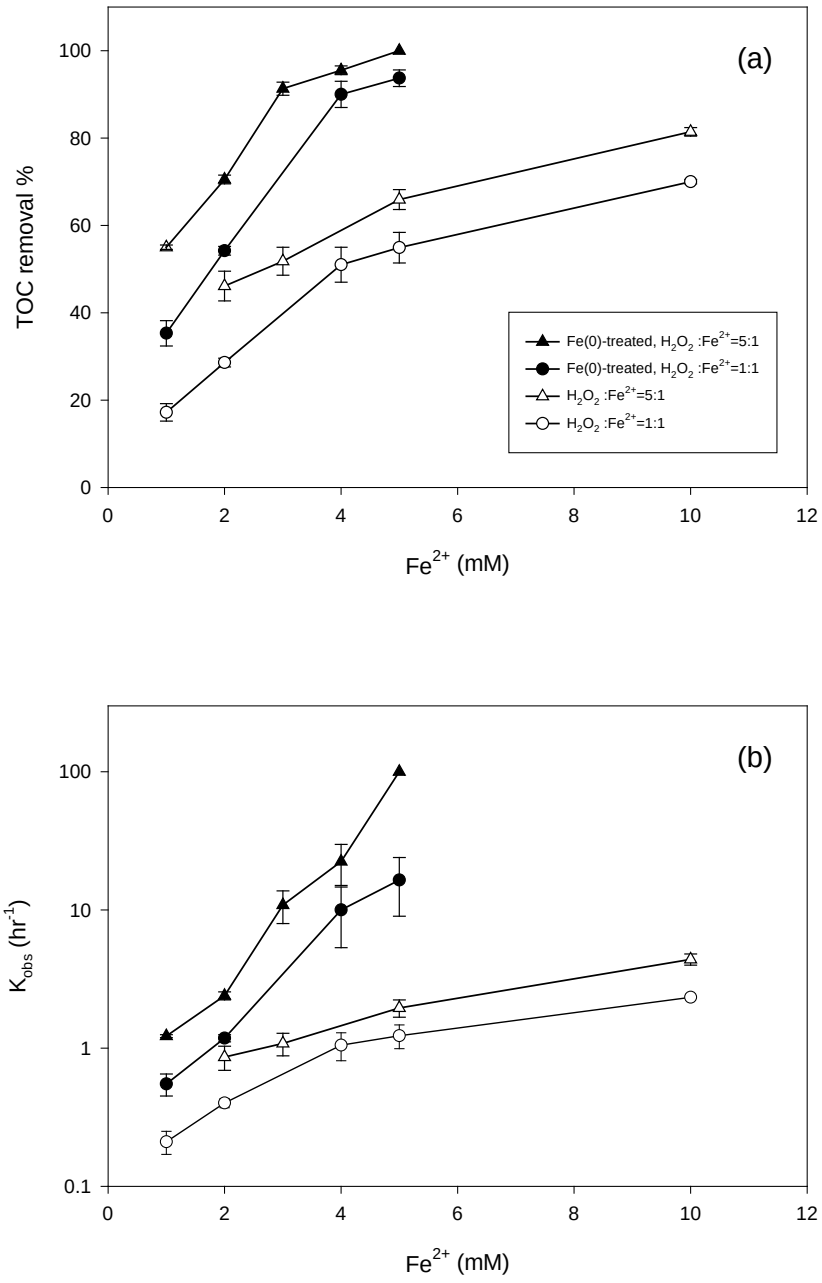

Figure 2.3 The extent of TOC removal (a) and pseudo-first-order rate constant (b) with various H_2O_2 and Fe^{2+} concentrations in Fenton oxidation of TNT and ZVI-treated TNT. Initial concentration of TNT and ZVI-treated TNT is 20.2-22.0 mg/L TOC (Oh et al., 2003a).

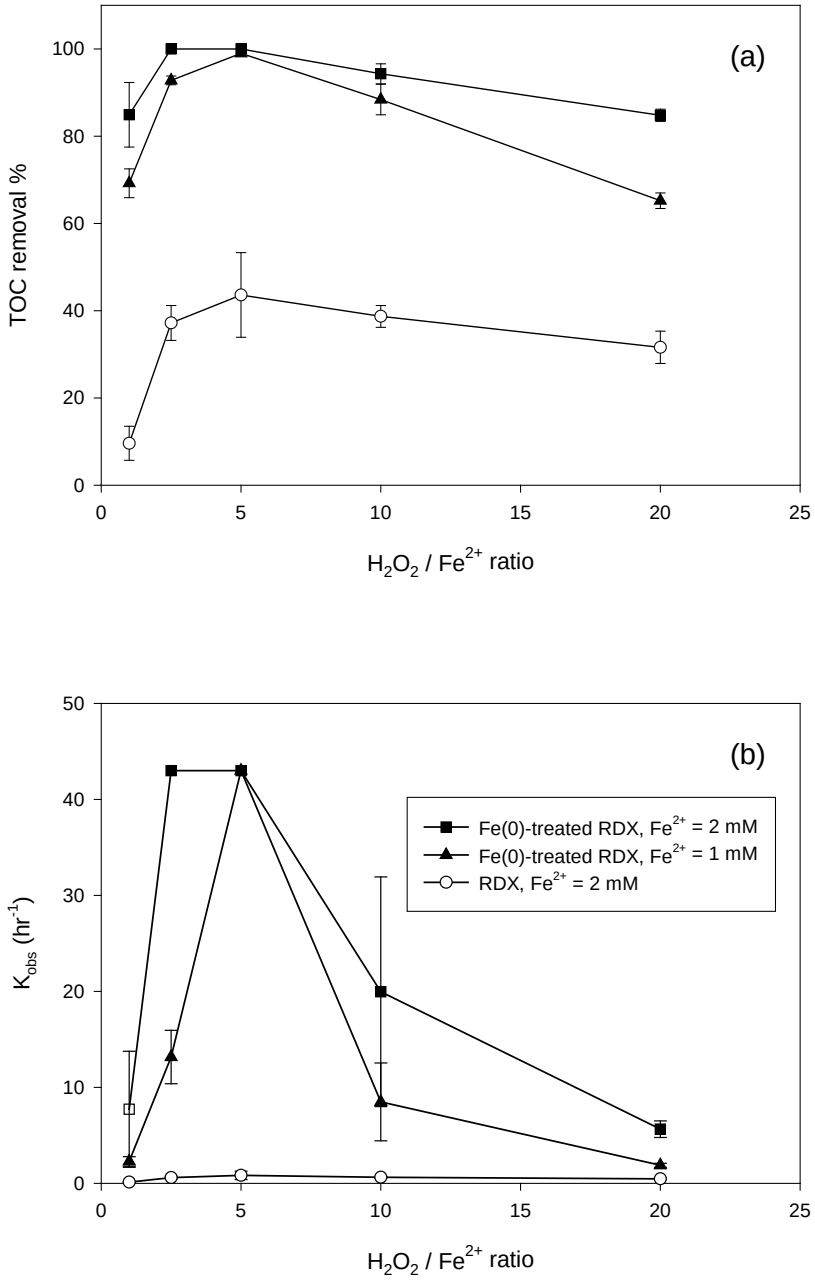

Figure 2.4 The extent of TOC removal (a) and pseudo-first-order rate constant (b) with various H_2O_2/Fe^{2+} molar concentration ratios in Fenton oxidation of RDX and ZVI-treated RDX. Initial concentration of RDX and ZVI-treated RDX is 8.8-9.4 mg/L TOC (Oh et al., 2003a).

in Section1). This ring cleavage may result in much easier the mineralization of ZVI-treated RDX. Similar to TNT, optimum H_2O_2 to Fe^{2+} ratio was found to be 5:1 for Fenton oxidation of RDX and ZVI-treated RDX. However, only 2 mM of Fe^{2+} was enough to obtain complete removal of TOC in ZVI-treated RDX solution under optimal condition. K_{obs} for TNT and ZVI-treated TNT under optimal condition was 0.8 (hr^{-1}) and 43 (hr^{-1}), respectively (Figure 2.4(b)).

Figure 2.5(a) shows the effect of H_2O_2 and Fe^{2+} concentrations on Fenton oxidation of RDX and ZVI-treated RDX. Similar to the oxidation of TNT and ZVI-treated TNT, TOC removal was enhanced as H_2O_2 and Fe^{2+} concentrations increased in both RDX and ZVI-treated RDX solutions. Complete removal of TOC in ZVI-treated RDX solution was achieved with 1 mM Fe^{2+} under optimal condition whereas 5 mM of Fe^{2+} was needed to obtain about 90% TOC removal of untreated RDX. Figure 2.5(b) shows that pseudo-first-order rate constant for TOC removal (K_{obs}) increased up to 43 (hr^{-1}) with only 1 mM Fe^{2+} under optimal condition. However, only 9.7 (hr^{-1}) of K_{obs} was obtained in Fenton oxidation of untreated RDX with even 5 mM of Fe^{2+} under optimal condition.

Nitrogen Balance in Fenton Oxidation

Nitrogen recovery was observed through analysis of NO_3^- and NH_4^+ as TOC was removed from explosive and Fe(0)-treated explosive solutions by Fenton oxidation (Table 2.1). 25 mM of H_2O_2 and 5 mM of Fe^{2+} was used for Fenton oxidation of TNT, RDX, and ZVI-treated TNT. For Fenton oxidation of ZVI-treated RDX, 10 mM of H_2O_2 and 2 mM of Fe^{2+} was used because those concentrations were enough to obtain complete TOC removal. In Fenton oxidation of TNT, 60.1% of nitrogen was recovered as NO_3^-, which is closely matched with 65.9% of TOC removal. This result suggests that NO_3^- may be a good indicator of TOC removal in Fenton oxidation of TNT. In Fenton oxidation of ZVI-treated TNT, 92.2% of nitrogen was recovered as NO_3^- and NH_4^+, which correlates well to 100% TOC removal. About 8% difference between TOC removal and nitrogen recovery may be due to unidentified nitrogen species like NO_2^- or analytical error in analysis of NH_4^+ and NO_3^-. Interestingly, before Fenton oxidation, 0.278 ± 0.004 mM of NH_4^+ was observed, which is not a reduction product of TNT with ZVI

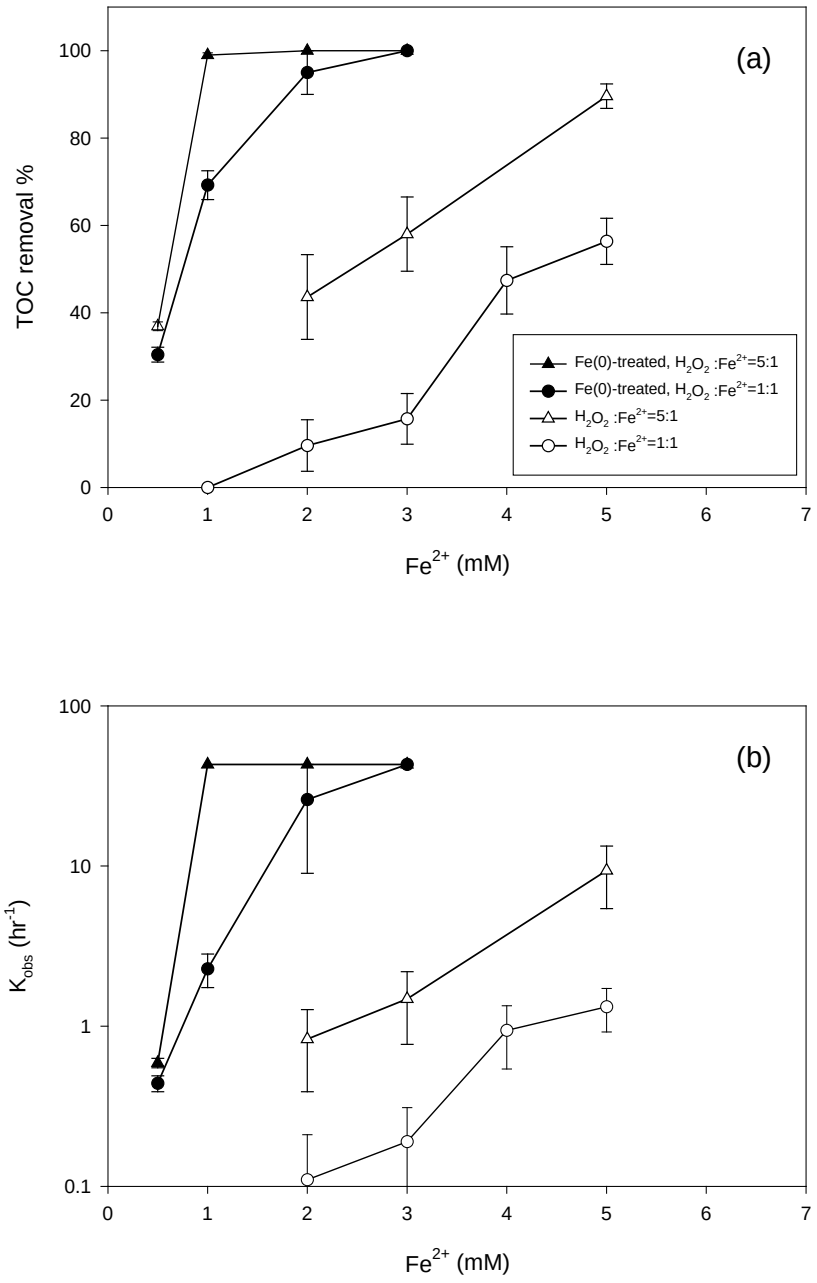

Figure 2.5 The extent of TOC removal (a) and pseudo-first-order rate constant (b) with various H_2O_2 and Fe^{2+} concentrations in Fenton oxidation of RDX and Fe(0)-treated RDX. Initial concentration of RDX and Fe(0)-treated RDX is 8.8-9.4 mg/L TOC (Oh et al., 2003a).

Table 2.1 Nitrogen recovery after Fenton oxidation of TNT, RDX, ZVI-treated TNT and ZVI-treated RDX solutions (Oh et al., 2003a).

	Before oxidation	
	Total N (mM)	NH_4^+ (mM)
TNT [1)]	0.714 ± 0.006	nd
Fe(0)-treated TNT [1)]	0.818 ± 0.015	0.278 ± 0.004
RDX [1)]	1.233 ± 0.035	nd
Fe(0)-treated RDX [2)]	1.027 ± 0.025	0.292 ± 0.011

	After oxidation			
	NH_4^+ (mM)	NO_3^- (mM)	N recovery (%)	TOC removal (%)
TNT [1)]	nd	0.429 ± 0.004	60.1	65.9
Fe(0)-treated TNT [1)]	0.511 ± 0.012	0.243 ± 0.004	92.2	100.0
RDX [1)]	0.164 ± 0.015	0.278 ± 0.007	35.8	89.6
Fe(0)-treated RDX [2)]	0.421 ± 0.005	0.393 ± 0.008	79.3	100.0

1) 25 mM H_2O_2 and 5 mM Fe^{2+}
2) 10 mM H_2O_2 and 2 mM Fe^{2+}
Nd: not determined

because complete mass recovery as TAT was observed in previous batch reduction experiments (Section 1). We hypothesize that NH_4^+ produced in ZVI-treated TNT solution resulted from the release of amino functions from TAT because TAT was reported to be unstable under aerobic environment (Preuss et al., 1993; Lewis et al., 1996; Hawari et al., 1998; Hwang et al., 2000). Hawari and coworkers (2000) reported abiotic formation of hydroxydiaminotoluene (HDAT) and dihydroxyaminotoluene (DHAT), which may be possible compounds in ZVI-treated TNT solution in this study. However, it is still unclear whether the mechanism in abiotic transformation of TAT is hydrolysis or oxidation. We also observed the abiotic transformation of TAT and the production of NH_4^+ in TAT solution under aerobic environment (data not

shown). In Fenton oxidation of NH_4^+ under the same condition, NH_4^+ was not oxidized to NO_3^- (data not shown), which indicates that increase of NH_4^+ concentration during Fenton oxidation (0.233 mM) resulted from Fenton oxidation of Fe(0)-treated TNT (Table 2.1). Molar concentration ratio of NH_4^+ to NO_3^- produced during Fenton oxidation was approximately 1:1. Formation of NH_4^+ and NO_3^- from N-bearing compounds by advanced oxidation processes was previously reported by several researchers (Low et al., 1991; Pignatello and Sun, 1995; Nohara et al., 1997; Maletzky and Bauer, 1998; Poulios et al., 2000). Low et al. (1991) showed that the ratio of NH_4^+ to NO_3^- formed during photo-catalytic oxidation of N-bearing organic compounds (e.g., phenylalanine) increased by increasing the irradiation time and pH. Maletzky and Bauer (1998) also reported that NH_4^+ was a dominant product of photo-Fenton oxidation of NH_2-containing compounds (e.g., *p*-aminophenol). On the other hand, Nohara et al. (1997) concluded that formation of NO_3^- in photocatalyzed oxidation of N-bearing compounds was highly dependent on the hydroxylation of amino group in compounds. Therefore, formation of NH_4^+ and NO_3^- in Fenton oxidation of ZVI-treated TNT is not an unexpected result. However, mechanism on the formation of NH_4^+ and NO_3^- in Fenton oxidation of ZVI-treated TNT still remains to be determined.

In Fenton oxidation of RDX, only 35.8% of nitrogen was recovered as NO_3^- and NH_4^+ in contrast to 89.6% of TOC removal, indicating that other nitrogen species, for example NO_2^- or N_2, might be formed in Fenton oxidation of RDX. According to Zoh and Stenstrom (2002), it was shown that 75% of initial nitrogen in RDX was transformed to N_2 during Fenton oxidation of RDX in a closed system. Therefore, about 55% of difference between TOC removal and nitrogen recovery may be attributed to formation N_2 in an open system. Molar concentration ratio of NH_4^+ to NO_3^- produced during Fenton oxidation of RDX was approximately 0.59 (Table 2.1). In Fenton oxidation of ZVI-treated RDX, 79.3% of nitrogen was recovered as 0.421 ± 0.005 mM of NH_4^+ and 0.393 ± 0.008 mM of NO_3^-. This difference between TOC removal and nitrogen recovery may be due to unidentified nitrogen species or analytical error in analysis NO_3^- and NH_4^+. Similar to ZVI-treated TNT solution, 0.292 ± 0.011 mM of NH_4^+ was observed in ZVI-treated RDX solution before Fenton oxidation. However, NH_4^+ in ZVI-treated RDX solution was not a product from abiotic transformation during storage

but a product from reduction of RDX by ZVI (Section 1). Molar concentration ratio of NH_4^+ to NO_3^- produced during Fenton oxidation of Fe(0)-treated RDX was approximately 0.33 (Table 2.1).

Degradation in a Bench-Scale Integrated System

Table 2.2 summarized TOC removal and nitrogen recovery in degradation of TNT and RDX using a bench-scale sequential ZVI column-Fenton oxidation integrated system. TNT was completely reduced to TAT in the ZVI column as 93.5% of initial TNT concentration (0.187 ± 0.017 mM) was accounted for in the column effluent. Reduction with ZVI did not reduce TOC concentration in TNT solution, indicating that sorption loss of TNT and its products in the column was minimal. After Fenton oxidation in the CSTR, 96.1 ± 1.2% of TOC was removed and 87.5% of initial nitrogen was recovered as 0.235 ± 0.007 mM of NH_4^+ and 0.257 ± 0.014 mM of NO_3^-. Similarly, RDX was also completely removed through reductive transformation in the iron column. After reduction in the iron column, 0.250 ± 0.004 mM of NH_4^+ was detected as a product, accounting for 23.8% of initial nitrogen. Subsequent Fenton oxidation in the CSTR showed 95.4 ± 1.5% TOC removal and 74.8% of nitrogen recovery (0.385 ± 0.038 mM of NH_4^+ and 0.400 ± 0.008 mM of NO_3^-), which were consistent with previous results in Fenton oxidation of ZVI-treated RDX (Table 2.1).

This study clearly shows that the proposed ZVI column-Fenton oxidation integrated system is a promising technology for treating pink water in munitions-manufacturing plants. This study showed that iron pretreatment enhanced the extent of TOC removal by approximately 20% and 60% for TNT and RDX, respectively. Enhancement of mineralization in ZVI-treated RDX was much more substantial than the mineralization of ZVI-treated TNT. This suggested that RDX-rich pink water may be more favorable for the application of ZVI pretreatment technology.

Furthermore, 92.2% and 79.3% of initial nitrogen was recovered as NH_4^+ and NO_3^- when ZVI-treated TNT and ZVI-treated RDX solutions were completely mineralized by Fenton oxidation, respectively. Finally, the bench-scale ZVI column-Fenton oxidation integrated system successfully demonstrated the feasibility of the proposed system in treatment of TNT and RDX solutions.

Table 2.2 TOC removal and nitrogen recovery in degradation of TNT and RDX solutions using a bench-scale ZVI column-Fenton oxidation integrated system (Oh et al., 2003a).

	TNT[1)]		
	TOC (mg/L)	NH_4^+ (mM)	NO_3^- (mM)
Initial	16.0 ± 1.2	nd	Nd
After reduction	15.7 ± 0.7	nd	Nd
After oxidation	0.6 ± 0.2	0.235 ± 0.007	0.257 ± 0.014

	RDX[2)]		
	TOC (mg/L)	NH_4^+ (mM)	NO_3^- (mM)
Initial	6.5 ± 0.2	Nd	Nd
After reduction	6.3 ± 0.1	0.250 ± 0.004	Nd
After oxidation	0.3 ± 0.1	0.385 ± 0.038	0.400 ± 0.008

1) 25 mM H_2O_2 and 5 mM Fe^{2+}

2) 10 mM H_2O_2 and 2 mM Fe^{2+}

nd: not determined

Decrease of pH during Fenton Oxidation

During Fenton oxidation of ZVI-treated TNT and ZVI-treated RDX, we observed rapid pH decrease as soon as Fenton oxidation started in the CSTR. In preliminary batch oxidation experiments with Fenton's reagent for those compounds in an unbuffered system, the pH of solution in the CSTR also decreased to between 2.2 and 2.4 in the earlier stage and throughout an 8-hour experiment. The decrease in pH during Fenton oxidation was previously

reported by several researchers. Sedlak and Andren (1991) showed that during Fenton oxidation of chlorobenzene in a batch reactor under unbuffered conditions, pH decreased from 3.0 to 2.4 when Fe^{2+} was completely depleted after 4 hours. Li et al. (1997) reported that pH declined by 1 to 2 pH units when the initial pH was above 4.5 during Fenton oxidation of TNT in an unbuffered batch reactor. They attributed the pH decrease in the Fenton oxidation to the oxidation and hydrolysis of Fe^{2+} and the generation of HNO_3 from TNT. Bier et al. (1999) also observed a decrease in pH to 2.6-2.8 in oxidation of RDX with Fenton's reagent, regardless of the initial pH in an unbuffered system (except the case of pH 2.0).

As proposed by Li et al. (1997), formation of HNO_3 from the reduction products by attack of hydroxyl radicals may be responsible for the decrease in pH during Fenton oxidation. Approximately 40-45% of initial nitrogen was recovered as NO_3^- after Fenton oxidation of TNT and RDX in the integrated system (Table 2.2). In order to calculate the acidity from the mineralization of TAT in Fenton oxidation, a stoichiometric equation was determined (eq. 2.2). We assumed that TAT was completely mineralized and that nitrogen was fully recovered as NO_3^- and NH_4^+ at a 1:1 ratio.

$$C_7H_5(NH_2)_3 + 21H_2O_2 \rightarrow 7CO_2 + 1.5NO_3^- + 1.5NH_4^+ + 23.5H_2O \qquad (2.2)$$

The initial concentration of TAT was 0.187 mM, corresponding to 0.281 mM of NO_3^- formation after complete mineralization. This calculation indicated that the acidity from HNO_3 was not responsible for observed decrease of pH during Fenton oxidation of TAT in the integrated system.

Another plausible explanation on the decrease of pH may be oxidation of Fe^{2+} and precipitation of Fe^{3+} during Fenton oxidation. During Fenton oxidation, Fe^{2+} is rapidly oxidized to Fe^{3+} with generation of OH^-. Though several side reactions may regenerate Fe^{2+}, Fenton oxidation is finally terminated with making excessive amounts of Fe^{3+} and OH^- in solution when dissolved Fe^{2+} is completely consumed. These excessive amounts of Fe^{3+} and OH^- result in precipitation of $Fe(OH)_3$ (eq. 2.3) and hydrolysis of Fe^{3+} in solution (equations 2.4-2.7).

$$Fe(OH)_{3(s)} \leftrightarrow Fe^{3+} + 3OH^-, K_1 = 10^{-38} \qquad (2.3)$$

$$Fe(OH)_{3(s)} \leftrightarrow Fe(OH)^{2+} + 2OH^-, K_2 = 10^{-26.16} \quad (2.4)$$

$$Fe(OH)_{3(s)} \leftrightarrow Fe(OH)_2^{+} + OH^-, K_3 = 10^{-16.74} \quad (2.5)$$

$$Fe(OH)_{3(s)} + OH^- \leftrightarrow Fe(OH)_4^-, K_4 = 10^{-5} \quad (2.6)$$

$$2Fe(OH)_{3(s)} \leftrightarrow Fe_2(OH)_2^{4+} + 4OH^-, K_5 = 10^{-50.8} \quad (2.7)$$

where Ks are equilibrium constants. When total dissolved Fe^{3+} concentration is 1 mM, 3 mM, and 5 mM, equilibrium between dissolved Fe^{3+} species and $Fe(OH)_{3(s)}$ is reached at pH 2.33, 2.17, and 2.10, respectively, and Fe^{3+} is the most dominant species in solution. This pH values agree reasonably well with final pH values observed in our experiments. Based on our calculation, it can be concluded that pH drop below 3 may be explained by the precipitation of ferric hydroxide during Fenton oxidation rather than the acidity form HNO_3. This acid production during Fenton oxidation eliminates the need for acid addition and may also provide the acidity needed for Fe^{2+} production from the iron column.

2.3 Validation of Proposed ZVI-Fenton Process with Pink Water

2.3.1 Introduction

In this study, we demonstrated the integrated system with real pink water. By batch and column experiments, we determined the reduction of TNT, RDX, and HMX with ZVI. We evaluated the extent of TOC removal from pink water in the integrated system.

2.3.2 Materials and Methods

Chemicals

Pink water was provided by the Iowa Army ammunition plant (Middletown, IA). $FeSO_4 \cdot 7H_2O$ (>99%) was purchased from Sigma (St. Louis, MO) and H_2O_2 (30%) was obtained from Fisher Scientific (Pittsburgh, PA). Cast iron was obtained from Master Builders, Inc. (Aurora, OH). Specific surface area of Master Builders iron was 1.29 m^2/g (Perey et al., 2002). The iron was used as received without pretreatment.

Batch and Column Experiments

Batch experiments were conducted in an anaerobic glove box (95% N_2 + 5% H_2, Coy, MI) using 8 mL borosilicate vials containing 5 mL of aqueous solution and 1 g of cast iron. In case of a pH controlled experiment, pink water contained 0.1 M HEPES buffer to maintain a constant pH of 7.4 throughout the experiments. The solution was purged in a glove box to completely remove oxygen for at least 1 day. After iron was added, the vials were shaken in a horizontal position using an orbital shaker at 100 rpm. At each sampling time, replicate vials were sacrificed and the supernatant was filtered through a 0.22-μm mixed cellulose membrane filter (Millipore, Bedford, MA) for analysis using a high performance liquid chromatograph (HPLC).

Column experiments were conducted using a glass column (2.5 cm i.d. $\times$ 30 cm L, Ace Glass, Vineland, NJ) with Teflon end fittings. The column was packed with Master Builders iron and had a porosity of 0.6. To ensure anaerobic conditions, pink water was purged with N_2 for 20 minutes prior to introduction into the column. The deoxygenated pink water was

pumped into the packed column using a peristaltic pump in an upward direction at the flow rate of 3.50 ± 0.05 mL/min. The retention time in the column was approximately 25 minutes. After more than three retention times, the column effluents were collected and passed through a 0.22-μm cellulose membrane filter (Millipore, Bedford, MA) for HPLC analysis.

Degradation in an Integrated System

Pink water was treated with a bench-scale integrated system, consisting of ZVI reduction and subsequent Fenton oxidation. The integrated system was constructed by connecting the iron column and the completely-stirred tank reactor (CSTR) for Fenton oxidation with silicone tubing and a glass fiber filter. The same column described above was used. Subsequent Fenton oxidation was conducted using an acrylic, cylindrical CSTR (8.8 cm dia. $\times$ 3.5 cm effective height). Solutions of $FeSO_4 \cdot 7H_2O$ and H_2O_2, and iron-treated pink water were pumped into the CSTR using peristaltic pumps (Cole-Parmer, Vernon Hills, IL). The flow rate of Fe^{2+} and H_2O_2 solutions were 0.08 mL/min and that of the pink water was 3.50 ± 0.05 mL/min. Molar ratio of H_2O_2 and Fe^{2+} was 5, which was shown to be the optimal ratio for TNT and RDX (Section 2.2). The pH of the reaction mixture was controlled at 3.0 ± 0.1 using an automatic pH controller (Cole-Parmer, Vernon Hills, IL) with 0.1-N NaOH solution. A hydraulic retention time was 1 hour. After more than 3 hours, CSTR effluent was collected and filtered with a glass fiber filter (Whatman, Clifton, NJ) for TOC analysis.

Analytical Methods

TNT, RDX, and HMX were analyzed using a Varian HPLC (Walnut Creek, CA) equipped with a Supelguard guard column (20 $\times$ 4.6 mm, Supelco, Bellefonte, PA), a Supelco LC-18 column (250 $\times$ 4.6 mm, 5 μm), a UV detector (2510 Varian, Walnut Creek, CA) and an isocratic pump (2550 Varian, Walnut Creek, CA). Methanol-water mixture (55/45, v/v) was used as the mobile phase at a flow rate of 1.0 mL/min. TAT was analyzed by HPLC with an Alltima C18 column (250 $\times$ 4.6 mm, 5 μm, Alltech, Deerfield, IL) and an Alltima guard column (7.5 $\times$ 4.6 mm, Alltech). Acetonitrile-phosphate buffer (40 mM, pH 3.2, 10/90, v/v) was used as an eluent at 1.0 mL/min. The injection volume for all samples was 10 μL and the wavelength for

the UV detector was 254 nm. TOC concentration was determined using a Tekmar-Dohrmann TOC analyzer (DC-190 Rosemount Analytical Inc., Santa Clara, CA). NH_4^+ and Fe^{2+} were analyzed with an UV-vis spectrophotometer (DR2010, HACH, Loveland, CO).

2.3.3 Results and Discussion

Pink Water Characterization

Table 2.3 summarizes pH and concentrations of TOC and three major explosives in pink water from the Iowa Army ammunition plant. Pink water was slightly acidic (pH 6.62 ± 0.01) and contained 17.4 ± 2.2 mg/L of inorganic carbon. Concentrations of TNT, RDX, and HMX were 108.2 ± 1.7 mg/L, 65.1 ± 7.8 mg/L, and 9.2 ± 0.4 mg/L, respectively. Concentrations of these explosives accounted for 82.9% (52.1 mg/L) of TOC in pink water (62.8 ± 0.6 mg/L). It appears that the unexplained 17.1% of TOC (10.7 mg/L) may be unidentified explosives in pink water or other organic compounds coming from loading, assembling, packing or demilitarization activities in the plant.

Table 2.3 Dissolved explosives, TOC and pH in pink water from the Iowa Army ammunition plant.

PH	TOC (mg/L)	TNT (mg/L)	RDX (mg/L)	HMX (mg/L)
6.62 ± 0.01	62.8 ± 0.6	108.2 ± 1.7	65.1 ± 7.8	9.2 ± 0.4

Batch and Column Experiments

Figure 2.6 shows the concentration of TNT, RDX, and HMX during reduction of pink water in an unbuffered ZV I-water system. The error bars in all figures indicate the standard deviation, which was calculated by data from analyses of replicate reactors. More than

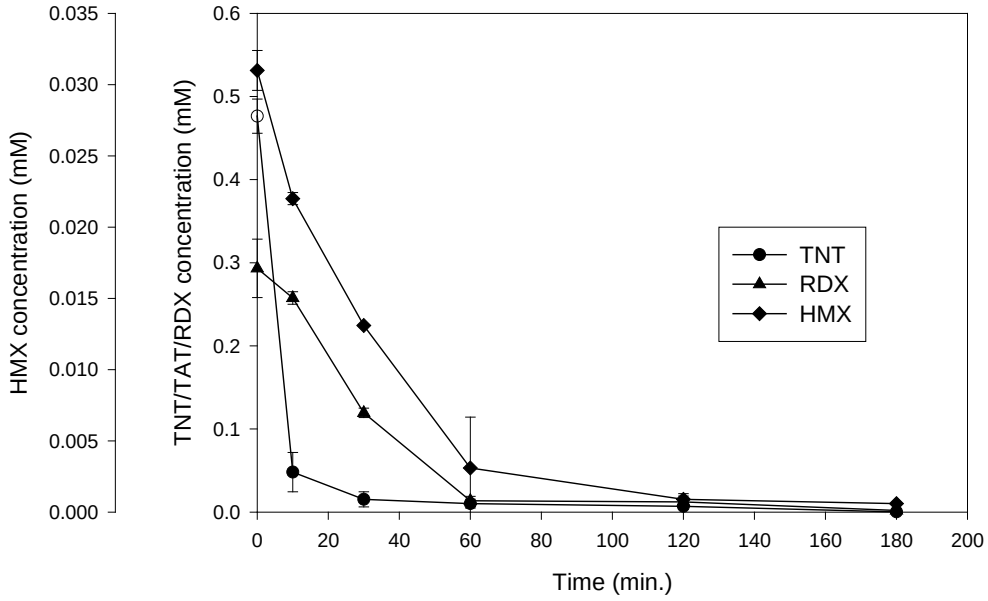

Figure 2.6 Concentrations of TNT, RDX, and HMX during reduction of pink water in an unbuffered iron-water system. The error bars are based on replicate reactors.

95% of TNT, RDX, and HMX were removed from the pink water after 2 hours. Even after 3 hours, removal of those explosives were not complete and about 40% of initial TNT was recovered as TAT (data not shown). Figure 2.7 shows the concentrations of TNT, RDX, and HMX during reduction of pink water with ZVI at pH 7.4. TNT and RDX were completely removed from the pink water within 30 min. After 1 hour, HMX was completely removed, indicating that HMX removal with ZVI was slower than TNT and RDX. After 30 min, TAT was increasingly formed as a product of TNT reduction. TAT showed 88.3% of initial TNT concentration after 2 hours.

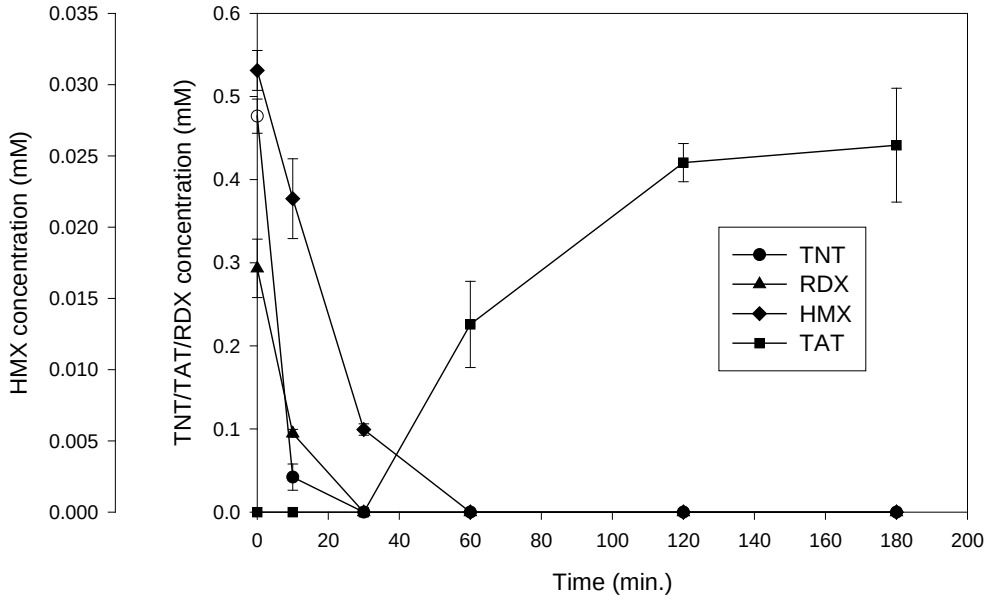

Figure 2.7 Concentrations of TNT, RDX, and HMX during reduction of pink water with zero-valent iron at pH 7.4. The error bars are based on replicate reactors (Oh et al., 2004b).

HPLC analysis of the column effluents indicated that TNT, RDX, and HMX were completely transformed in the ZVI column. TNT was fully reduced to TAT and no intermediates were detected. Concentrations of TAT and NH_4^+ were 58.9 mg/L (0.433 mM) and 12.2 mg/L (0.679 mM), respectively. The steady-state concentration of Fe^{2+} in the effluent was below 0.1 mg/L. With 0.1 M HEPES buffer, the column effluent contained 115.5 ± 3.0 mg/L of Fe^{2+}, suggesting that the ZVI column may be used for generating Fe^{2+} for subsequent Fenton oxidation.

TOC Removal in an Integrated System

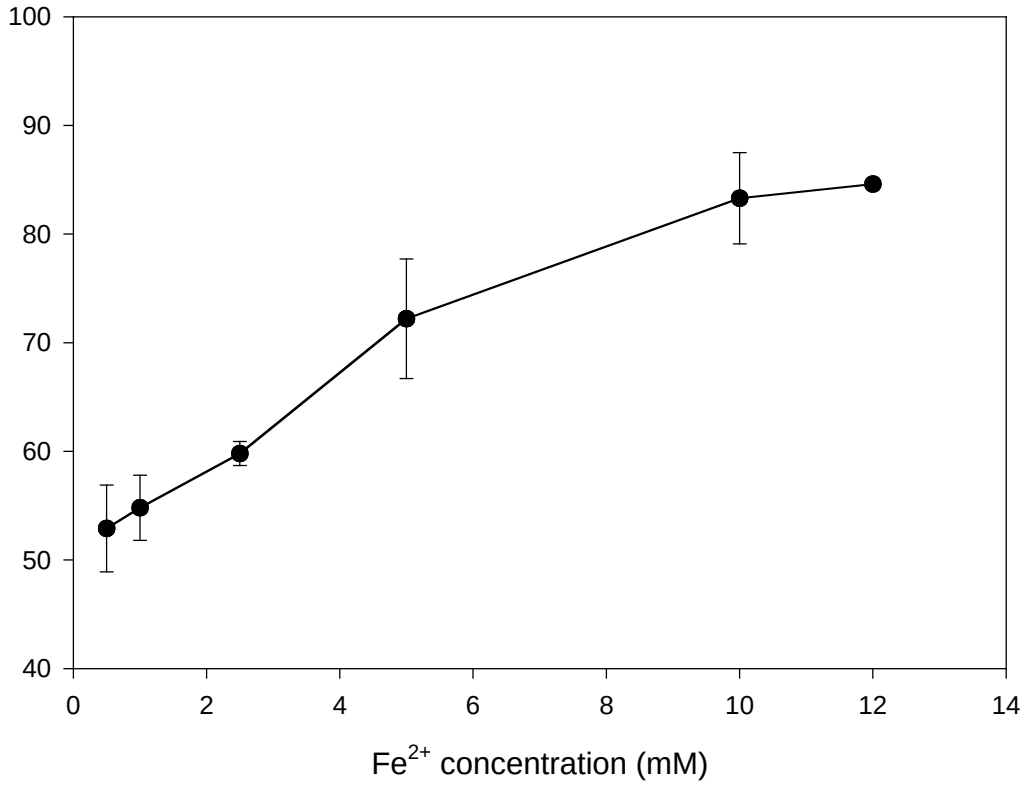

Figure 2.8 The extent of TOC removal with various H_2O_2 and Fe^{2+} concentrations in Fenton oxidation of pink water. Molar ratio of H_2O_2 to Fe^{2+} is 5 (Oh et al., 2004b).

Figure 2.8 shows the TOC removal in the bench-scale integrated system. With 0.5 mM of Fe^{2+} and 2.5 mM of H_2O_2, 52.9 ± 4.0% of TOC was removed in a CSTR. As concentrations of Fe^{2+} and H_2O_2 were increased, TOC removal in a CSTR was correspondingly increased. With 5 mM of Fe^{2+} and 25 mM of H_2O_2, 72.2 ± 5.5% of TOC was removed in Fenton oxidation. However, even with higher concentrations of Fe^{2+} and H_2O_2 under optimal condition, complete TOC removal was not achieved. With 10 mM of Fe^{2+} and 50 mM of H_2O_2, 83.3 ±

4.2% of TOC was removed. This incomplete TOC removal with large amounts of Fenton's reagent may be due to high concentration of TNT in the pink water. TNT concentration in the pink water was approximately 2.5 times higher than that in the solutions used for the integrated system in Section 5. The TOC content (10.7 mg/L) unexplained by three major explosives may also be responsible for incomplete TOC removal in Fenton oxidation.

In summary, our results show that TNT, RDX, and HMX were rapidly removed from pink water and that TAT and NH_4^+ were produced as products with ZVI. Using the integrated system, $83.3 \pm 4.2\%$ of TOC was removed from pink water with 10 mM Fe^{2+} and 50 mM of H_2O_2. It appears that larger amounts of Fenton's reagent will be required to achieve the complete TOC removal in the integrated system. Follow-up study on cost-effective design of Fenton process may be needed to generate sufficient amount of dissolved Fe^{2+} and minimize the amount of iron sludge in field application.

Cost Analysis

The cost analysis was performed on the integrated ZVI-Fenton process using the average flow rate (7.5 gallon/min) and the average TNT concentration (30.1 mg/L) in the pink water at the McAlester Army ammunition plant (McAlester, OK). Based on the specification of the designed column, the cost for the iron column was estimated. For estimating the cost for the Fenton reactor, previously reported capital and operational cost for the pilot-scale Fenton reactor (Choi, 1999) was modified.

For designing the iron column, minimum retention time of 15 min, which was shown to be enough to completely transform TNT in Section 1, and 60% of porosity were used. With the selected retention time, porosity, and the flow rate of pink water in the plant, we proposed the cylindrical iron-packed column having 2 ft in diameter and 10 ft of height (140 gallon of pore volume and 18.7 min of retention time). The amount of iron that would fill the column was also determined to be 2.77 ton/column based on the density of iron (7.86 g/cm^3) and the porosity of the column. To estimate the column life, we calculated the rate of iron consumption by coupling the TNT reduction with the oxidation of ZVI to Fe^{2+}. This is conservative approximation

because nitroaromatics were known to be reduced by surface-bound Fe^{2+}. Stoichiometric calculation was performed using the following equation with the average concentration of TNT in the pink water:

$$TNT + 9Fe + 12H_2O \rightarrow TAT + 9Fe^{2+} + 18OH^- \quad (2.8)$$

Iron consumption rate by TNT was estimated to be 2.87 kg/day, corresponding to 965 days of service time based on the 2.77 ton of iron in the column. This estimation suggests that the iron column may last more than two and a half years. We estimated the cost for the iron reduction process using the purchasing and disposal cost of cast iron for the iron-packed column. Using the price of Master Builders cast iron (app. $ 500/ton), the service time of the iron column (app. 2 years), and the solid waste disposal cost (app. $ 40/ton), the cost for the iron reduction process was approximately estimated to be $ 1,505/year. Construction cost for the iron column was not included in the estimated cost. We used the estimated cost for the iron column to calculate the total capital cost.

Choi (1999) operated the pilot-scale Fenton-reactor to treat the landfill leachate. The pilot-scale plant was designed to treat the 5 gal/min leachate and installed in a trailer of 8 ft. (W) $\times$29 ft. (L)$\times$9 ft. (H). The plant was composed of a four-step process: mixing, Fenton oxidation, alkaline neutralization, and sedimentation. In this pilot-scale study, capital cost was $ 70,505.58, including cost for materials, utility, safety, electrical works, and construction. This cost was used for the capital cost for the Fenton reactor in the integrated process. If the lifetime of the Fenton reactor at the plant was assumed as 20 years, total capital cost per gallon of pink water in the integrated ZVI-Fenton process was calculated as 0.13 cents/gal using equations 2.9 -2.11.

Total amount of pink water treated = 20 (yrs) × 365 (days/yr) × 24 (hrs/day) × 60 (mins/hr) × 7.5 (gal/min) = 78,840,000 (gal) (2.9)

Total capital cost = $ 1,505(/yr)$\times$20 (yrs) + $ 70,505.58 = $ 100,605.58 (2.10)

Capital cost per gal = $ 100,605.58 $\div$ 78,840,000 (gal) = 0.13 cents/gal (2.11)

According to the previously estimated prices of chemicals and power (Choi, 1999), operational cost for the zero-valent iron-Fenton process was calculated using the average flow rate of pink water (7.5 gallon/min). Concentrations of Fe^{2+} and H_2O_2 were assumed as 10 mM and 50 mM, respectively, which were evaluated in the bench-scale integrated system. Labor cost was not included. Table 2.4 summarizes the estimated cost for treatment of the pink water. Estimated treatment cost was 1.71 cents/gal. Operational cost was responsible for 92.6% of the total cost. If follow-up study on the generation of Fe^{2+} from the iron column is completed, the operational cost for Fe^{2+} may be replaced with the operational cost for acid.

In order to perform the cost comparison with the existing GAC adsorption process and the anaerobic biological GAC fluidized bed reactor, only cost for the iron reduction process in the integrated system was used because other two processes were used only to remove explosives from pink water. The estimated costs for the GAC adsorption process and the anaerobic biological GAC fluidized bed reactor in the McAlester Army ammunition plant were $ 71,000/year and $ 19,090/year, respectively (Maloney et al., 2002). These yearly costs were one order of magnitude higher than that for the iron column ($ 1,505/yr). This indicated that the iron reduction process might be much more cost-effective than other two processes. However, evaluation of the pilot-scale iron column still remains to be determined in future works to completely verify the cost-effectiveness of the iron reduction process in the integrated system.

Table 2.4 Estimated treatment cost of pink water with the integrated zero-valent iron-Fenton process.

Item	Required amount	Price*	Cost (cents/gal)	(%)
Operational cost			1.5856	92.6
Fe^{2+}	0.0378 (M/gal)	9.1938 (cents/M)	0.3480	20.3
H_2O_2	0.1893 (M/gal)	5.8025 (cents/M)	1.0981	64.1
NaOH*	0.3718 (M/gal)	0.0304 (cents/M)	0.0097	0.6
Electricity*	0.0122 (KWH/gal)	10.6167 (cents/KWH)	0.1298	7.6
Capital cost			0.1276	7.4
Total			1.7132	100.0

* Choi (1999)

Section 3
Pilot-Plant Evaluation of an Integrated ZVI-Fenton Process for RDX Containing Process Water Treatment

3.1 Introduction

3.1.1 Background

For the last quarter century, the U.S. Army has been searching for an alternative technology to granular activated carbon (GAC) for the treatment of munitions-manufacturing wastewater (or pink water), which are generated in large quantities in the U.S. (Adrian and Campbell, 1999). The dominant constituents of pink water are 2,4,6-trinitrotoluene (TNT) and hexahydro-1,3,5-trinitro-1,3,5-triazine (RDX), octahydro-1,3,5,7-tetranitro-1,3,5,7-tetrazocine (HMX), 2,4-dinitrotoluene (DNT), trinitrobenzenes (TNB), and dinitrobenzenes (DNB). Many of these compounds resist aerobic degradation and are toxic and/or potentially carcinogenic (Yinon, 1990; Peters et al., 1991). Currently, no federal effluent limitation exists for pink water and every State establishes its own limitation specific to each site. The most common method to remove energetic compounds from pink water is GAC adsorption. This process is expensive and nondestructive and generates large quantities of explosives-laden spent carbon, a hazardous material that is expensive to regenerate and dispose of.

3.1.2 Objectives of the Demonstration

The objectives of this research are (1) to conduct a pilot-scale study to demonstrate and validate ZVI reduction technology for RDX containing process water treatment. A three-year bench-scale project by ERDC-CERL and the University of Delaware (UD) has shown that ZVI technology is effective in removing TNT, RDX, HMX and other energetic compounds under ideal laboratory conditions; however, large-scale testing of ZVI against real RDX wastewater has not been conducted to validate this technology for field applications. In addition, studies to date on degradation of energetic compounds by ZVI are relatively short-term.

3.2 Technology Description

The original scope of this project was a demonstration of the ZVI technology for treatment of an RDX wastewater from Holston AAP. In the previous section, it was shown we could effectively treat energetic compounds (TNT, RDX and NG) using ZVI. RDX transformation by ZVI involves rapid ring cleavage (Oh et al., 2005a) and the products are aerobically biodegradable to a large extent (Oh et al., 2005b). Because the Holston AAP generate RDX process water and an industrial wastewater treatment plant (IWTP) is already available at the site to provide biological oxidation, Fenton oxidation was not necessary for the Holston wastewater. A schematic of the proposed ZVI reactor system followed by a biological IWTP for the Holston wastewater is shown in Figure 1. The Holston AAP demonstration was the first application of ZVI in a trailer-mounted reactor system for RDX process water treatment.

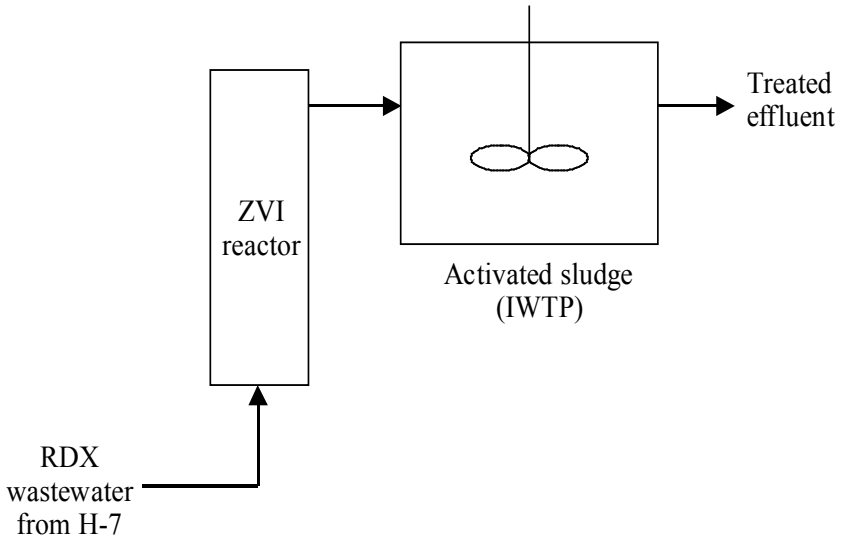

Figure 3.1. Schematic of the proposed ZVI treatment system for RDX wastewater.

3.2.1 Advantages and Limitations of the Technology

The ZVI process has many of the advantages that have been recognized for subsurface PRBs. In addition, in contrast to PRBs, the ZVI process is above-ground and therefore easy to control, modify, and replace if necessary. The advantages of the ZVI process can be summarized as follows: (1) commercial ZVI is readily available and rather inexpensive, (2) the ZVI process is simple and robust and the system is easy to construct and operate, (3) the technology is flexible and can be incorporated into new or existing facilities, (4) the reactions of all explosives tested with ZVI are fast and hence the treatment would require short contact times and small footprints, (5) the process does not require active operation or frequent maintenance and can be interrupted and re-started without significant loss of time or efficiency, in contrast to biological processes, and (6) unlike GAC, ZVI actually breaks down energetic molecules without producing secondary pollution problem. It also mineralizes the explosives when combined with biological or chemical oxidation.

Risk associated with this technology demonstration is low. One concern is potential clogging of ZVI reactors, which may result from porosity losses due to iron oxides and mineral precipitation, blockage of pore space by trapped gases, and excessive microbial growth in ZVI reactors. The clogging problem can be readily prevented, as shown in our preliminary study, and precautions have been taken to address the possible causes above.

We conducted a laboratory column (1 cm dia. x 10 cm L) study where one column was filled entirely with commercial ZVI while the other column was filled with a 1:1 (w/w) mixture of ZVI and Ottawa (quartz) sand. We observed that the "100% ZVI column" clogged after several weeks of operation, presumably due to inter-particle bridging as a result of mineral precipitation. In contrast, clogging was not observed and the porosity was relatively constant in the ZVI-sand column over approximately 2,000 pore volumes, suggesting that inclusion of quartz sand into ZVI reactors can largely circumvent the clogging problem caused by mineral precipitation. This has been incorporated into our reactor design.

3.3 Preliminary Laboratory Testing

As noted above, reductive degradation of TNT, RDX and other energetic compounds by ZVI has been studied by many, and a significant amount of kinetic and mechanistic information is available (Agrawal and Tratnyek, 1996; Singh et al., 1998; Devlin et al., 1998; Oh, Just and Alvarez, 2001; Oh et al., 2002a,b; Oh, 2003, Oh et al., 2003; Oh et al., 2004; Oh et al., 2005a,b; Balakrishnan et al., 2004). However, because most of earlier studies were conducted in batch reactors, we conducted preliminary laboratory study to verify the performance of continuous-flow ZVI columns on the treatment of "real" energetic wastewater from Holston AAP.

3.3.1 RDX Process Water from Holston AAP

To examine the removal of RDX from the Holston wastewater by ZVI columns, four identical 20 cm (L) x 2.5 cm (dia.) glass columns were filled with iron granules (porosity of 0.72) and RDX process water from Holston was continuously fed to each column using a peristaltic pump. RDX concentration in the column effluent was measured under a range of different hydraulic retention time (HRT), which was controlled by varying the flow rate of the wastewater. Results of the study are shown in Figures 3.2 and 3.3. As shown in Figure 3.2, RDX concentration in column effluent decreased with increasing HRT (or decreasing flow rate), and removal of RDX to below detection (4 ppb) was achieved within an HRT of 6.2 minutes.

An additional column test was carried out at an elevated temperature of 75 ^{o}C by placing the ZVI column in a heated water bath. The high-temperature test was performed because Holston AAP has available steam for this demonstration, which may accelerate RDX degradation and therefore reduce the HRT and ZVI reactor size required for complete RDX removal. As shown in Figure 3.3, RDX concentration in column effluent for the same HRT was significantly lower at 75 ^{o}C and was below detection in about 4 minutes. These results show that complete removal of RDX in the Holston wastewater requires only minutes of HRT in a ZVI reactor, and that the HRT and ZVI reactor size may be further reduced by pre-heating the wastewater with steam. These tests with real wastewaters from Holston support the conclusion that ZVI is effective in degrading energetic compounds and may be a viable method to treat this munitions-manufacturing wastewater.

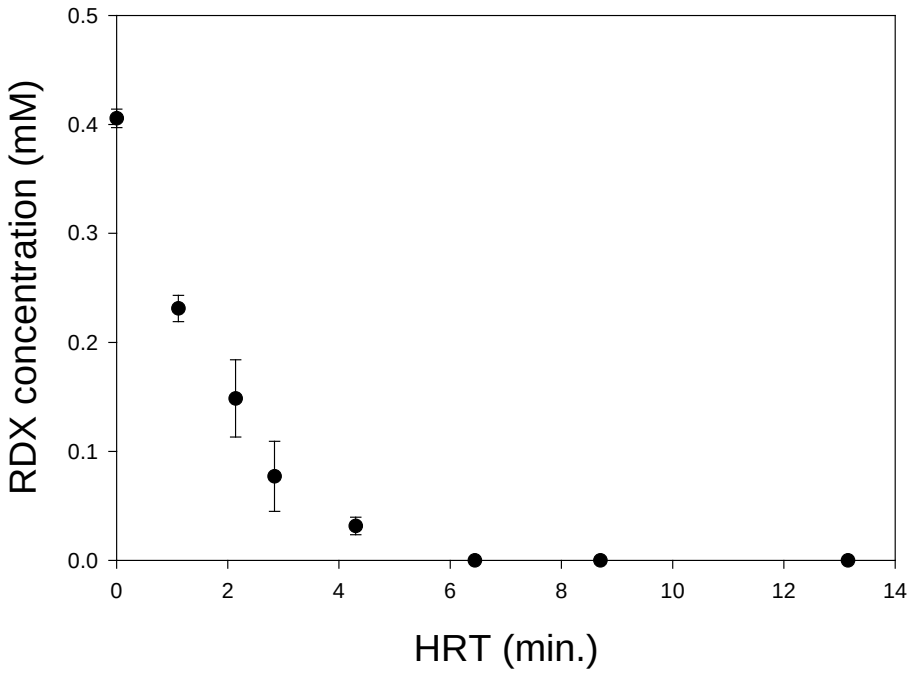

Figure 3.2 Reduction of RDX in Holston AAP wastewater in laboratory ZVI-packed column at 20 ^{o}C (HRT = hydraulic retention time).

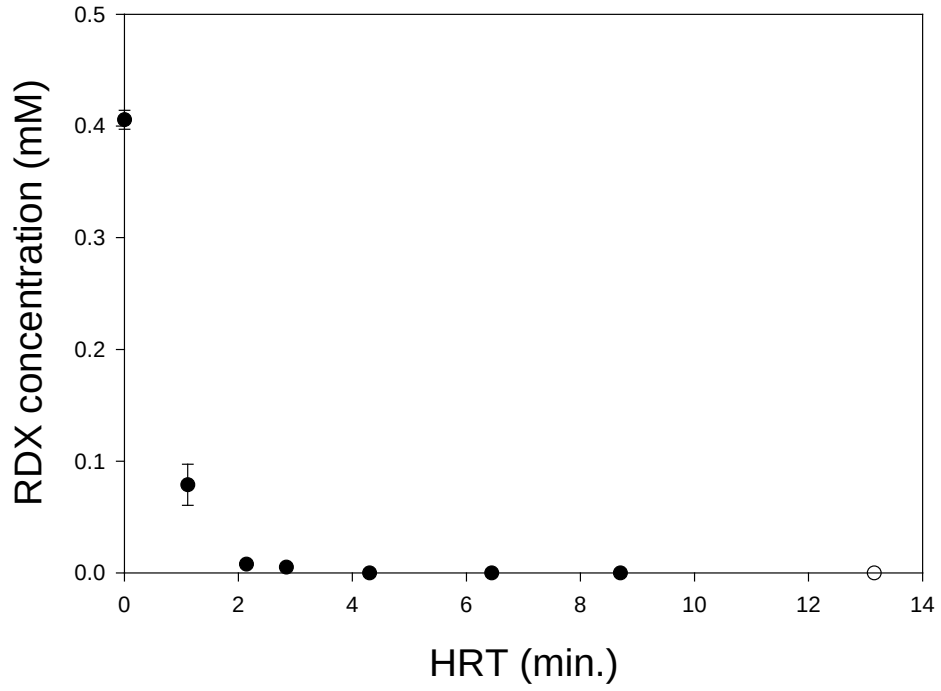

Figure 3.3 Reduction of RDX in Holston AAP wastewater in laboratory ZVI-packed column at 75 ^{o}C (HRT = hydraulic retention time).

3.4 Design And Construction of Demonstration Unit: Holston AAP

The objectives of the study at the Holston AAP are to demonstrate the effectiveness of ZVI to degrade RDX in the Holston AAP wastewater and to evaluate the long-term performance and economics of the ZVI technology. The primary reason for selecting Holston AAP for this demonstration was that it is the predominant RDX-producing facility in the U.S. The wastewater also has chemical characteristics (see Table 3.1) that are conducive to ZVI treatment. In addition, the facility can provide the necessary support, such as space, electricity, steam, auxiliary equipment, and personnel for this project. Holston AAP also has an existing industrial wastewater treatment plant (IWTP) that can polish the ZVI-treated wastewater for more complete RDX mineralization prior to discharge.

Holston AAP is located in Kingsport, Tennessee, and occupies a site of 120 acres. The plant was constructed in the early 1940s by Tennessee Eastman Corporation. The plant used to produce Composition B, which consists of RDX and TNT, between World War II and the Vietnam War. It later switched to the manufacture of RDX and HMX as these explosives are used more by the Army due to their superior energy to TNT. As of 1988, Holston AAP produced all of the RDX and HMX used in the U.S. and 90 percent of that consumed by all of the nations friendly to the U.S. The current production capacity of Holston AAP is 20 million pounds of RDX and 700,000 pounds of HMX a month (http://www.globalsecurity.org).

The RDX wastewater for the demonstration is produced in building H-7 of Holston AAP. It consists of primarily filtrate of RDX slurry from a vacuum filtration operation, which is on 12 hours a day around the year. The wastewater flow fluctuates but averages about 9,000 gallons a day. The chemical characteristics of the RDX wastewater from are shown in Table 3.1.

Table 3.1. Chemical characteristics of the wastewater from Holston AAP, building H-7.

Solute / Parameter	Concentration / Value	Units
pH	4.71 ± 0.03	—
TOC	452.7 ± 7.8	mg/L
RDX	90.7 ± 4.4	mg/L
Conductivity	520	µS/cm
NO_3^-	114.3	mg/L
NH_4^+	18.0	mg/L
SO_4^{2-}	67.0	mg/L

The demonstration unit was designed to handle the entire waste stream produced from building H-7. The system is a trailer-mounted mobile unit, which permits potential testing of the ZVI technology against energetics wastewaters produced at other locations. The system consists of two identical packed-bed reactors that contain commercial ZVI as a reactive material and quartz sand and gravel as inert fillers. In addition to the reactors, the trailer houses a heat exchanger and piping and valves for wastewater and steam. A mechanical layout of the trailer unit is shown in Figure 3.4 and the detailed schematic drawings of ZVI reactors are shown in Figures 3.5 and 3.6.

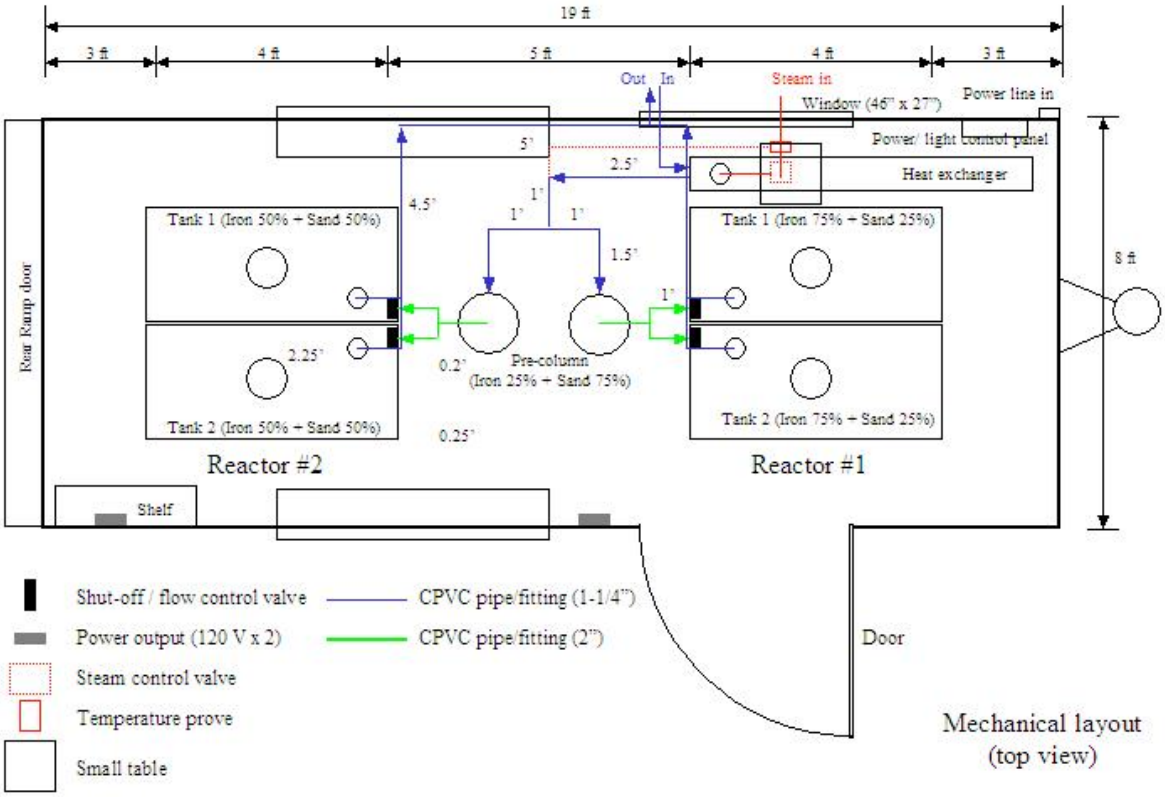

<u>Summary of Heat Exchanger:</u>
Bell & Gossett Steam U-tube type (Model QSU 46-4)
4" diameter x 6' length
Capacity: 13 gpm, 38 psig steam, 135 lbs
Outlet temperature : 25 ^{o}C
Water inlet and outlet : 1-1/4"
Steam inlet: 3"
Condensate outlet: 1"
Temperature controller

Figure 3.4 Layout of the trailer-mounted ZVI reactor system.

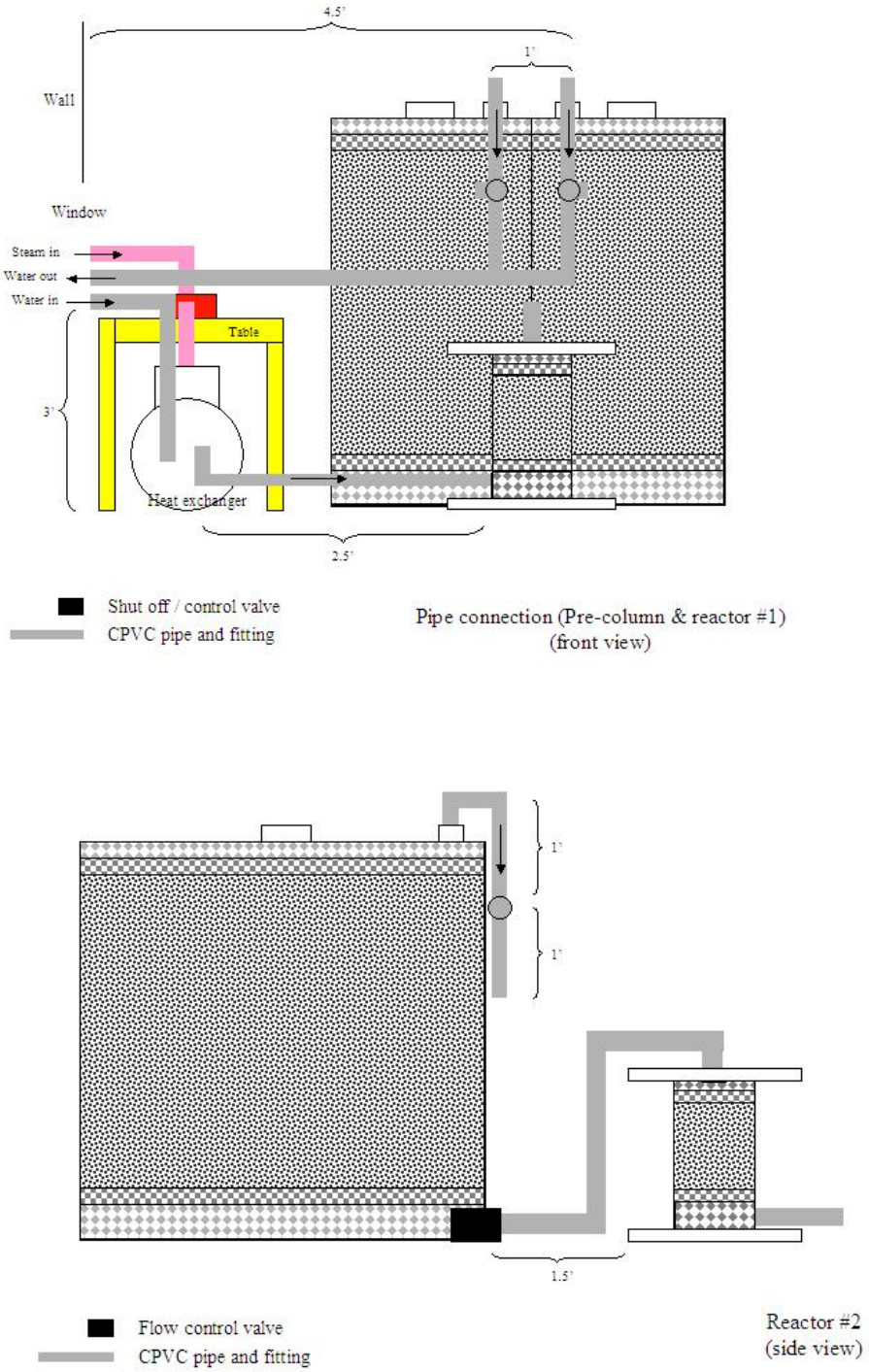

Figure 3.5 Schematic Diagram of ZVI reactor system.

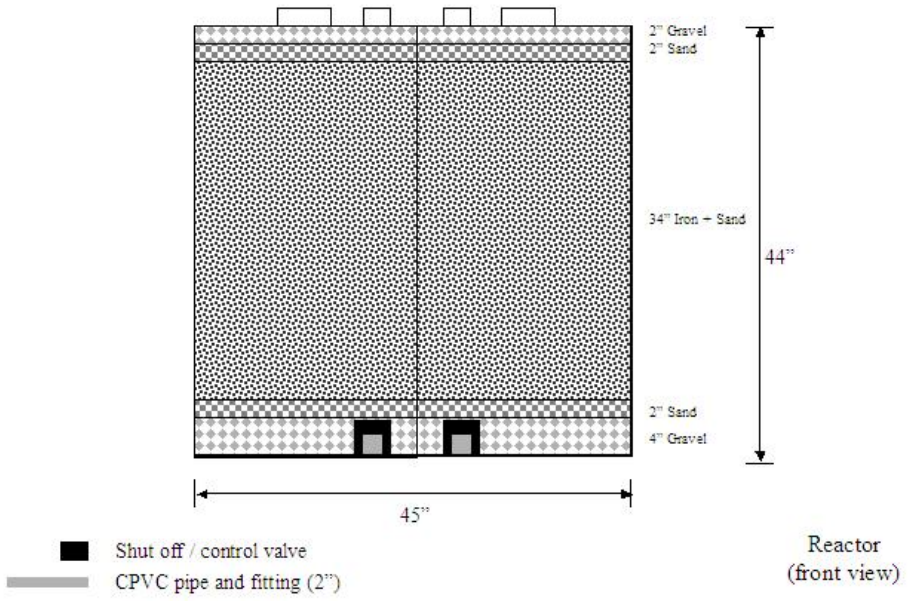

Summary of Reactors:
Model BT-110 (Dixie Poly-Drum Corp.) (x 2)
Twin 110 gallon tanks (poly ethylene) in Steel frame cage (x 2)
L: 45", W: 45", H: 44"
Weight: 425 lbs
2" inlet valve for each tank
Flow rate = 9,000 gpd (total); 1.56 gpm for each tank
24 hr operation
Estimated HRT = 50 (gallon, pore volume)/3.1 = 32 min each tank (empty bed)
50:50 (iron:sand) mixture ratio = iron contact time 16 min.
75:25 (iron:sand) mixture ratio = iron contact time 24 min.

Figure 3.6 Schematic of the dual ZVI reactors.

3.5 Start-Up of ZVI Demonstration Unit: Holston AAP

The trailer-mounted ZVI reactor unit was constructed by University of Delaware personnel at its facility before transporting it to Holston, TN. Both main iron column reactors and pre-columns were packed with iron/sand mixture one month after the arrival at Holston AAP. The lessons learned from the first trial of the demonstration unit were discussed in the following section. New design concepts proposed for subsequent demonstration was also briefly described.

3.5.1 Lesson Learned

Following observations were noted from the first trial of the demonstration unit and the modifications to the demonstration unit were recommended:

- Influent pump was frequently shut-off due to low water levels in the equalization/storage tank, causing "back siphoning" of the flow from the iron reactor back to the storage tank. This reverse flow lowered the water level in the iron reactor and exposed the wetted iron granules to atmospheric air. We postulate that this periodic exposure of iron granules to air may have resulted in accelerated oxidation and accumulation of corrosion products in the iron reactors, causing premature clogging and pressure build-up in the iron columns and tanks.

  In order to prevent unwanted interruption in influent flow, we recommend a separate pump to supply the influent directly from the storage tank rather than tapping into the recirculation line. Currently, the stored raw water is continuously recirculated for freeze protection and the influent to the iron demonstration unit is tapped into recirculation line. We observed that the recirculation pump shuts off frequently perhaps due to sensitive water-level control mechanism. In order to protect against back flow of water during shut-down events, we recommend an installation of check valve in the influent line.

- Flow shut-off valves installed downstream of iron reactors were damaged due to the presence of sand and iron particles in the liquid stream. We recommend mounting the

valves on (or after) the vertical sections of the pipes along with the installation of stainless screens upstream of each valve. In addition, heavier duty industrial-grade valves should be used instead of PVC ball valves.

- The sections of the floor underneath the main iron reactor were sagging. Although the trailer floor was designed and constructed to withstand the weight of iron reactors, the floor loading was likely rated for dry operation conditions. The floor strength may have been compromised due to frequent wetting of the floor from the leaking reactors. We recommend reinforcing of the floor with heavy-duty plywood sheet.

- The removal of spent (or clogged) iron granules from the reactors may be difficult and impractical. The plastic iron reactors were filled with iron/sand mixtures through a 6-inch screw-top opening and the top was permanently sealed after filling. The pre-fabricated polyethylene tanks were convenient and economical, but small opening was not practical for the removal of the reactor contents. We recommend using column reactors with flanged end caps for easier extraction of reactor contents.

  Since the withdrawal of iron granules from the reactors was not viable, the removal of reactor units from the trailer may also be difficult and labor intensive because of the heavy weight of iron-filled reactors and the location of reactors in the trailer. We recommend the reactors to be positioned closer to the trailer doors as possible so that they can be easily maneuvered from the outside with a fork lift.

3.6 Design and Construction of Demonstration Unit at University of Delaware

In order to demonstrate and validate the ZVI technology, a continuous flow of 50 gallons per hour pilot plant was constructed in a 8 ft (W) x 9 ft (L) x 29 ft (L) mobile trailer. Initial design parameters and operation conditions were based on the data from our laboratory study. The pilot plant was fabricated and constructed by the mechanical shop and the electrical shop at University of Delaware. The ZVI demonstration unit consists of pre-column and main ZVI

reactors. A schematic layout of the system is shown in Figure 3.7. In order to prevent unwanted draining of the iron reactors and exposing the wetted iron granules to atmospheric air, RDX-laden water was pumped pass through two columns in U-shaped manner. Detailed layout of iron columns is shown in Figures 3.8.

RDX-containing water was continuously pumped at 50 gallon/hour to the pre-column (50% iron and 50% sand) to eliminate suspended particles and dissolved oxygen prior to the main ZVI reactors. The deoxygenated RDX-containing wastewater was then treated in the two PVC columns (25 gallons each) in series. ZVI reactors have iron-to-sand ratio of 50:50. The selection of iron-to-sand ratios was based on our previous experience with laboratory columns.

Performance of the system was evaluated based on RDX removal efficiency calculated from influent and effluent RDX concentrations, which was measured by analysis of grab samples. Triplicate samples of the influent at the demonstration unit wer obtained directly from the influent storage basin near the pump inlet. The effluent samples were obtained from the effluent pipes in triplicate. All samples were analyzed for RDX, total organic carbon (TOC), total suspended solids (TSS), and pH. In addition, selected samples were analyzed for RDX reduction intermediates (e.g., methylenedinitramine, or MDNA) and products (e.g., ammonium and formaldehyde) to ensure complete reduction of RDX. Samples were also be analyzed periodically for dissolved iron and nitrate. Dissolved iron may serve as an indicator of the reducing conditions in the reactors, whereas nitrate is a reactive constituent in the wastewater that may negatively affect the longevity of the ZVI reactors.

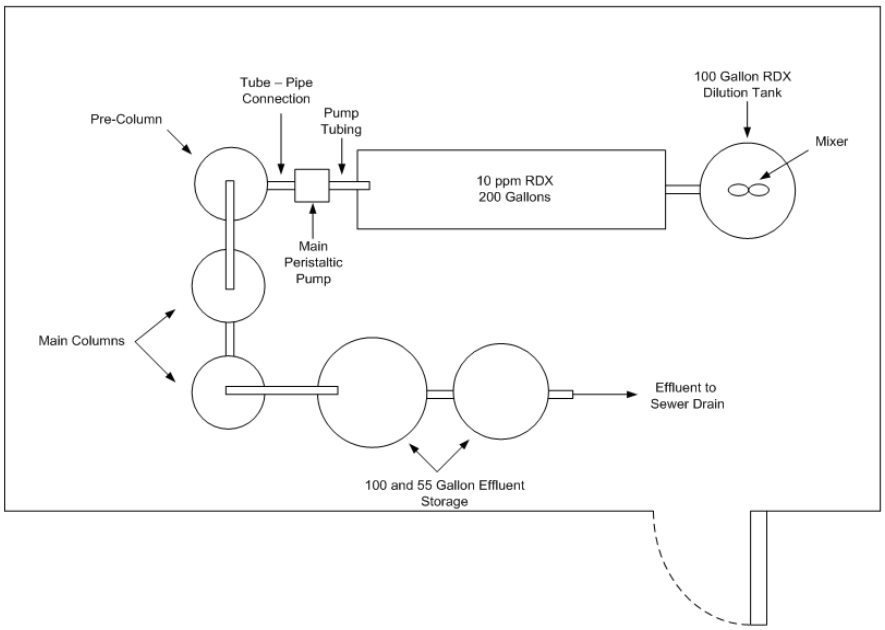

Figure 3.7. Schematic layout of trailer-mounted demonstration system.

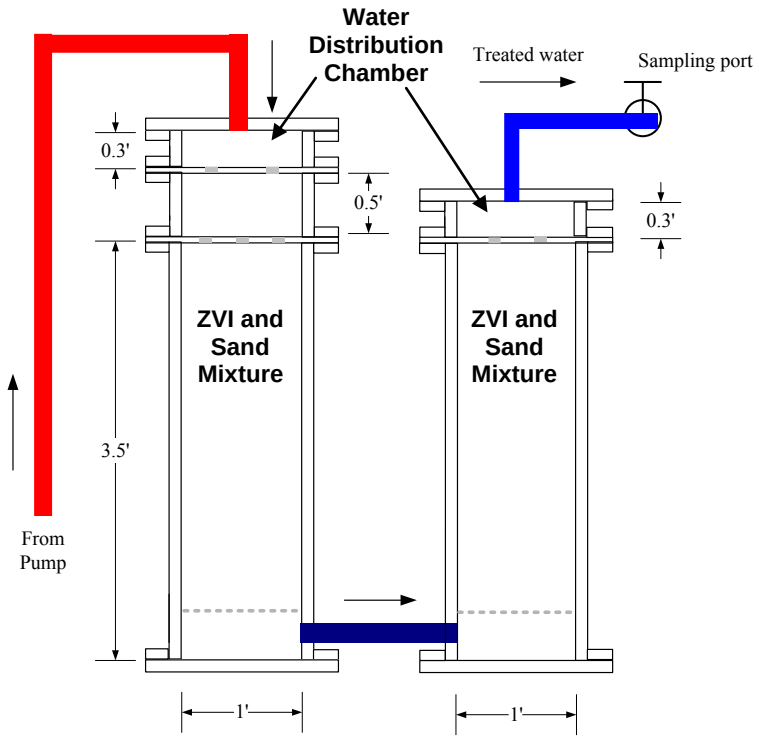

Figure 3.8. Iron columns in the demonstration system

3.7 Results of Pilot-plant Study at Delaware

The construction of trailer mounted ZVI system was completed in October, 2007 and initially operated for the treatment of 50 gallons/hour of DNT-containing solution (10 mg/L). DNT solution was prepared daily in the laboratory by dissolving 2,4-dinitrotoluene powder in tap water. The pilot-plant was operated for 4 hours/day for 30 days. The influent DNT was completely removed in the iron column (Figure 3.9) and the majority of DNT was recovered as diaminotoluene (Figure 3.10). Although DNT was not energetic compounds of interest at the proposal, we tested DNT as a warming up test because treatment data from other processes (for example, anaerobic granular activated carbon fluidized bed reactor) at various AAPs were available.

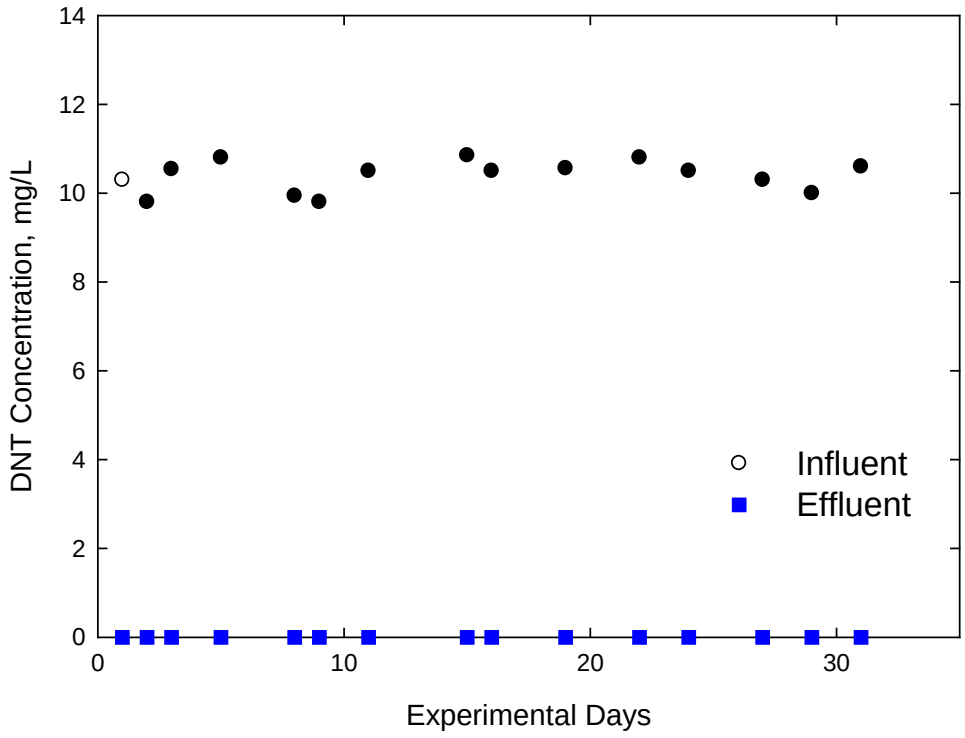

Figure 3.9 Removal of DNT by pilot-scale iron columns (Total HRT = 40 min.).

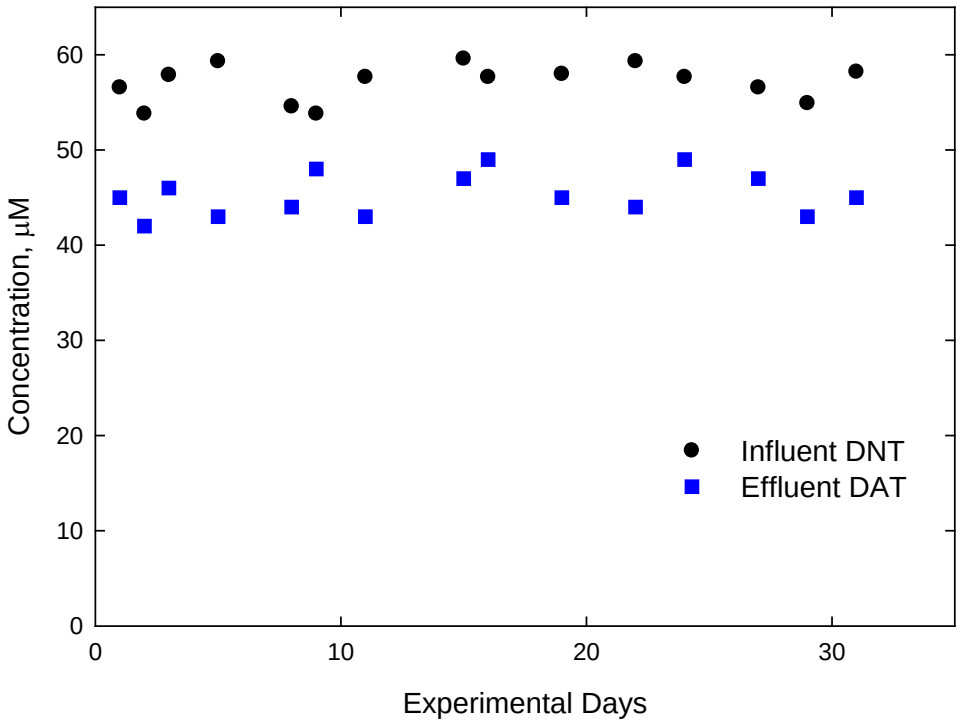

Figure 3.10 Dinitrotoluene as the major products of DNT reduction by ZVI.

After DNT treatment, a series of demonstration study with synthetic RDX wastewater was conducted with the trailer-mounted iron columns. Four different influent RDX concentrations (10 – 40 mg/L) and two different influent pH values were tested. Two hundred gallons of synthetic RDX wastewater was prepared daily. Supersaturated RDX solutions were first obtained by dissolving RDX powder in tap water at elevated temperatures (~ 70^{o}C). The saturated supernatant was analyzed for RDX and then systematically diluted to target RDX concentrations with warm tap water.

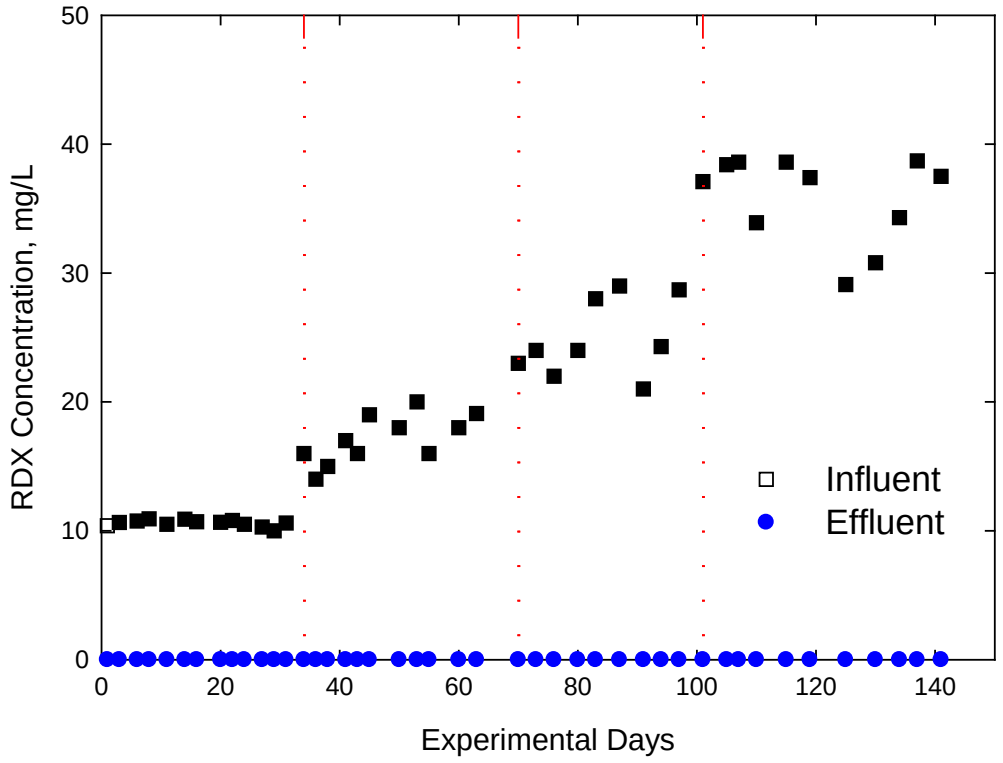

Figure 3.11 Removal of RDX by pilot-scale iron columns (Total HRT = 40 min.; influent pH = 7.5).

For all four influent RDX concentrations tested, no RDX was detected in final effluent throughout the 5-month experimental period (Figure 3.11). Periodic sampling of pre-column effluent showed that RDX reduction was completely removed in the pre-column (HRT =8 min), confirming the results obtained from our laboratory studies (Figure 3.2). Formaldehyde concentrations in the effluent samples indicated that 55 – 75% of carbon in RDX was recovered as formaldehyde.

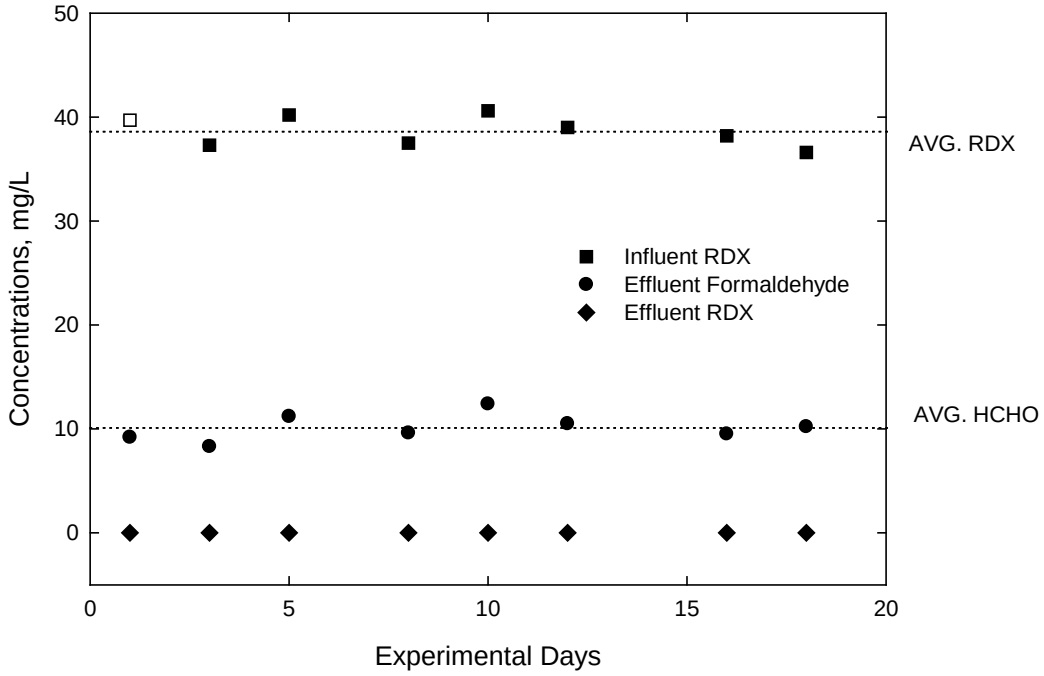

Figure 3.12 Removal of RDX by pilot-scale iron columns (Total HRT = 40 min.; influent pH = 4.5). Average concentration of influent RDX was 38.6 mg/L (0.174 mM) and average concentration of effluent formaldehyde was 10.1 mg/L (0.337 mM).

In order to simulate the pH of RDX wastewater from Holston AAP, the pH of influent RDX solution (RDX ~ 40 mg/L) to the trailer unit was adjusted to 4.5. Complete removal of RDX in the influent by iron columns was also observed with low pH influent. Average concentration of influent RDX was 38.6 mg/L (0.17 mM) and the average concentration of effluent formaldehyde was 10.8 mg/L (0.36 mM) during 3 weeks of low pH operation (Figure 3.12). Formaldehyde measured in the effluent samples accounted for 65% of carbon in influent RDX.

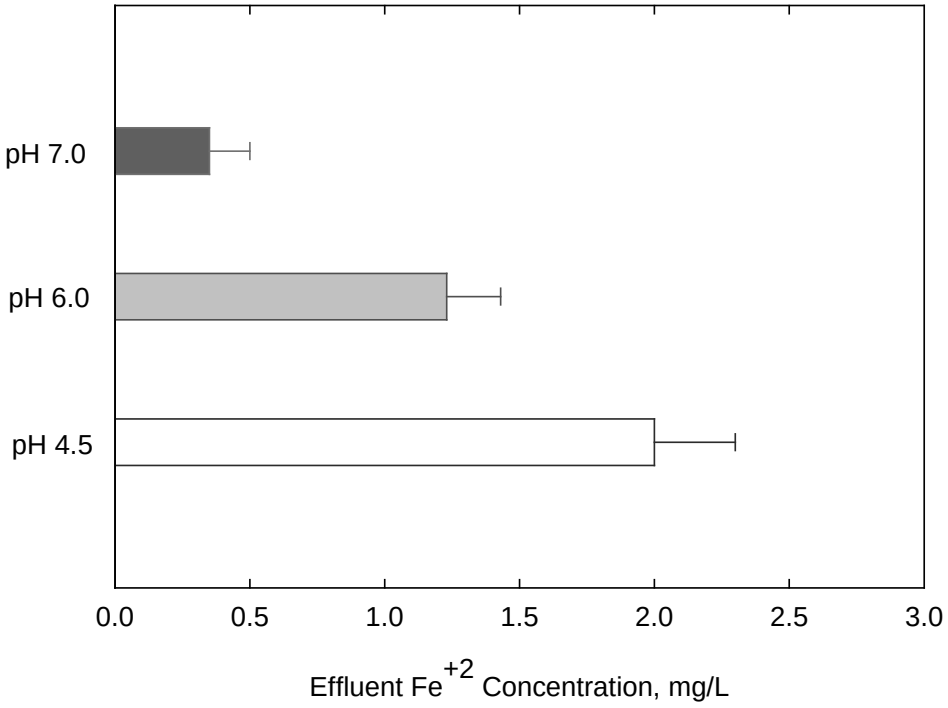

Figure 3.13 Effect of influent pH on effluent ferrous iron concentrations.

Ferrous ion concentrations in column effluent were periodically determined during the RDX reduction study and Fe^{+2} concentrations ranged from 0.35 to 2.4 mg/L. Amount of Fe^{+2} ions leached from iron columns increased with decreasing solution pH (Figure 3.13).
This increase in Fe^{+2} concentrations are most likely due to increased rate of corrosion at lower pH.

Section 4
Conclusions and Recommendations

4.1 Conclusions

In this study, the potential and feasibility of using ZVI to degrade several important energetic compounds - TNT, RDX, DNT, and NG - were demonstrated. The results indicate that ZVI can rapidly reduce these energetic compounds either to non-toxic and/or readily biodegradable products (in the case of nitroglycerin) or to products that are much more susceptible to oxidative degradation (in the case of TNT, RDX, and HMX). Using Fenton reaction as a subsequent oxidative treatment, we proposed an integrated iron-Fenton process and showed that reductive iron treatment greatly enhanced both the rate and extent of mineralization of these energetic compounds in synthetic and real process water. The study further demonstrates the advantages and cost-effectiveness of the iron-Fenton process for pink water treatment relative to other technologies, such as the conventional carbon adsorption process.

Through batch experiments, we determined the reaction rates and pathways for the reduction of TNT and nitroglycerin with ZVI and obtained high carbon and nitrogen balances for these compounds. TNT and NG were quantitatively transformed through successive reduction of the nitro and nitrate functions to TAT and glycerol, respectively. RDX and HMX were also reduced with iron to innocuous end products such as formaldehyde, nitrous oxide, and ammonium, but the mass balance was incomplete, indicating there were unidentified products. Nonetheless, the result shows that after Fenton oxidation, most of the carbon mass was accounted for by TOC removal and most of the nitrogen was recovered as ammonium and nitrate.

The results from the pilot-scale iron column study showed that RDX and DNT were readily degraded by ZVI under a wide range of influent conditions.
About 65% of carbon in influent RDX was recovered as formaldehyde. This study demonstrated that ZVI-based treatment process is an efficient way to convert RDX in wastewater into products that is more easily degradable through chemical or biological oxidation.

4.2 Recommendations

The applicability and cost-effectiveness of ZVI to degrade energetic compounds demonstrated in this laboratory and pilot study strongly suggest that this novel approach has great potential to become a superior technology for treating explosive-laden wastewaters and thus merits further investigation. Specifically, it is recommended that a pilot study be conducted to evaluate the proposed iron-Fenton process more fully and over a longer time period. A larger-scale evaluation of the technology not only will allow identification of issues that are important in system scale-up but will also provide an estimate of the capital and operational cost.

One important issue that can/should be addressed in a pilot study is the performance of ZVI over long periods of time while treating real energetic wastewater. Although the iron columns in our study remained effective for many months, the reactivity of cast iron and the permeability of the column medium may decrease over time due to passivation and porosity losses. A longer-term study using different column medium compositions (e.g., iron-to-sand ratios) and particle sizes is essential for assessing the longevity of iron, selecting the optimal iron content, and determining the frequency of rejuvenating (e.g., back-washing or acid treatment) or replacing the column medium, if necessary.

Other issues that would be important in full-scale operation and should be examined in a pilot study include pH control (for both iron column and Fenton reactor) and control of ferrous ion production in the iron column to enhance Fenton oxidation. These issues are not only inter-related but also will influence many of the issues discussed above – iron reactivity and service life, medium composition and replacement frequency, column permeability, chemical needs and operating cost. Clearly, the iron-Fenton process can be further optimized with respect to these parameters (pH and ferrous ion concentration) in order to minimize treatment cost without compromising efficiency.

REFERENCES

Accashian, J. V., Vinopal, R. T., Kim, B. J., and Smets, B. F. (1998) Aerobic growth on nitroglycerin as the sole carbon, nitrogen, and energy source by a mixed bacterial culture. *Appl. Environ. Microbiol.*, 64:3300-3304.

Adrian, N. and Campbell, E. (1999) TNT and RDX degradation by cell-free extracts of *clostridium acetobutylicum*. Technical report 99/102, Construction Engineering Research Laboratories, U.S. Army Corps of Engineers, Champaign, IL.

Agrawal, A. and Tratnyek, P. G. (1996) Reduction of nitro aromatic compounds by zero-valent iron metal. *Environ. Sci. Technol.*, 30:153-160.

Allen-King, R. M., Halket, R. M., and Burris, D. R. (1997) Reductive transformation and sorption of cis- and trans-1,2-dichloroethene in a metallic iron-water system. *Environ. Toxicol. Chem.*, 16:424-429.

Alnaizy, R. and Akgerman, A. (1999) Oxidative treatment of high explosives contaminated wastewater. *Water Res.*, 33:2021-2030.

Alowitz, M. J. and Scherer, M. M. (2002) Kinetics of nitrate, nitrite, and Cr(VI) reduction by iron metal. *Environ. Sci. Technol.* 36:299-306.

Arnold, W. A., Ball, W. P., and Roberts, A. L. (1999) Polychlorinated ethane reaction with zero-valent zinc: pathway and rate control. *J. Contam. Hydrol.*, 40:183-200.

Balakrishnan, V. K., Monteil-Rivera, F., Halasz, A., Corbeanu, A., Hawari, J. (2004) Decomposition of the polycyclic nitramine explosive CL-20 by Fe^0. *Environ. Sci. Technol.*, **38**: 6861-6866.

Berchtold, S. R., VanderLoop, S. L., Suidan, M. T., and Maloney, S. W. (1995) Treatment of 2,4-dinitrotoluene using a two-stage system: fluidized-bed anaerobic granular activated carbon reactors an aerobic activated sludge reactors. *Water Environ. Res.*, 67:1081-1091.

Bhaumik, S., Christodoulatos, C., Korfiatis, G. P., and Brodman, B. W. (1997) Aerobic and anaerobic biodegradation of nitroglycerin in batch and packed bed bioreactors. *Water Sci. Technol.*, 36:139-146.

Bier, E. L., Singh, J., Li, Z., Comfort, S. D., and Shea, P. J. (1999) Remediating hexahydro-1,3,5-trinitro-1,3,5-triazine-contaminated water and soil by Fenton oxidation. *Environ. Toxicol. Chem.*, 18:1078-1084.

Blehert, D. S., Knoke, K. L., Fox, B. G., and Chambliss, G. H. (1997) Regioselectivity of nitroglycerin denitration by flavoprotein nitroester reductase from two Pseudomonas species. *J. Bacteriol.*, 179:6912-6920.

Blowes, D. W., Ptacek, C. J., and Jambor, J. L. (1997) In-situ remediation of Cr(VI)-contaminated groundwater using permeable reactive walls: laboratory studies. *Environ. Sci. Technol.*, 31:3348-3357.

Boopathy, R. and Manning, J. F. (2000) Laboratory treatability study on hexahydro-1,3,5-trinitro-1,3,5-triazine-(RDX-) contaminated soil from the Iowa Army ammunition plant, Burlington, Iowa. *Water Environ. Res.*, 72:238-242.

Brenner, A., Ronen, Z., Harel, Y., and Abeliovich, A. (2000) Use of hexahydro-1,3,5-trinitro-1,3,5-triazine as a nitrogen source in biological treatment of munitions wastes. *Water Environ. Res.*, 72:469-475.

Bruhn, C., Lenke, H., and Knackmuss, H. J. (1987) Nitrosubstituted aromatic compounds as nitrogen source for bacteria. *Appl. Environ. Microbiol.*, 53:208-210.

Burris, D. R., Allen-King, R. M., Manoranjan, V. S., Campbell, T. J., Loraine, G. A., and Deng, B. (1998) Chlorinated ethene reduction by cast iron: sorption and mass transfer. *J. Environ. Eng. ASCE*, 124:1012-1019.

Burris, D. R., Campbell, T. J., and Manoranjan, V. S. (1995) Sorption of trichloroethylene and tetrachloroethylene in a batch reactive metallic iron-water system. *Environ. Sci. Technol.*, 29:2850-2855.

Choi, H. J. (1999) Evaluation of Fenton's process for the treatment of landfill leachate. Ph.D. dissertation, University of Delaware.

Christodoulatos, C., Bhaumik, S., and Brodman, B. W. (1997) Anaerobic biodegradation of nitroglycerin. *Water Res.*, 31:1462-1470

Concurrent Technologies Corporation (1995) Pink water treatment options. Report No. SFIM-AEC-ETD-CR-95036, U.S Army Environmental Center, Aberdeen Proving Ground, MD.

Deng, B., Burris, D.R., and Campbell, T.J. (1999) Reduction of vinyl chloride in metallic iron-water systems. *Environ. Sci. Technol.*, 33:2651-2656.

Devlin, J. F., Klausen, J., and Schwarzenbach, R. P. (1998) Kinetics of nitroaromatic reduction on granular iron in recirculating batch experiments. *Environ. Sci. Technol.*, 32:1941-1947.

French, C. E., Nicklin, S., and Bruce, N. C. (1996) Sequence and properties of pentaerythritol tetranitrate reductase from *Enterobacter cloacae* PB2. *J. Bacteriol.*, 178:6623-6627.

Gillham, R. W. and O'Hannesin, S. F. (1994) Enhanced degradation of halogenated aliphatics by zero-valent iron. *Groundwater*, 32:958-967.

Gu, B., Liang, L., Dickey, M. J., Yin, X., and Dai, S. (1998) Reductive precipitation of uranium(VI) by zero-valent iron. *Environ. Sci. Technol.*, 32:3366-3373.

Hach Co. (1998) *DR/2010 Spectrophotometer Handbook.* Hach Co., Loveland, CO, USA.

Halasz, A., Spain, J., Paquet, L., Beaulieu, C., and Hawari, J. (2002) Insights into the formation and degradation mechanisms of methylenedinitramine during the incubation of RDX with anaerobic sludge. *Environ. Sci. Technol.*, 36:633-638.

Hardy, L. I. and Gillham, R. W. (1996) Formation of hydrocarbons from reduction of aqueous CO_2 by zero-valent iron. *Environ. Sci. Technol.*, 30:57-65.

Harvey, S. D., Fellows, R. J., Cataldo, D. A., and Bean, R. M. (1991) Fate of the explosive hexahydro-1,3,5,-trinitro-1,3,5-triazine (RDX) in soil and bioaccumulation in bush bean hydroponic plants. *Environ. Toxicol. Chem.*, 10:845-855

Hawari, J., Halasz, A., Paquet, L., Zhou, E., Spencer, B., Ampleman, G., and Thiboutot, S. (1998) Characterization of metabolites in the biotransformation of 2,4,6-trinitrotoluene with anaerobic sludge: role of triaminotoluene. *Appl. Environ. Microbiol.*, 64:2200-2206.

Hawari, J., Halasz, A., Sheremata, T., Beaudet, S., Groom, C., Paquet, L., Rhofir, C., Ampleman, G., and Thiboutot, S. (2000) Characterization of metabolites during biodegradation of hexahydro-1,3,5-trinitro-1,3,5-triazine (RDX) with anaerobic sludge. *Appl. Environ. Microbiol.*, 66:2652-2657.

Heilmann, H. M., Wiesmann, U., and Stenstrom, M. K. (1996) Kinetics of the alkaline hydrolysis of high explosives RDX and HMX in aqueous solution and adsorbed to activated carbon. *Environ. Sci. Technol.*, 30:1485-1492.

Huang, C. P., Dong, C., and Tang, Z. (1993) Advanced chemical oxidation: Its present role and potential future in hazardous waste treatment. *Waste Management*, 13:361-377.

Huang, C. P., Wang, H. W., and Chiu, P. C. (1998) Nitrate reduction by metallic iron. *Water Res.*, 32:2257-2264.

Hundal, L. S., Shea, P. J., Comfort, S. D., Powers, W. L., and Singh, J. (1997) Long-term TNT sorption and bound residue formation in soil. *J. Environ. Qual.*, 26:894-904.

Hwang, P., Chow, T., and Adrian, N. R. (1998) Transformation of TNT to triaminotoluene by mixed culture incubated under methanogenic conditions. Technical report 98/116, Construction Engineering Research Laboratories, U.S. Army Corps of Engineers, Champaign, IL.

Hwang, P., Chow, T., and Adrian, N. R. (2000) Transformation of TNT to triaminotoluene by mixed cultures incubated under methanogenic conditions. *Environ. Toxicol. Chem.*, 19:836-841.

Jafarpour, Y, Imhoff, P. T., and Chiu, P. C. (2003) Mathematical modeling of 2,4-dinitrotoluene reduction with high-purity and cast iron. *Natl. Mtg.-Am. Chem. Soc., Div. Environ. Chem.*, 43 (Abstr.)

Jolas, J. L., Pehkonen, S. O., and Maloney, S. W. (2000) Reduction of 2,4-dinitrotoluene with graphite and titanium mesh cathodes. *Water Environ. Res.*, 72:179-188.

Kaplan, D. L. and Kaplan, A. M. (1982) 2,4,6-Trinitrotoluene-surfactant complexes: decomposition, mutagenicity, and soil leaching studies. *Environ. Sci. Technol.*, 16:566-571.

Kielemoes, J., De Boever, P., and Verstraete, W. (2000) Influence of Denitrification on the corrosion of iron and stainless steel powder. *Environ. Sci. Technol.*, 34:663-671.

Knackmuss, H. J. (1996) Basic knowledge and perspectives of bioelimination of xenobiotic compounds. *J. Biotech.*, 51:287-295.

Lewis, T. A., Goszczynski, S., Crawford, R. L., Korus, R. A., and Admassu, W. (1996) Products of anaerobic 2,4,6-trinitrotoluene (TNT) transformation by *Clostridium bifermentans*. *Appl. Environ. Microbiol*., 62:4669-4674.

Li, Z. M., Comfort, S. D., and Shea, P. J. (1997) Destruction of 2,4,6-trinitrotoluene by Fenton oxidation. *J. Environ. Qual.*, 26:480-487.

Low, G. K. C., McEvoy, S. R., and Matthews, R. W. (1991) Formation of nitrate and ammonium ions in titanium dioxide mediated photocatalytic degradation of organic compounds containing nitrogen atoms. *Environ. Sci. Technol.*, 25:460-467.

Maletzky, P. and Bauer, R. (1998) The photo-Fenton method - degradation of nitrogen containing organic compounds. *Chemosphere*, 37:899-909.

Mantha, R., Taylor, K. E., Biswas, N., and Bewtra, J. K. (2001) A continuous system for Fe^0 reduction of nitrobenzene in synthetic wastewater. *Environ. Sci. Technol.*, 35:3231-3236.

McCormick, N. G., Cornell, J. H., and Kaplan, A. M. (1981) Biodegradation of hexahydro-1,3,5-trinitro-1,3,5-triazine. *Appl. Environ. Microbiol.*, 42:817-823.

Meng, M., Sun, W. Q., Geelhaar, L. A., Kumar, G., Patel, A. R., Payne, G. F., Speedie, M. K., and Stacy, J. R. (1995) Denitration of glycerol trinitrate by resting cells and cell extracts of *Bacillus thuringiensis/cereus* and *Enterobacter agglomerans*. *Appl. Environ. Microbiol.*, 61:2548-2553.

Nam, S. and Tratnyek, P. G. (2000) Reduction of azo dyes with zero-valent iron. *Water Res.*, 34:1837-1845.

Nohara, K., Hidaka, H., Pelizzetti, E., and Serpone, N. (1997) Processes of formation of NH_4^+ and NO_3^- ions during the photocatalyzed oxidation of N-bearing compounds at the titania/water interface. *J. Photochem. Photobiol.*, 102:265-272.

Oh, B. T., Just, C. L., and Alvarez, P. J. J. (2001) Hexahydro-1,3,5-trinitro-1,3,5-triazine mineralization by zerovalent iron and mixed anaerobic cultures. *Environ. Sci. Technol.*, 35:4341-4346.

Oh, S. Y., Cha, D. K., Kim, B. J. and Chiu, P. C. (2002a) Effect of Adsorption to Elemental Iron on the Transformation of 2,4,6-Trinitrotoluene and Hexahydro-1,3,5-trinitro-1,3,5-triazine in solution, *Environ. Toxicol. Chem*., 21:1384-1389.

Oh, S. Y., Cha, D. K. and Chiu, P. C. (2002b) Graphite-Mediated Reduction of 2,4-Dinitrotoluene with Elemental Iron, *Environ. Sci. Technol*., 36:2178-2184.

Oh, S. Y., Chiu, P. C., Kim, B. J. and Cha, D. K. (2003a) Enhancing Fenton Oxidation of TNT and RDX through Pretreatment with Zero-Valent Iron. *Water Research*, 37:4275-4283.

Oh, S. Y., Cha, D. K., Chiu, P. C. and Kim, B. J. (2003b) Enhancing Oxidation of TNT and RDX in Wastewater: Pretreatment with Elemental Iron. *Water Sci. Technol*., 47(10):93-99.

Oh, S. Y., Cha, D. K., Kim, B. J. and Chiu, P. C. (2004a) Reduction of Nitroglycerin with Cast Iron: Pathway, Kinetics, and Mechanisms. *Environ. Sci. Technol*., 38: In Print.

Oh, S. Y., Cha, D. K., Chiu, P. C. and Kim, B. J. (2004b) Conceptual Technology Comparison for Pink Water Treatment: Zero-Valent Iron/Fenton Reagent Reactor, Anaerobic Fluidized Bed Reactor, and Granular Activated Carbon. *Water Sci. Technol*., 49(5-6): In Print.

Oh, S.-Y., Cha, D. K., Kim, B. J. and Chiu, P. C. (2005a) Transformation of Hexahydro-1,3,5-trinitro-1,3,5-triazine (RDX), Octahydro-1,3,5,7-tetranitro-1,3,5,7-tetrazocine (HMX), and

Methylenedinitramine (MDNA) with Elemental Iron. *Environ. Toxicol. Chem.*, **24**: 2812-2819.

Oh, S. Y., Chiu, P. C., Kim B. J. and Cha, D. K. (2005b) Zero-Valent Iron Pretreatment for Enhancing the Biodegradability of RDX. *Water Res.*, **39**: 5027-5032.

Orth, W. S. and Gillham, R. W. (1996) Dechlorination of trichloroethene in aqueous solution using Fe^0. *Environ Sci. Technol.*, 30:66-71.

Perey, J. R., Chiu, P. C., Huang, C. P. and Cha, D. K. (2002) Zero-valent iron pretreatment for enhancing the biodegradability of azo dyes. *Water Environ. Res.*, 74:221-225.

Pesari, H. and Grasso, D. (1993) Biodegradation of an inhibitory nongrowth substrate (nitroglycerin) in batch reactors. *Biotech. Bioeng.*, 41:79-87.

Peters G. T., Burton D. T., Paulson R. L. and Turley S. D. (1991) The acute and chronic toxicity of hexahydro-1,3,5-trinitro-1,3,5-triazine (RDX) to 3 fresh-water invertebrates. *Environ Toxicol Chem.* **10**:1073-1081.

Philips, D. H., Gu, B., Watson, D. B., Roh, Y., Liang, L., and Lee, S. Y. (2000) Performance evaluation of a zerovalent iron reactive barrier: mineralogical characteristics. *Environ. Sci. Technol.*, 34:4169-4176.

Pignatello, J. J. and Sun, Y. (1995) Complete oxidation of metolachlor and methyl parathion in water by the photoassisted Fenton reaction. *Water Res.*, 29:1837-1844.

Poulios, I., Avranas, A., Rekliti, E., and Zouboulis, A. (2000) Photocatalytic oxidation of Auramine O in the presence of semiconducting oxides. *J. Chem. Technol. Biotechnol.*, 75:205-212.

Preuss, A., Fimpel, J., and Diekert, G. (1993) Anaerobic transformation of 2,4,6-trinitrotoluene (TNT). *Arch. Microbiol.*, 159:345-353.

Puls, R. W., Paul, C. J., and Powell, R. M. (1999) The application of in situ permeable reactive (zero-valent iron) barrier technology for the remediation of chromate-contaminated groundwater: a field test. *Appl. Geochem.*, 14:989-1000.

Reardon, E. J. (1995) Anaerobic corrosion of granular iron: measurement and interpretation of hydrogen evolution rates. *Environ. Sci. Technol*., 29:2936-2945.

Roberts, A. L., Totten, L. A., Arnold, W. A., Burris, D. R., and Campbell, T. J. (1996) Reductive elimination of chlorinated ethylenes by zero-valent metals. *Environ. Sci. Technol.*, 30:2654-2659.

Rodgers, J. D. and Bunce, N. G. (2001) Electrochemical treatment of 2,4,6-trinitrotoluene and related compounds. *Environ. Sci. Technol.*, 35:406-410.

Rosemount Analytical Inc. (1994) DC-190 high-temperature TOC analyzer operation manual. Rosemount Analytical Inc., Santa Clara, CA.

Saxe, J. P., Lubenow, B. L., Chiu, P. C., Huang, C.-P. and Cha, D. K. (2006a) Enhanced Biodegradation of Azo Dyes Using an Integrated Elemental Iron-Activated Sludge System: I. Evaluation of System Performance. *Water Environ. Res.*, **78**: 19-25.

Saxe, J. P., Lubenow, B. L., Chiu, P. C., Huang, C.-P. and Cha, D. K. (2006b) Enhanced Biodegradation of Azo Dyes Using an Integrated Elemental Iron-Activated Sludge System: I. Evaluation of System Performance. *Water Environ. Res.*, **78**: 26-30.

Schmelling, D. C., Gray, K. A., and Kamat, P. V. (1996) Role of reduction in the photocatalytic degradation of TNT. *Environ. Sci. Technol.*, 30:2547-2555.

Schwarzenbach, R. P., Gschwend, P. M., and Imboden, D. M. (1993) Environmental organic chemistry. Wiley, New York, NY.

Sedlak, D. L. and Andren, A. W. (1991) Oxidation of chlorobenzene with Fenton's reagent. *Environ. Sci. Technol.*, 25:777-782.

Singh, J., Comfort, S. D., and Shea, P. J. (1998) Remediating RDX-contaminated water and soil using zero-valent iron. J. Environ. Qual., 27:1240-1245.

Singh, J., Comfort, S. D., and Shea, P. J. (1999) Iron-mediated remediation of RDX-contaminated water and soil under controlled Eh/pH. *Environ. Sci. Technol.* 33:1488-1494.

Smith, L. L., Carrazza, J., and Wong, K. (1983) Treatment of wastewaters containing propellants and explosives. *J. Hazard. Mater.*, 7:303-316.

Smock, L. A., Stoneburner, D. L., and Clark, J. R. (1976) The toxic effects of trinitrotoluene (TNT) and its primary degradation products on two species of algae and the fathead minnow. *Water Res.*, 10:537-543.

Spain, J. C., Hughes, J. B., and Knackmuss, H. J. (2000) Biodegradation of nitroaromatic compounds and explosives. Lewis Publishers, New York, NY.

Summers, W. R. (1990) Characterization of formaldehyde and formaldehyde-releasing preservatives by combined reversed-phase cation-exchange high-performance liquid chromatography with postcolumn derivatization using Nash's reagent. *Anayl. Chem.* 62:1397-1402.

Tratnyek, P. G., Johnson, T. L., Scherer, M. M., and Eykholt, G. R. (1997) Remediating ground water with zero-valent metals: chemical considerations in barrier design. *Ground Water Monit. Rem.*, 17:108-114.

U.S. EPA (1999) Field application of in-situ remediation technologies: permeable reactive barriers. EPA 542-R-99-002, U.S. EPA, Washington, DC.

United States Army Toxic and Hazardous Materials Agency (1989) Ball powder production wastewater biodegradation support studies. Report No. CETHA-TE-CR-88344, USATHMA, Aberdeen, MD.

Urbański, T. (1985) Chemistry and technology of explosives vol. 4. Pergamon, New York, NY.

VanderLoop, S. L., Suidan, M. T., Moteleb, M. A., and Maloney, S. W. (1998) Two-stage biotransformation of 2,4,6-trinitrotoluene under nitrogen-rich and nitrogen-limiting conditions. *Water Environ. Res.*, 70:189-196.

Vidic, R. D. and Pohland, F. G. (1996) Treatment Walls. TE-96-01, Technology Evaluation Report, Groundwater Remediation Technologies Analysis Center (GWRTAC), Pittsburgh, PA.

Walling, C. (1975) Fenton's reagent revisited. *Acc. Chem. Res.*, 8:125-131.

Weber, E. J. (1996) Iron-mediated reductive transformations: investigation of reaction mechanism. *Environ. Sci. Technol.*, 30:716-719.

Wendt, T. M., Cornell, J. H., and Kaplan, A. M. (1978) Microbial degradation of glycerol nitrate. *Appl. Environ. Microbiol.*, 36:693-699.

White, G. F., Snape, J. R., and Nicklin, S. (1996) Biodegradation of glycerol trinitrate and pentaerythritol tetranitrate by *Agrobacterium radiobacter*. *Appl. Environ. Microbiol.*, 62:637-642.

Won, W. D., DiSalvo, L. H., and Ng, J. (1976) Toxicity and mutagenicity of 2,4,6-trinitrotoluene and its metabolites. *Appl. Environ. Microbiol.*, 31:576-580.

Yinon, J. (1990) Toxicity and metabolism of explosives. CRC Press, Boca Raton, FL.

Yinon, J. and Zitrin, S. (1993) Modern methods and applications in analysis of explosives. John Wiley & Sons, New York, NY.

Zhang, Y. Z., Sundaram S. T., Sharma, A., and Brodman, B. W. (1997) Biodegradation of glycerol trinitrate by *Penicillium corylophilum* Dierckx. *Appl. Environ. Microbiol.*, 63:1712-1714.

Zoh, K. D. and Stenstrom, M. K. (2002) Fenton oxidation of hexahydro-1,3,5-trinitro-1,3,5-triazine (RDX) and octahydro-1,3,5,7-tetranitro-1,3,5,7-tetrazocine (HMX). *Water Res.*, 36:1331-1341.